Knock Behavior of a Lean-Burn, Hydrogen-Enhanced Engine Concept

by

Jennifer A. Topinka

B.S., Mechanical Engineering
University of Wisconsin – Madison, 2001

Submitted to the Department of Mechanical Engineering
in Partial Fulfillment of the Requirements for the Degree of

Master of Science in Mechanical Engineering

at the

Massachusetts Institute of Technology

September 2003

Signature of Author: _____
Department of Mechanical Engineering
September 2003

Certified by: _____
John B. Heywood
Sun Jae Professor of Mechanical Engineering
Thesis Advisor

Accepted by: _____
Ain A. Sonin
Professor, Department of Mechanical Engineering
Chairman, Department of Graduate Committee

(This page was intentionally left blank.)

Knock Behavior of a Lean-Burn, Hydrogen-Enhanced Engine Concept

by

JENNIFER A. TOPINKA

Submitted to the Department of Mechanical Engineering
September, 2003 in partial fulfillment of the
requirements for the Degree of Master of Science in
Mechanical Engineering

Abstract

Experiments to identify the knock trends of lean gasoline-air mixtures, and such mixtures enhanced with hydrogen (H_2) and carbon monoxide (CO), were performed on a single-cylinder research engine with boosting capability. The experimental method used to investigate knock trends consisted of determining the octane number (ON) of the primary reference fuel (mixture of isooctane and n-heptane) supplied to the engine that just produced audible knock. All tests were completed at 1500 rpm, MBT spark timing, with coolant temperature at fully warmed-up conditions and intake air temperature at 20° C. Various relative air-fuel ratio (lambda) sweeps were performed, while holding different parameters constant. First, testing with primary reference fuels investigated knock limits of lean operation; selected tests were then repeated with H_2 and CO-enhancement. These mixtures simulated 15% and 30% of the engine's gasoline being reformed in a plasmatron fuel reformer.

Experimental results show that leaner operation does not decrease the knock tendency of an engine under conditions where a fixed output torque is maintained; rather it slightly increases the octane requirement. The onset of knock does decrease with lean operation when the intake pressure is held constant, but engine torque is then reduced. When H_2 and CO are added to the mixture, the knock susceptibility is reduced, as illustrated by a decrease in the measured octane number of the primary reference fuel resulting in knock. Experiments conducted with the addition of H_2 show similar trends, but to a lesser degree. Therefore, both H_2 and CO act as octane enhancers when added to a hydrocarbon-air mixture. The extent to which H_2 and CO improve the knock resistance of a mixture can be estimated by finding the bond-weighted octane number for the mixture of fuels.

To substantiate these results, a chemical kinetic ignition model was used to predict autoigntion of the end-gas for various conditions and fuel-air mixtures. Predicted model trends of knock onset partially agree with experimental observations. A comprehensive isooctane chemistry mechanism was used to demonstrate that H_2 and CO-enhancement are effective in lengthening the ignition delay, and thereby reduce knock tendency.

Thesis Advisor: John B. Heywood
Title: Sun Jae Professor of Mechanical Engineering

(This page was intentionally left blank.)

Acknowledgements

The Sloan Automotive Laboratory is a world-class laboratory because of the people – the professors, scientists, students, and staff. I feel fortunate to have worked with many talented individuals in this exciting and supportive environment. There are many people who have helped shape and complete this work. Just as importantly, there are many who provided healthy friendships and encouragement on a personal level. This page acknowledges those who have helped make my experience in graduate school positive and unforgettable.

I would like to thank Professor Heywood for guiding this research project and my development as a graduate student. I feel very privileged to have had the opportunity to work with and learn from him. Professor Heywood's profound insight, solid reasoning, and professional tact are just the beginning of his impressive character. He set an excellent example of how to conduct research and business. This thesis and the research results herein would not have been possible without him.

Professor Keck also contributed to this project by helping to utilize the reduced chemistry model and by offering his expertise on combustion. The other Sloan Automotive Laboratory students working on the plasmatron engine concept have been terrific teammates. I thank Ed Tully for his brilliant explanations and patience with me during my first year in graduate school. Ziga Ivanic and Josh Goldwitz helped a great deal by improving the engine experimental setup and working through the engine issues that cropped up over this past year.

Laboratory guru, Brian Hallgren, helped tremendously with the Volvo/Ricardo experimental setup. He also provided pep talks whenever necessary to encourage me at every step of my journey through graduate school. My officemates, Yuetao (Tony) Zhang, Yianni Kitsopanidis, and Nuria Margarit, provided great friendships and technical support. Tony was always willing to "take a look" at the puzzles that arose throughout my research. Yianni was the star lecturer of the lab... simply give him a white board and 50 minutes. Nuria, my dear friend, helped make long days bearable by welcoming small talk and coffee runs. I also appreciated the special friendships of Morgan Andreas, Vince Costanzo, Tiffany Groode, Yong Li, Jeremy Llaniguez, and Fiona McClure. Although I cannot mention all of their names, I have enjoyed the company and the support of all the students at the laboratory. I wish you the best and I look forward to meeting again in the future!

There are others associated with the Sloan Automotive Laboratory who provided invaluable support. I thank Professor Cheng for his willingness to help troubleshoot issues in the lab and for supporting laboratory camaraderie in many ways. I appreciate Dr. Wong for his dedication to the lab. Thane DeWitt provided me with solid technical guidance in the lab. Karla Stryker was flexible and accommodating, always finding room for me in Professor Heywood's busy schedule. She also was the fun-loving lab mother, who added pizzazz to lab business and social events. I would like to thank Alexis Rozantes, our dynamic administrative assistant and my great friend, for her kindness, sense of humor, and good advice.

Finally, I'd like to acknowledge my family and my friends at the University of Wisconsin-Madison for providing unconditional support. Thank you for helping me to find the courage to follow my dreams.

This overall project wouldn't exist without plasmatron reformer champions at the MIT Plasma Fusion Science Center: Leslie Bromberg, Dan Cohn, and Alexander Rabinovich. Rudy Smaling deserves much credit for the project's commercial status and for the system design work related to this technology.

This research was supported by a grant from Ford Motor Company. I would like to extend a special thanks to Jim Clarke and Graham Hoare for giving me the opportunity to participate in this research.

Table of Contents

(This page was intentionally left blank.)

List of Tables

List of Figures

Chapter 1 Introduction

1.1 Overview

Knock is caused by the spontaneous combustion of unburned fuel and air ahead of the propagating flame front in a Spark-Ignition (SI) engine [1]. This rapid release of energy causes a rise in local pressure. The pressure waves propagating across the gas in the combustion chamber cause the engine block and cylinder head to vibrate, generating a clanging or pinging noise. This noise is unfavorable to customers; in addition, extended operation under knocking conditions can cause damage to engine components.

Knock has been well studied for many decades, but it is still a concern. Advances in fuel processing have resulted in gasolines with increased knock resistance; in addition, fast burning combustion chamber designs help to control knock. Nevertheless, engine performance and efficiency are constrained by knock. If new methods to control knock are developed, engine performance and efficiency could be significantly improved.

One way to suppress knock in a naturally aspirated engine is to operate the engine with excess air in the cylinder. However, under these lean operating conditions, the engine torque decreases. If the engine is then boosted to maintain constant torque, then the knock situation relative to operation with stoichiometric mixtures is unclear.

The traditional motivation for using lean engine operation is to decrease harmful emissions and to increase fuel conversion efficiency. In general, the leaner the mixture, the greater the efficiency and emissions benefit; however, at some point the engine cannot support stable combustion and the lean limit is encountered. To extend the stable range of lean operation small amounts of hydrogen, which burn faster than gasoline, can be added to the fuel-air mixture. To obtain hydrogen onboard a vehicle, a fuel reformer can be used to produce a hydrogen (H_2), carbon monoxide (CO), and nitrogen (N_2) mixture from gasoline and air.

The work herein explores the opportunities for suppressing knock by lean, hydrogen-enhanced engine operation. The engine's Octane Number Requirement (ONR) indicates its propensity to knock. This project examines the changes in knock limits, as measured by the base fuel octane number at the onset of audible knock, of an engine under lean operating conditions, with gasoline alone and with gasoline enriched with H_2, CO, and N_2. The changes in octane number requirement of the primary reference fuel supplied to the engine will be discussed and related to fundamental explanations using engine experiments and modeling.

1.2 Engine Technologies

With increasing concern about the greenhouse gas effect, and air pollution reduction requirements, automobile manufactures must prepare to meet both tighter emission standards and more aggressive Corporate Average Fuel Economy (CAFE) regulations. A variation of spark ignition technology, the lean burn engine, could help overcome the hurdles.

Present-day gasoline engines operate with low NOx and HC emissions at the expense of fuel efficiency and CO_2 emissions. Exhaust NO_x, CO and HC are reduced with the use of a three-way catalyst. The three-way catalyst requires that the exhaust gases alternate between slightly rich to slightly lean of stoichiometric, constraining gasoline engines to an average stoichiometric mixture. This leads to inefficiencies such as pumping losses and lower indicated fuel conversion efficiency at part load operation.

At part load, filling the cylinder with a stoichiometric mixture would result in too much power; so the incoming mixture is throttled, decreasing the density of mixture in the cylinder. The pressure drop across the intake system of a throttled engine causes pumping losses over the exhaust and intake stokes, decreasing part load efficiency.

A stoichiometric mixture has non-optimal properties as a working fluid, due to a relatively low ratio of specific heats. In addition, the burned gas temperatures produced by combustion of a stoichiometric mixture are higher than lean mixture temperatures so heat losses are higher which reduces efficiency.

Diesel engines do not suffer the same restrictions as gasoline engines, but have a different set of concerns. Diesels engines are not limited by knock because burning involves a diffusion flame instead of flame propagation. Thus higher compression ratios can be used, thereby increasing efficiency. Diesels are unthrottled, varying the torque by adjusting the amount of fuel injected instead of the amount of fuel-air mixture, which avoids much of the pumping losses. Because the air-fuel mixture in a diesel has excess air, the ratio of specific heats is higher, increasing the amount of energy that is removed from the burned gases during expansion. However, the inhomogeneous nature of diesel combustion produces NOx and particulate matter. Good diesel aftertreatement is not yet available. Hence, significant technical hurdles have to be overcome before diesels can become important in the US light duty vehicle market.

This work considers a way to improve gasoline engines by combining features of diesel and SI into one concept. The concept involves lean operation, which combines the surplus air of a diesel with the homogeneous mixture characteristic of a gasoline engine. A lean burn concept is attractive for many reasons: engines with lean air-fuel mixtures are more efficient, pumping losses are lower because of less throttling, and NOx emissions are reduced due to the lower flame temperatures. The advantages of using

a lean burn engine increase as more air is used. To justify abandoning the current gasoline engine approach -- a stoichiometric gasoline engine and a 3-way catalyst -- very lean mixtures must be burned. Ultra-lean combustion could alleviate the need for NOx after treatment. However, lean engines are not widespread today due to problems that arise in lean operation before reaching the relative air/fuel ratio (λ) of approximately two, where the benefits of very low NOx can be realized.

The significant obstacle associated with lean operation involves the loss of flame speed and combustion stability. When excess air is present in the cylinder, the flame propagates more slowly leading to long burn duration and less stability. Flame stability is manifested in the amount of combustion variation that occurs from one cycle to the next. Cycle-to-cycle variation is the result of three main phenomena: 1.) Non-optimal combustion phasing, in which cycles whose burning is not phased for maximum brake torque have a lower indicated output when compared with an average cycle that is properly phased with the piston motion, 2.) Partial burns, resulting when the flame is quenched before completely consuming the mixture, and 3.) Misfires, occurring when the mixture is too lean to be ignited by the spark plug. When combustion stability worsens, engine output decreases and overall engine efficiency declines. The point where the mixture's burning properties are unacceptable is called the lean limit. Typical gasoline-fueled SI engines operating in the lean regime encounter the lean limit of operation before the major benefits of lean operation can be realized. This project examines the knock limits of SI engine operation with very lean, hydrogen-enhanced mixtures. The objective is to help optimize this lean-burn SI concept so the full benefits of lean operation can be realized.

1.3 The Plasmatron-Engine System

1.3.1 Hydrogen Enhancement

The hydrogen-enhanced engine concept uses H_2 and CO produced with an onboard fuel reformer to enable ultra-lean engine operation with low engine-out NOx emissions and increased fuel conversion efficiency. This approach would use existing SI engines and could be realized short-term to allow ultra-lean mixtures to be burned in a SI engine technology.

Hydrogen addition allows ultra-lean mixtures to burn without misfire or high variability. Hydrogen has a high flame speed compared with other conventional fuels (see Table 1-1). When hydrogen is added to a mixture, the high flame speed helps to maintain flame stability, even when excess air is present. Hydrogen diffusion properties increase the flame speed in a mixture, decreasing burning duration and variability. Finally, the high spontaneous ignition temperature of hydrogen alludes to the

idea that hydrogen is a knock-resistant fuel. Hydrogen is therefore an optimal additive to extend the lean limit of a SI engine.

Table 1-1 Combustion characteristics for hydrocarbon fuels, H_2, and CO [2].

Fuel	Flame Speed at 100 °C and 1 atm. [cm/sec]		Spontaneous Ignition Temperature in Air [°C]
	Stoichiometric	Maximum	
Isooctane	57.8	58.2	447
Normal-heptane	63.8	63.8	247
Hydrogen	170.0	325.0	572
Carbon monoxide	28.5	52.0	609

Previous and ongoing research at MIT has examined the benefits of hydrogen-enhanced lean combustion. So far, results indicate hydrogen is very effective in extending the lean limit. Hydrogen-enhanced lean operation has shown up to a 99% reduction in NOx and a 12% increase in overall fuel conversion efficiency [3]. Hydrogen-enhanced combustion is not a new idea. Although the benefits of hydrogen have been shown, problems typically associated with hydrogen (cost, storage, and infrastructure) have discouraged it use. Most of these challenges can be alleviated when hydrogen is produced onboard the vehicle as needed for consumption.

1.3.2 System Description

Figure 1-1 illustrates the generalized plasmatron engine concept. A fraction of the fuel flow is diverted to the plasmatron. Inside the plasmatron reformer, gasoline is partially oxidized to a H_2, N_2 and CO mixture, with modest amounts of H_2O and CO_2, and some smaller hydrocarbons. The reformate gas is then cooled if necessary and directed into the engine with additional air and gasoline. This reformer engine concept has several advantages:

- Current engine technology can be employed. A drastic change in engine or automotive design is not necessary.
- This system could be added to existing engines.
- The customer does not perceive degradation in engine performance or operation.

Disadvantages of the system are:

- The plasmatron has an electrical power requirement; this electrical power must be generated onboard the vehicle.
- Fuel conversion inefficiency within the plasmatron penalizes overall energy efficiency.
- The plasmatron – engine system introduces increased complexity

These issues are currently being investigated to minimize their impact.

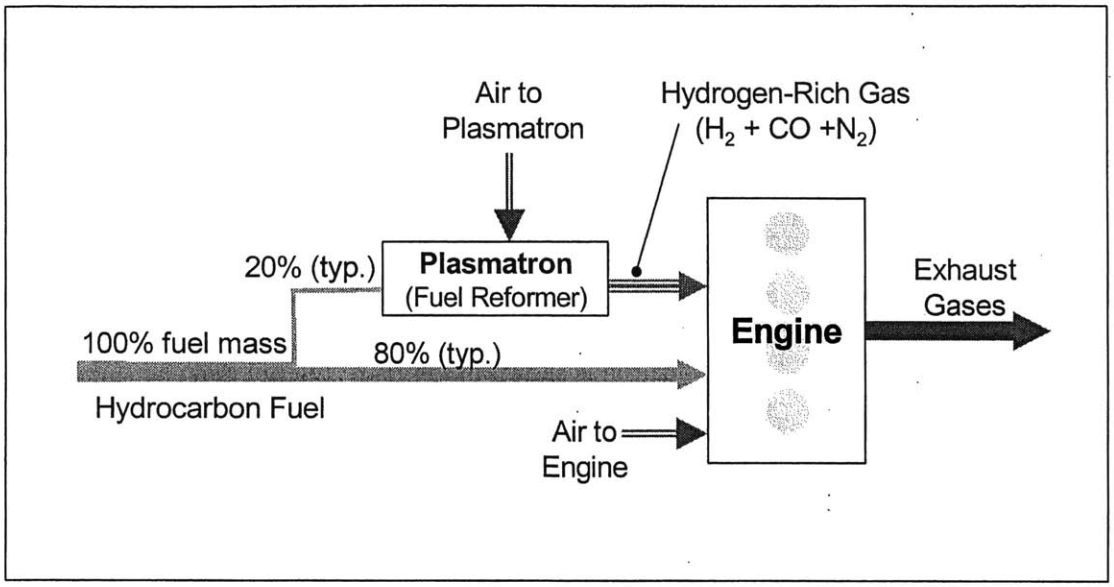

Fig. 1-1 Typical set-up for the plasmatron fuel reformer.

1.3.3 The Plasmatron

The plasmatron fuel reformer (Fig. 1-2) is being developed at the MIT Plasma Fusion Science Center. A plasma arc is used to partially oxidize a rich mixture of fuel and air, which passes through the reactor. The ideal oxidation reaction is shown in Eq (1-1).

$$C_m H_n + \frac{m}{2}(O_2 + 3.773N_2) \rightarrow mCO + \frac{n}{2}H_2 + \frac{m}{2}\cdot 3.773N_2 \qquad \textbf{Eq. 1-1}$$

The mass air/fuel ratio for this reaction is approximately 4, depending on the hydrocarbon supplied. A majority of the fuel and air participate in the ideal reaction. However, a small portion of the hydrocarbon undergoes complete oxidation, producing CO_2 and water. On the other extreme, some fuel escapes any

oxidation and exits unchanged or as smaller hydrocarbons. The ideal and typical current output compositions of the plasmatron are shown in Table 1-2.

Table 1-2 **Ideal and typical composition and efficiency of the plasmatron fuel reformer, subject to hydrocarbon supplied.**

Parameter	Ideal Plasmatron	Typical Plasmatron
H_2	25%	20%
CO	26%	22%
N_2	49%	51%
CO_2	0%	2%
H_2O	0%	4
Smaller Hydrocarbons	0%	<1%
Fuel Conversion Efficiency	84%	76.5%

A simple energy balance schematic for the plasmatron is shown in Fig. 1-3. Energy must be supplied to power the plasmatron; the proposed energy requirement is 5-6 MJ/kg H2. In addition, the chemical reaction is exothermic, indicating that the chemical energy contained in the incoming stream of hydrocarbon fuel is greater than the chemical energy contained in the plasmatron reformate leaving the reactor. The plasmatron fuel conversion efficiency, η_{Plas}, is defined as the chemical energy out divided by the hydrocarbon energy in Eq. 1-2)

$$\eta_{Plas} = \frac{\dot{m}_{H2} \cdot LHV_{H2} + \dot{m}_{CO} \cdot LHV_{CO}}{\dot{m}_{GASOLINE} \cdot LHV_{GASOLINE}} \qquad \textbf{Eq. 1-2}$$

where $\dot{m}$ is the mass flow rate [kg/sec], LHV is the lower heating value [MJ/kg].

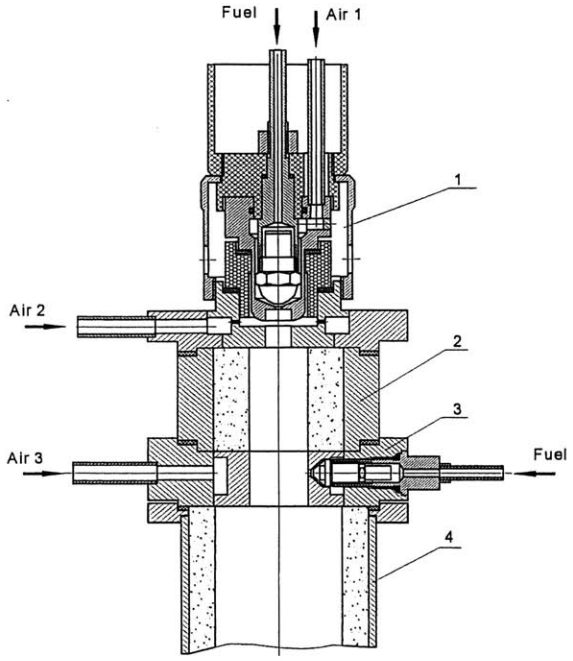

1-Plasmatron
2-1st Stage Reactor
3-Nozzle Section
4-2nd Stage Reactor

(Courtesy of Alexander Rabinovich)

Fig. 1-2 Schematic of the plasmatron fuel reformer.

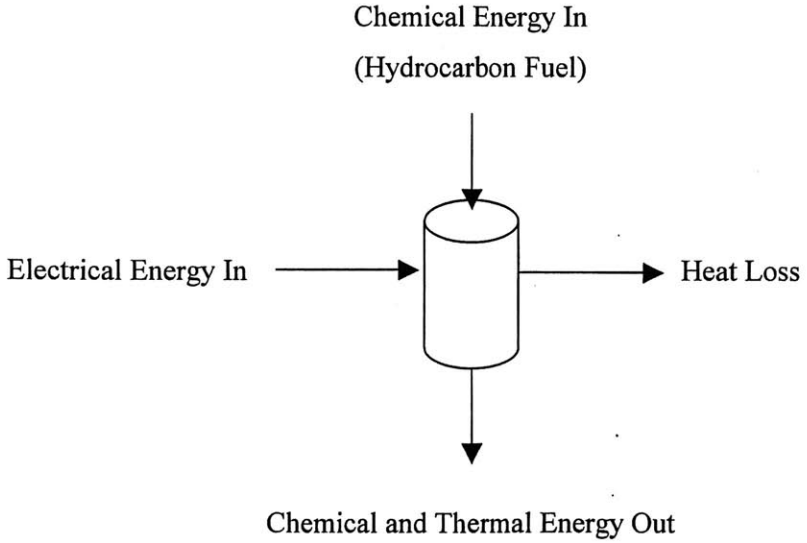

Fig. 1-3 Simple energy balance for the plasmatron fuel reformer.

1.4 Knock Fundamentals

1.4.1 General Description of Phenomena

Knock is an abnormal mode of combustion for SI engines in which the unburned mixture reaches sufficiently high temperature and pressure to cause rapid ignition (or autoignition), before being consumed by the turbulent flame front. The unburned mixture, commonly referred to as end-gas is compressed first by the piston in the compression stroke, and then by the expanding burned gases. The compression causes an increase in temperature, triggering autoigntion reactions and resulting in the mixture igniting before the arrival of the flame. Thus, autoigntion is a race between the preignition reactions in the end-gas and the turbulent flame front. If the flame consumes the end gas before the preignition reactions become significant, autoigntion does not occur. When the unburned mixture ignites, a large amount of chemical energy can be released rapidly, causing a rapid rise in local pressure. The resulting pressure oscillations cause a ringing noise commonly called "knock". If severe enough, knock can damage the engine by introducing high amplitude stress oscillations and rates of heat transfer. The following research focuses upon autoignition that is severe enough to cause an audible sound.

1.4.2 The Role of Knock on SI Engine Design and Performance

When knock is present during combustion, autoignition occurs in one or several locations in the end-gas before the flame propagation is complete. Light knock can increase the engine performance slightly, in the same way that a fast burning cycle may result in a higher output. However, customers perceive even light knock as a problem. Moderate to heavy knock shows pressure oscillations of up to several bar and often a decrease in torque output, similar to that which is experienced with an over-advanced spark timing [4]. Heavy knock results in damage to the engine components. Engine designers attempt to avoid knock for these reasons.

Knock is normally a problem at high loads and low speeds. It is avoided in current engine designs by limiting maximum temperature and pressures in the cylinder. If encountered during operation, spark timing can be retarded to phase the combustion event later in the cycle, reducing peak temperatures and pressure, until knock is eliminated. Although spark retard is an effective way to control knock to some extent, overall engine design is constrained by knock. Maximum Net Indicated Mean Effective Pressure (NIMEP) is limited by the inability to increase peak pressure, thereby limiting engine output. Compression ratio is also limited, preventing use of higher compression ratios and realizing higher efficiencies.

1.4.3 Parameters which Influence Knock

The tendency of an engine to knock depends on many factors. However, there are three key parameters which affect knock: end-gas thermodynamic state (i.e. temperature and pressure), end-gas chemistry, and end-gas time spent at high pressure and temperature. These three variables are affected by both engine design parameters (compression ratio, combustion chamber design, bore to stroke ratio) and engine operation (intake pressure, intake temperature, equivalence ratio, engine speed).

1.4.3.1 Temperature Effect

The maximum unburned mixture temperature has the greatest influence on knock because chemistry rates are strongly dependent on temperature. Therefore, when addressing the extent to which factors affect knock, those that change the unburned mixture temperature are most important. The following quantities are known to have an impact on maximum unburned mixture temperature:

- Residual fraction - These burned gasses left over from a previous cycle have high temperatures and directly increase the air, fuel, and residual gas mixture temperature within each cylinder. Nakada [5] shows that residual fraction can increase the charge temperature by up to 55° K at Top Dead Center (TDC), directly impacting knock.
- Temperature of intake air - Higher intake air temperatures will result in higher maximum unburned gas temperature.
- Temperature of engine coolant (and therefore the temperature of the intake port, cylinder head, piston, and cylinder walls) - This variable determines the amount of heat transfer to and from the mixture.
- Mixture humidity - Water in the charge adds heat capacity, therefore affecting charge temperature.
- Ratio of specific heats (γ) - A higher value of gamma causes a larger temperature raise during compression.

The extent to which the initial temperature of the charge and the ratio of specific heat affect the maximum mixture temperature can be estimated assuming the end-gas is uniform in temperature and pressure and is isentropically compressed. Using the intake mixture temperature and initial in-cylinder pressure, and maximum pressure, the maximum unburned gas temperature can be estimated as shown in Eq. (1-3).

$$T_{\max} = T_{initial}\left(\frac{P_{\max}}{P_{initial}}\right)^{\frac{\gamma-1}{\gamma}} \qquad \text{Eq. 1-3}$$

1.4.3.2 Pressure (Density) Effect

Other factors directly influence the pressure of the charge. These factors are less important than to those that change the temperature directly. However, pressure and temperature are coupled by Eq. (1-3) and the ideal gas law, hence temperature and pressure change together.

- Spark Timing - Retarded spark timing causes combustion to occur later in the cycle. The late burning results in less work being extracted from the burned gases, and peak pressures are reduced, thereby decreasing knock tendency. Spark retard is commonly used on engines, providing the flexibility to transition out of knocking operation in the case where poor octane fuel is used, or when engine deposits form and increase the knock tendency.
- Compression Ratio - Defined as the maximum cylinder volume divided by the minimum cylinder volume, the compression ratio dictates the amount of compression that the gas experiences due to motion of the piston. The higher the compression ratio, the greater the pressure increase experienced by the end gas.
- Intake Pressure - A high intake pressure will result in a higher pressure profile throughout the compression process.
- Energy released during the combustion - The pressure raise due to the chemical energy heat release is a function of air/fuel ratio and mass trapped in the cylinder. Higher inlet pressures and near-stoichiometric mixtures provide the largest energy release.

1.4.3.3 Mixture Composition – Chemical Reactivity of the End-Gas

The chemistry composition of the end-gas is also important in determining knock. The fuel properties have a significant impact on the chemical reactivity of the end-gas. The knock resistance of fuels is quantified by their octane number. Typically hydrocarbon fuels are blended to increase their resistance to knock. Knock inhibiting additives, which are sometimes used, work by consuming radicals thereby slowing the reactions leading to autoigntion. The concentration of the fuel is important, with near-stoichiometric mixtures showing the shortest ignition delay time. Both excessively rich and lean mixtures cause the rates of these autoignition reactions to decrease.

1.4.3.4 End-Gas Residence Time

Factors that influence the length of time the end-gas experiences high temperature and pressure, before being consumed by the flame, affect the knock tendency. Engine speed governs the absolute time the end-gas remains in the cylinder. Knock is less of a problem at high speed because residence times are lower and high turbulence increases the flame speed.

The flame speed of the mixture changes the end-gas residence time in the cylinder. For a given engine speed, the flame speed is primarily a function of the air/fuel ratio and the fuel properties. Quickly burning mixtures will be less likely to knock as the flame consumes the end-gas before reaction become significant. Slow-burning mixtures allow more time to pass before the end-gas is consumed.

1.4.4 Gasoline and Compression Ratio Trends

A brief history of gasoline octane and engine compression ratio is included here to illustrate the importance of fuel in engine design and performance. Fuels and engines have evolved together. The first engines were required to have a very low compression ratio to run without knock. After WWI, it became apparent that better fuel was needed to allow an increase in the compression ratio and specific output. The knock resistance of commercially available gasoline has been increasing since by means of additives or better hydrocarbon processing. Tetraethyl lead (TEL) was used as an octane-enhancing additive from the late 1920's to the 1970's and 80's, at which time it was phased out due to the environmental and health hazards, and its poisoning effect on catalysts. Currently, oxygenates are used in fuels to improve exhaust emissions, and increase octane number.

Figure 1-4 shows long-term history of octane number increase. Due to the increase in octane number it has been possible for compression ratio to be increased as is also shown in Fig. 1-4 [6]. Figure 1-5 [7] shows a continued gradual increase in compression ratio over the past few years. Implications of this research include increasing the compression ratio of gasoline engines, enabled by higher knock resistant fuel/air mixtures.

Until there is a way to dynamically change the effective compression ratio, it will be limited by the antiknock quality of the fuel and the combustion characteristics of the chamber. Novel concepts including variable valve timing and dynamic engine geometry allow for a continuously variable compression ratio. However, these ideas involve significant modifications of the engine design.

The plasmatron concept does not significantly change the engine design, but rather adds a fuel converter that enables changes in the mixture composition by species and by dilution. This research finds that the changes in mixture specie composition cause the knock tendency to decrease; that is, by

reforming part of the gasoline to a H_2, CO mixture, the overall octane number of the fuel mixture (H_2+CO+gasoline) is increased. If implemented, this concept has the potential to facilitate an increase in average compression ratio without requiring a higher octane number hydrocarbon fuel supply or significant engine modifications.

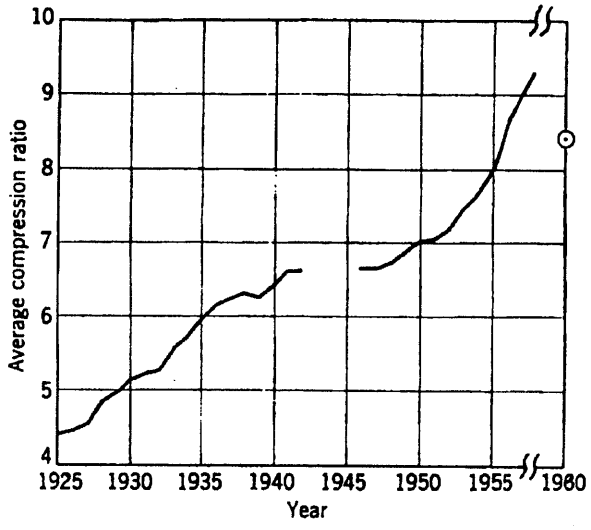

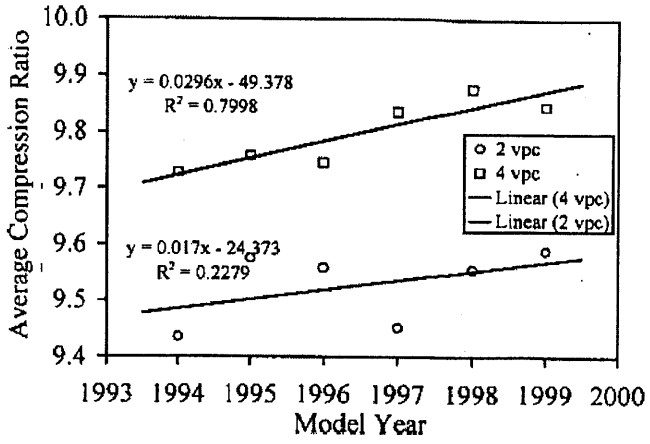

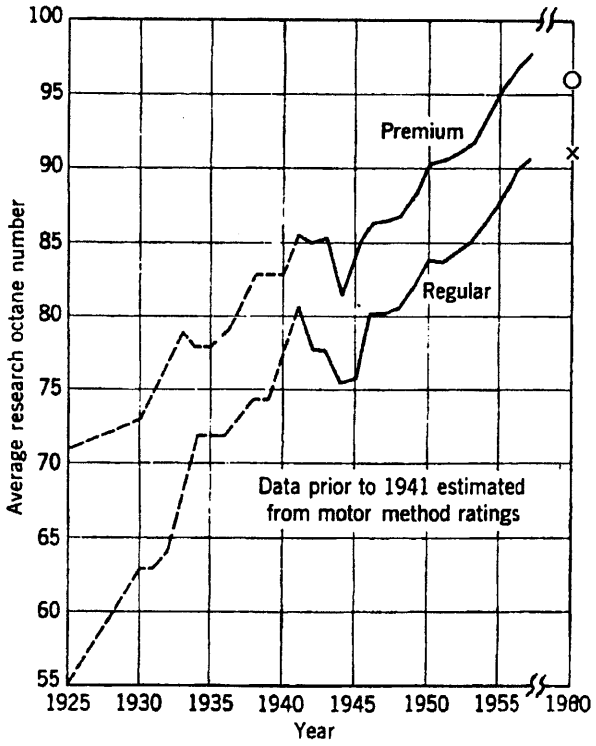

Fig. 1-4 **Long-range history of average octane number fuel available and corresponding average compression ratio trends [6].**

Fig. 1-5 **(Top Right) Short-term history of average compression ratio [7].**

1.5 Previous Work

Most research associated with lean-burn and hydrogen-enhanced combustion has been done on emissions and efficiency benefits of these modes of operation. Few studies have addressed knock behavior, in such a way that their results can be used in designing an improved engine. The relevant studies are summarized below.

1.5.1 Autoignition in Lean Mixtures

The most referenced literature on knock trends of lean mixtures was published in 1979 by Gruden and Hahn [8]. In their study, a production engine was converted to a lean burn engine. Researchers explored the effect of many parameters on engine economy including: high compression ratio, optimization of ignition timing and layout of the combustion chamber shape with intensive charge turbulence. Knock trends were explored by generating a curve of highest possible compression ratio for a range of relative air-fuel ratios. Figure 1-6 shows the conclusion of this study. The shaded areas in the chart show the possible points of operation, bounded above by the knock limit, on the right by the lean limit, and on the left by the inflammability (rich) limit. The chart shows that the compression ratio can be increased with lean operation, implying that lean mixtures are more knock resistant. However, the operating condition for which the trend is valid is not clearly stated. Research is needed to address the autoignition trends in lean engines where the torque output per volume matches that of a stoichiometric engine.

Betts et al. [9] described a lean, boosted, high compression engine with some caution. The authors' experiences with high compression engines encountered a region of runaway knock, occurs very quickly and with little warning. They speculated that lean, high compression engines would likely show a similar trend. In addition, they noted that most lean-burn engines are operating lean under part load conditions; therefore, knock characteristics of lean mixtures are only valid at part throttle.

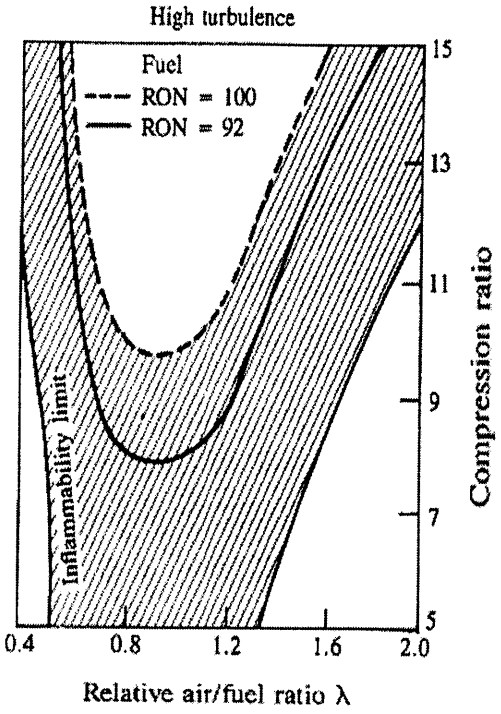

Fig. 1-6 **Illustration by Gruden [8] suggesting higher compression ratios are possible with lean operation. The shaded area is the safe for operation, bounded above by the knock limit, to the left by the inflammability limit, and to the right by the misfire limit.**

Stokes et al of Ricardo [10] suggest that a lean, boosted engine system has engine knock benefits. A Gasoline Direct Injection (GDI) engine was used, with a simulated turbocharger. Excess air was shown to be effective in suppressing knock, even at high inlet manifold pressure. The engine concept they proposed takes advantage of Gruden's Fig. 1-6. The authors foresee a feedback loop where lean operation allows an increased compression ratio, and an increased compression ratio allows leaner mixtures to be burned. These two interactions form a positive feedback loop allowing great benefit according to this paper.

Work from Chalmers and Lund Universities [11] has compared knock in lean mixtures versus stoichiometric mixtures with and without exhaust gas recirculation (EGR). Testing was done on a single-cylinder research engine, which was modified to facilitate end-gas temperature measurement with dual broadband rotational Coherent Anti-Stokes Ramen Spectroscopy (CARS). Experiments were done at relatively constant IMEP, MBT spark timing, and constant air and engine fluid temperatures, while supplying the engine with gasoline of ON 75. For each mixture, the knock characteristics, such as knock intensity and onset of knock, were recoded over many cycles as well as the end-gas temperature leading

to the autoignition event. The experiments showed that lean mixtures have the earliest onset of knock, and the highest knock intensity. While doing experiments and modeling, it was noted that lean mixtures are particularly sensitive to the charge heating due to compression. This research implies that excess air at high loads does not suppress knock.

1.5.2 Hydrogen and Carbon Monoxide Autoignition Properties

Past researchers have investigated engines fueled with pure hydrogen and hydrogen-hydrocarbon mixtures. Hydrogen, an alternative fuel for spark ignition engines, is not a new idea. However, hydrogen production and storage has always been a technical hurdle. Most H_2 or H_2-enhanced research concepts focus on the increased efficiency and low emissions associated with the engines concepts. However, with increasing interest in Homogeneous Charge Compression Ignition (HCCI) engine combustion concepts, there are researchers examining the autoigntion properties of dual mixtures as well.

The autoigntion properties of H_2 are not so clear. Some have tried to assign an octane number to hydrogen. However, using the standard methods of octane testing is inconclusive. Various sources state that the ON of hydrogen is very high, from 130-140 [12][13][14].

There has been considerable work done on autoignition properties of dual fuel mixtures with one fuel being hydrogen. Karim and coworkers at the University of Calgary [15] have worked with experiments and models exploring the autoignition properties of duel mixtures containing methane + hydrogen and propane + hydrogen. Conclusions hint that the addition of small amounts of hydrogen can delay the ignition of methane. Too much hydrogen will have the opposite effect. This work suggests that the hydrogen ignition reactions are slower in nature than the ignition reactions in methane.

The concept of controlling HCCI combustion by using bi-fuels has been studied. Shudo and coworkers [16] have looked at blends of Dimethylether (DME) and CO-H_2-CO_2 mixtures. Results show that the addition of H_2 and CO lengthens autoigntion delay time. Comparative tests of DME + H_2 and DME + CO show that H_2 is more effective than CO in extending the ignition delay.

1.6 Objectives

The original question proposed for this project was: "What is the knock-limited compression ratio of a lean, hydrogen-enhanced, and also boosted engine concept?" Since changing compression ratio on the research engine was not a trivial task, it was decided to explore the knock behavior by varying fuel qualities, which would give directional indications of a knock-limited compression ratio. This study thus investigated the octane number requirement of the single-cylinder engine used, for various engine operating conditions and mixtures. Two tasks were carried out:

1. Explore the knock behavior of lean mixtures
2. Determine how the addition of H_2 and CO change the knock resistance properties of the hydrocarbon, H_2 and CO mixture.

Chapter 2 Experimental Method

The methodology used to explore the knock behavior of lean and plasmatron reformate-enhanced mixtures involved determining the gasoline Octane Number Requirement (ONR) for a series of operating points. Primary Reference Fuels (PRF), isooctane and normal-heptane, were used to represent gasoline of different Octane Number (ON). By mapping the primary reference fuel octane number requirement at various operating conditions, the relative knock behavior was examined. Tests were first completed with gasoline (primary reference fuel), then selected tests were repeated using simulated plasmatron reformate or hydrogen. By running the same test conditions with different fuel compositions, the effect of the fuels was isolated and examined. In all cases the primary metric measured was the octane number of gasoline supplied to the engine at the onset of audible knock.

2.1 Experimental Procedure

Before defining the operating conditions that were investigated, the procedure used to acquire the data is outlined.

Step 1: The operating conditions were established and defined using isooctane (ON 100). This involved determining the appropriate combination of fuel and air to yield the prescribed relative air fuel ratio and torque. Specifications required to define an engine operating condition are: intake manifold air pressure, airflow, fuel flow, intake air temperature, coolant temperature, spark timing, and speed. The spark timing was adjusted for maximum brake torque (MBT).

Step 2: For each operating condition established in Step 1, the octane number of primary reference hydrocarbon fuel supplied to engine was decreased until audible knock - the point where knock just becomes audible - occurred. This involved multiple tests run with the octane number of the hydrocarbon fuel decreasing by approximately two numbers for each successive run. Between fuel changes, the engine was motored and the fuel lines purged. Once the new fuel was supplied, it was necessary to return precisely to the operating condition that was being tested. Before the measurement (determination of knock) was made, the engine's operating conditions were recorded to make sure that all parameters were set as specified. This method presumes that the combustion characteristics do not significantly change with different mixtures of primary reference fuels, therefore the same operating condition specifications defined in step 1 are suitable to use over the range of different fuels.

2.2 Lean Operating Conditions

The first group of experiments investigates the octane number requirement trends with lean operation. To understand the trends with lean operations, these sets of data were collected:

- lambda sweep at constant inlet pressure
- lambda sweep at constant fuel flow
- lambda sweep at constant NIMEP
- inlet pressure sweep at constant lambda

To explore the octane number requirement of different engine torque or NIMEP outputs, the lean tests were carried out at high and low load.

Some parameters that are known to affect knock, such as the temperatures of the intake air and the engine fluids, were held constant for all of the tests. Speed variations were not considered in this study because the knock trends with speed are well understood. At each condition, MBT spark timing was used.

Table 2-1 Experimental test matrix for mid-load operation with primary reference fuel.

Operation Points	Parameter Varied	Parameter Held Constant
Series 1 (4 data points)	Lambda = 0.95, 1.1, 1.3, 1.5	NIMEP ≅ 6.7 bar
Series 2 (4 data points)	Lambda=0.95, 1.1,1.3,1.5	Intake Pressure ≅ 0.9 bar
Series 3 (4 data points)	Lambda=0.95, 1.1,1.3,1.5	Fuel IPW[1] = 8.8ms
Series 4 (3 data points)	Intake Pressure = 0.8, 0.9 bar, and WOT	Lambda=1.5

Table 2-2 Experimental test matrix for high-load operation with primary reference fuel.

Operation Points	Parameter Varied	Parameter Held Constant
Series 5 (4 data points)	Lambda = 1.1, 1.3, 1.5, 1.7	NIMEP ≅ 8.5 bar
Series 6 (4 data points)	Lambda=1.1,1.3,1.5, 1.7	Intake Pressure ≅ 1.1 bar
Series 7 (4 data points)	Lambda=1.1,1.3,1.5, 1.7	Fuel IPW= 10.89ms
Series 8 (3 data points)	Intake Pressure = 1.1bar, 1.2bar, 1.3bar	Lambda=1.5

[1] Injection Pulse Width (IPW) is an injector-specific metric, which indicates the length of time the injector orifice is open.

2.3 Plasmatron Reformate and Hydrogen Addition

To explore the knock behavior of primary reference fuels enhanced with hydrogen and carbon monoxide, points from the first experiment were repeated with the plasmatron reformate and hydrogen addition. The lambda sweep at constant load is considered the most important because it represents a lean-burn engine replacing a conventional stoichiometric-operated engine. Therefore, these test series for both high and mid-load were completed with the novel fuels to determine if the hydrogen or plasmatron reformate mixture had an influence on knock.

The definition of the plasmatron reformate fraction is related to its application on an actual vehicle. In these experiments, lambda is defined for the entire system as depicted in Fig. 2-1 and Eq. (2-1)-(2-2). The fraction of the gasoline fuel by mass directed to the plasmatron is referred to as the "plasmatron fraction," shown in Eq. (2-3).

Since the plasmatron gas includes hydrogen and carbon monoxide, separate tests were completed with pure hydrogen to isolate the effect of hydrogen alone. In the hydrogen-only experiments, the fraction of energy derived from the hydrogen matched that in the plasmatron experiments. Tables 2-3 and 2-4 show how this was done.

Table 2-3 Experimental test matrix for high and mid-load operation with plasmatron reformate-enhanced primary reference fuels.

Relative Air/Fuel Ratio	0% Plasmatron Fraction *0% energy from H_2* *0% energy from CO* *0% energy loss in reformer*	15% Plasmatron Fraction *~5.5% energy from H_2* *~7% energy from CO* *2.5% energy loss in reformer*	30% Plasmatron fraction *~11% energy from H_2* *~14.5 energy from CO* *4.5% energy loss in reformer*
1.1, 1.3, 1.5	Mid-Load (NIMEP≅6.7 bar)	Mid-Load (NIMEP≅6.7 bar)	Mid-Load (NIMEP≅6.7 bar)
1.1, 1.3, 1.5, 1.7	High-Load (NIMEP ≅8.5 bar)	High-Load (NIMEP ≅8.5 bar)	High-Load (NIMEP ≅8.5 bar)

Table 2-4 Experimental test matrix for high and mid-load operation with hydrogen enhanced primary reference fuels.

Rel. Air/Fuel Ratio	0% Energy from H2	~5.5% Energy from H2	~11% Energy from H2
1.1, 1.3, 1.5	Mid-Load (NIMEP ≅6.7 bar)	Mid-Load (NIMEP ≅6.7 bar)	Mid-Load (NIMEP ≅6.7 bar)
1.1, 1.3, 1.5,1.7	High-Load (NIMEP ≅8.5 bar)	High-Load (NIMEP ≅8.5 bar)	High-Load (NIMEP ≅8.5 bar)

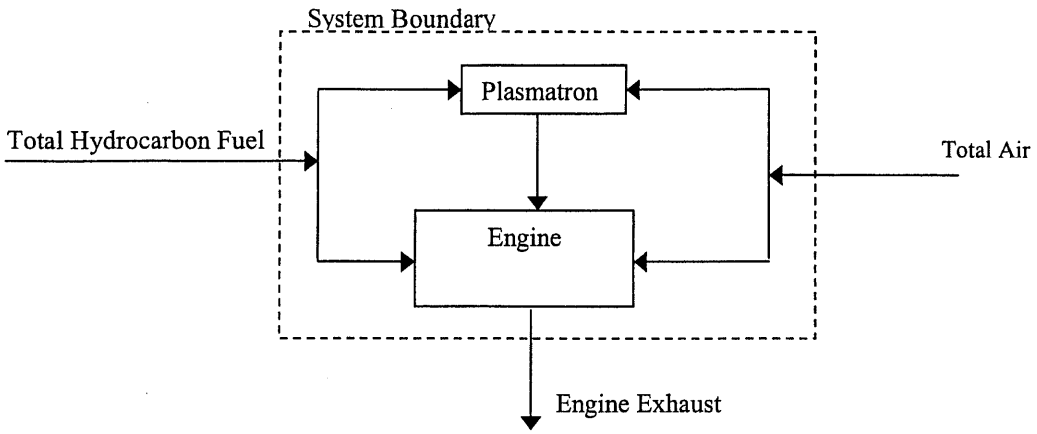

Fig. 2-1 **Plasmatron engine schematic depicting air and hydrocarbon fuel flows. System boundary is shown by dashed line.**

$$\lambda_{system} = \frac{AFR_{actual}}{AFR_{stoichiometric}} \qquad \textbf{Eq. 2-1}$$

$$\text{Air Fuel Ratio} = AFR = \frac{\dot{m}_{\text{air total}}}{\dot{m}_{\text{fuel total}}} \qquad \textbf{Eq. 2-2}$$

$$\%\ \text{Plasmatron Fraction} = \frac{\dot{m}_{\text{HC into Plasmatron}}}{\dot{m}_{\text{HC into Plasmatron}} + \dot{m}_{\text{HC into Engine}}} \qquad \textbf{Eq. 2-3}$$

2.4 Engine Setup

The base engine used in this study is a single-cylinder Ricardo Hydra MK III. The engine cylinder head has been replaced with a B5254 Volvo to better represent current engines. The spark plug is located in the center of the pentroof combustion chamber. There are four valves, which are actuated by belt-driven dual overhead camshafts. Turbulence is increased with a charge motion control plate in the intake port as described by Tully [3]. The complete specifications of the engine are shown in Table 2-5.

2.4.1 Engine Specifications

Table 2-5 Specifications for Volvo-Ricardo research engine.

Displaced Volume (cm^3)	487
Clearance Volume (cm^3)	54
Bore (mm)	83
Stroke (mm)	90
Con Rod Length (mm)	158
Compression Ratio	10.1
Valve Timing:	IVC 60° ABDC; IVO 0° ATDC
	EVC 8° ATDC; EVO 68° BBDC

2.4.2 Dynamometer

The engine crankshaft is directly coupled to a 6000 series EATON dynamometer. The air-cooled, 3-phase electric dynamometer has the ability to motor the engine or absorb power and maintain a user-specified engine speed while the engine is firing. The steady state capacity of the dynamometer is 50 HP. The dynamometer gives a rough brake output. However, this measurement did not provide the accuracy needed for data collecting and it was used to determine approximates engine loads only.

2.4.3 Engine Control Unit

The engine ignition timing and fuel injection is controlled by a MoTeC M4 engine controller. The engine operator controls engine operation by adjusting spark timing and injector pulse width. Other critical parameters specified by the engine control system are injection timing (end of injection is set to 385 CA Deg ATDC) and coil dwell time (4 ms).

2.4.4 Air Intake System

Air can be supplied from ambient or from an Atlas Copco air compressor. The compressor supplies air to a large buffer tank at 60 psi. The air is then routed into the test cell via a PCV pipe. It is regulated to 2 bar before entering the engine pneumatic damping tank. The damping tank upstream of the throttle is used to minimize pressure pulsations throughout the system. With the damping tank holding 2 bar air, the throttle can be used in the conventional fashion.

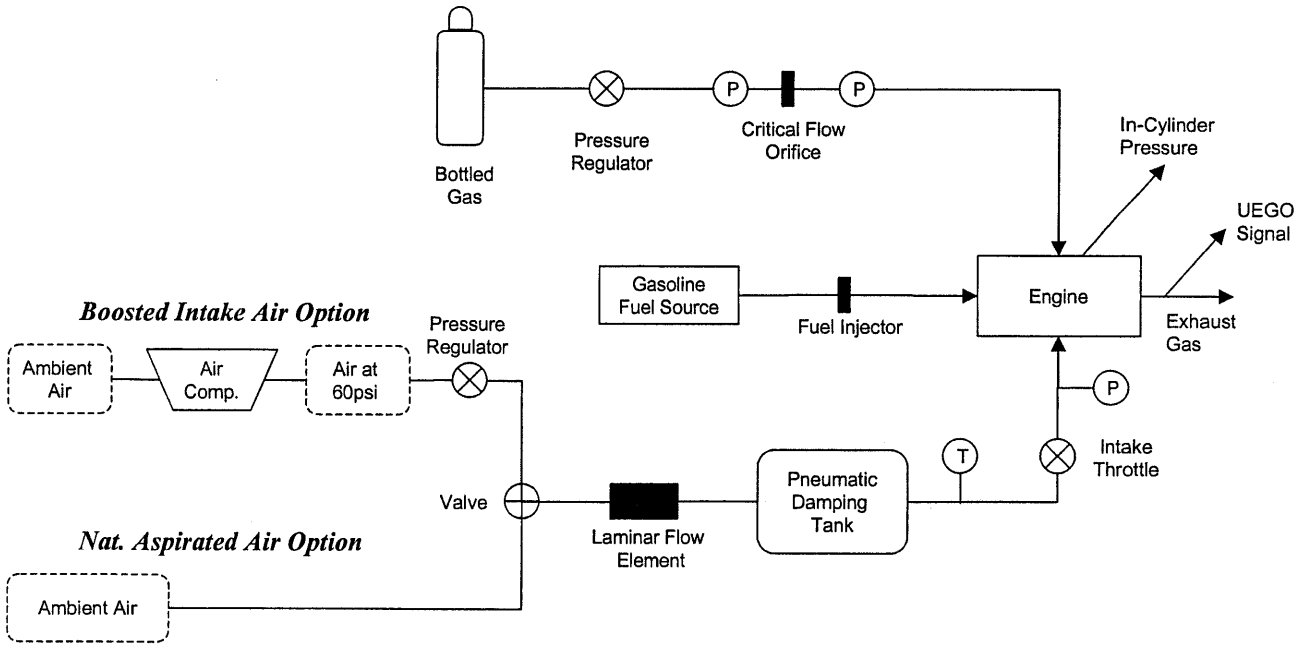

Fig. 2-2 Engine instrumentation and air intake system showing simulated boosted and natural aspirated systems.

2.5 Engine Control and Measurement

The nature of the octane number requirement tests required establishing the specifications for a given operating condition, and then returning to that precise operating condition with each successively decreasing octane fuel. Since the supply fuel needed to be interrupted for the fuel change, the engine had to be motored during the fuel changes. After the new fuel was installed, it was necessary to return accurately to the same operating condition with each successive fuel. Overall, an operating condition is defined by the relative air/fuel ratio, the net indicated mean effective pressure and the fuel composition (meaning relative proportions of hydrocarbon fuel, H_2, and CO). The independent variables that the operator adjusts are inlet pressure, fuel flow rate (gasoline, and plasmatron gas or hydrogen). Engine speed was always held at 1500 rpm.

2.5.1 Intake Air (Volume, Pressure, Temperature)

The amount and the properties of air entering the engine are critical parameters to control and monitor. A butterfly valve throttle controlled with a stepper motor controls the flow of air. The air pressure after the throttle is measured by an Omega pressure sensor (PX 176, 0-50 PSI range). The volume of air that is pulled into the engine is monitored by a Ricardo Viscous Flow Air Meter (laminar flow element), which measures the volumetric flow of the air entering the baffle from the pressure drop across a laminar flow. The pressure differential across the meter is measured by an Omega PX140 differential pressure sensor. This sensor can read extremely small pressure differentials (0-1 psi), yet withstand elevated line pressures up to 20 psi gage. The mass flow rate of air is calculated from the volume flow rate using the temperature and pressure of the air, as measured in the baffle, to obtain the density.

These measurements specify the mass and the temperature of the air entering the engine. Although the humidity of the atmospheric air was measured, it is not clear how the compressor influences humidity. Since humidity changes the knock behavior, all tests were completed while the ambient conditions were approximately 20° C with a relative humidity less than 40%.

2.5.2 Engine Fluids Temperatures

The coolant temperature was held constant at a warmed-up condition for all tests. An inline heater is used to raise the coolant temperature at engine startup, or when overcooling takes place. When the coolant becomes too warm, it is cooled by city water in a fluid-to-fluid heat exchanger. The flow of the cold [city] water is maintained with a temperature sensitive valve. With these heating and cooling measures,

the temperature of the coolant is automatically kept at 88-90°C , without continuous manual adjustment. The oil temperature is not controlled, but under warmed up conditions will be nearly the same as the coolant temperature.

2.5.3 Gasoline Flow Rate

The amount of fuel supplied is well controlled and repeatable. The fuel injector used is a single hole injector. The liquid fuel flow rate is determined by the injection pulse width, characterized by length of time the injector orifice is open. Pulse widths in this project range from 5-10 ms. The fuel in the supply lines is pressurized relative to the intake manifold pressure. As a result, the pressure drop across the orifice is constant, and the mass flow is only a function of the duration that the orifice is open. The injector was calibrated by measuring the mass of fuel injected when firing the injector for a set number of times at a given pulse width. The fuel mass flow was linearly related to the injection pulse width.

2.5.4 Gaseous Fuel Flow Rate

For some experiments, gaseous fuels, hydrogen and synthetic plasmatron reformate, were supplied to the engine. The gaseous fuel is introduced at the engine's intake port entrance. To control the flow rate of the plasmatron gas and the hydrogen, which are supplied from high-pressure bottles, a critical flow orifice was used. The mass flow rate for a critical flow orifice is proportional to upstream pressure only, when the flow is choked. The upstream pressure was controlled with a regulator on the high pressure gas bottle. The range of upstream pressures was kept well above twice the downstream pressure (MAP pressure) to ensure choked flow. The manufacturer of the orifices provided calibration tables supplying the volume flow rate of air at standard temperature and pressure for a given upstream pressure. From this information, the mass flow of any gas was determined as a function of upstream pressure.

2.5.5 Lambda Measurement

A wideband Horiba MEXA-110 λ Universal Exhaust Gas Oxygen (UEGO) meter was used to measure the equivalence ratio. The mass ratio of fuel to air was also calculated and compared to the reading. Agreement to within 3% was reached for all tests indicating that the measurements of air and fuel are well regulated.

2.5.6 In-Cylinder Pressure Measurement

In-cylinder pressure measurement was the most reliable way to determine the indicated performance of an engine. Cylinder pressure was measured with a side-mounted Kistler Model 6125A piezoelectric pressure transducer (SN 1 227847). Before running experiments, the pressure transducer was calibrated with a dead weight tester to verify linearity and establish the scaling factor.

Piezoelectric transducers have the capability to measure changes in pressure very accurately, however, they do not record absolute pressure independently. In order to get an absolute pressure measurement, the pressure signal must be pegged to a known pressure at some point in the cycle. This pegging process was accomplished by processing the data with an MIT Cycle Analysis program [17] [18]. For these experiments, the voltage at bottom dead center (start of compression) was set equal to the intake manifold pressure, which is an absolute pressure measurement.

Since quality of pressure data is of great importance in fundamental combustion tests, efforts were taken to prevent thermal shock. Thermal shock is an effect due to the transducer diaphragm deforming due to thermal strain. This model of transducer has a double diaphragm to protect the transducer against thermal shock. To further reduce any thermal shock, a flame arrestor is placed on the transducer. The output signal from the transducer was sent to a Kistler charge amplifier. The amplified signal was then sampled by a PC based data acquisition system running LabVIEW. During the tests, two data files were collected. "Fast" sampled pressure data was collected at 1000 kHz and used to record knock oscillations. "Slow" pressure data was sampled once per crank angle and processed to calculate indicated engine performance. The trigger for the slow data was provided by a square wave (generated by the shaft encoder) corresponding to once per crank angle. The slow data also contained an additional reference flag at Bottom Dead Center (BDC) compression stroke, which was generated from a camshaft position sensor. Given these signals, the location on the pressure trace could be referenced to a precise piston position. The bottom dead center pulse is superimposed onto the pressure trace to serve as a reference point in the pressure data. In-cylinder pressure data was used to determine indicated engine load, burning characteristics, pressure statistics, and knock characteristics. The pressure data, which was sampled once per crank angle, was processed in the burn rate analysis to perform the calculations and compile the statistics.

2.6 Fuel

Primary Reference Fuels (PRF) are used to define fuel Octane Numbers (ON). The ONR testing needed a range of different octane fuels, and a convenient way to switch from another in such a manner that fuel mixing did not occur, and that large amounts of fuel were not wasted. This section describes the blending method and fuel switching system

2.6.1 Properties and Blending

A range of primary reference fuels was blended with isooctane (ON=100) and n-heptane (ON=0) for this experiment. The ON is defined as the volume fraction of isooctane in a mixture of n-heptane and isooctane, as shown in Eq. (2-4). They were mixed in one-gallon quantities and varied in octane number from 100 to 65, typically in increments of two. The mixing accuracy of the PRF is ± 0.5 ON.

$$ON = \frac{V_{isooctane}}{V_{isooctane} + V_{nheptane}} \qquad \textbf{Eq. 2-4}$$

where V is volume.

2.6.2 Fuel System Design

A fuel system that allowed convenient purging and convenient fuel changes was installed for this study. A schematic is shown in Fig. 2-3. During fuel changes, the fuel pump, fuel injector and spark ignition trigger were turned off and the engine was motored. To purge the current fuel out of the lengthy fuels lines, nitrogen was introduced into the fuel line just downstream of the fuel pump. All of the fuel in the line running *to the engine* and *from the engine* was pushed through the return lines back to the container of fuel. When the return line showed nitrogen returning, the fuel lines were free of fuel. At this point, the one gallon container was removed and the next ON fuel was installed. The fuel pump could be manually controlled to fill the lines in a process where first the old fuel was released from the lines, and next the nitrogen was vented out as the fuel entered. The next steps involved filling the pump and lines with the new fuel. A detailed procedure can be found in the engine test cell.

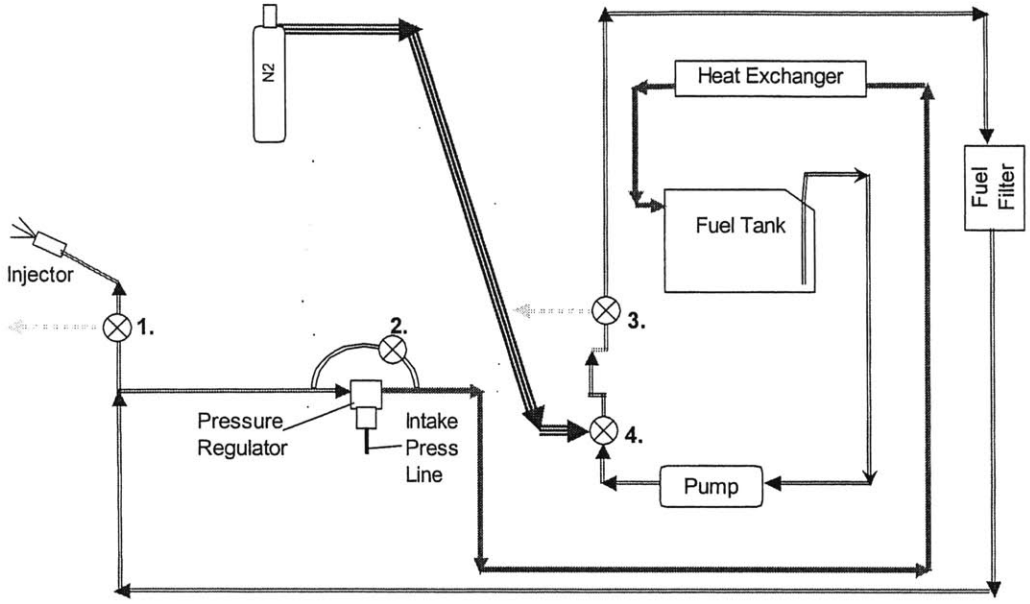

Fig. 2-3 Fuel apparatus schematic illustrating system to purge the fuel lines.

(This page was intentionally left blank.)

Chapter 3 Experimental Results

Audible knock characteristics, Octane Number Requirement (ONR) trends with lean operation, and the impact of H_2 and CO on the knock resistance of fuel mixtures are presented in this section. The knock behavior tests were performed based on the procedure described in Chapter 2. A summary of the specifications required to arrive at a given operating condition is presented in Appendix A. These tables show pertinent information including MBT spark timing, inlet pressure, and fuel regulation parameters. The process of defining these operating conditions was the first step to obtaining data; however, these trends will not be discussed. Operation with lean, hydrogen-enhanced mixtures has been previously explored and discussed by Tully [3].

3.1 Audible Knock Characterization

The ONR is defined as the highest ON fuel where audible knock is detected. Audible knock determination is a traditional way to perform knock experiments, and preferred over other methods to detect knock for this research. A typical knock sensor is not optimal for this study for two reasons:
1.) A typical knock sensor would first need a special calibration for the single cylinder research engine, 2.) A knock sensor can be "fooled" by very fast combustions or preigntion – both of which can occur with hydrogen as a fuel. Another way to do knock tests involves detailed pressure data analysis; however, this method requires unneeded complexity for the knock trends sought in this study. Audible knock is a well-established limit, and was used to acquire the data presented here. The ONR determined and discussed here is that of the hydrocarbon (primary reference) fuel.

Although the main experimental data taken consisted of finding the ONR, a limited amount of fast-sampled pressure data was also taken at each knocking condition to define the audible knock characteristics. Selected data sets were examined to characterize the knock parameters at the audible threshold. An example of a typical set of pressure traces at the audible level is shown in Fig. 3-1. This figure shows that knock is a highly irregular event, which is susceptible to cycle-to-cycle variations in combustion characteristics. Knock Intensity (KI) is a common measure of knock severity; it is often defined as the peak-to-peak magnitude of the filtered pressure data. This fast-sampled, filtered data showed that around half the cycles have a KI of 1 bar or higher. This is similar to what is found by Valtadoros [20].

Much past research has been done to characterize knock in SI engines. While progress has been made, predicting knock characteristics based on pre-knock details of the pressure trace is complex [19].

For later use in the knock prediction model (described in Chap. 5), a manual analysis was done on approximately 100 pressure traces at the audible knock limit. The statistics show that location of peak pressure is a good indication of the cycle's tendency to knock. Fast burning cycles have an early location of peak pressure, causing the end gas to reach a higher maximum temperature and pressure, thus promoting knock. Figure 3-2 shows a typical distribution of location of peak pressure for the pressure traces analyzed. Figure 3-3 illustrates that fast burning cycles, characterized by early location of peak pressure, are more likely to knock (arbitrarily defined as a KI of at least 1 bar). Combining the cycle scatter information, and the link between knock probability and location of peak burning (Fig. 3-4), it can be concluded that at the audible knock limit, an engine cycle with a location of peak pressure which is at least one standard deviation before the average location is likely to autoignite with sufficient intensity to knock.

3.2 Knock Behavior with Lean Operation

A series of tests were completed to map the ONR of the engine under different operating conditions. The series of operating conditions were chosen to examine the effect of lean operation on knock. The trends show the independent effect of inlet pressure and fuel flow; this was done to better understand the trends observed operating the engine under increasingly lean conditions at constant torque output.

3.2.1 General Trends

Figures 3-5 and 3-6 show two ONR "roadmaps." They show how the ONR changes with variations in fuel and air. Both figures show the same trends – but they were carried out at different loads levels. Each node represents an operating condition. The italics number in parenthesis is the experimental octane number requirement. The axes designate the fuel flow, and MAP - which is a good indication of air flow rate.

The vertical line shows that as the fuel flow rate is reduced at a constant inlet pressure, the mixture becomes lean and the ONR decreases. However, the output torque also decreases. Instead of reducing fuel to increase lambda, the opposite approach is to increase the air flow rate and hold the flow of fuel constant. In this case, shown by the horizontal line, the ONR increases, as well as the NIMEP, due to increasing fuel conversion efficiency when operating under leaner conditions.

To achieve constant torque with leaner mixtures, a combination of less fuel and higher intake pressure are required. The ONR under leaning operation with constant torque output is the result of two competing effects – a decrease in the ONR due to less fuel, and an increase in ONR due to higher MAP.

The results show that the ONR for a lean sweep with constant torque output is relatively constant. For a given load, the ONR requirement increases slightly as lambda increases above approximately 1.2. The last set of data included is a series of points at constant lambda at a range of pressures. This shows that the knock behavior of a lean mixture is highly dependent on the intake pressure.

The ONR roadmaps are good for evaluating how and why the ONR changes with lean operation at constant torque. However, to map ONR over a wider range of operation, additional data were needed. Extra data points were tested for areas of operation not covered by the roadmaps described above. The entire set of additional points was completed with air supplied from the laboratory compressor. The data presented hereafter are a compilation of all the data.

3.2.2 Role of Lambda on ONR

Figure 3-7 shows how the ONR changes as a function of equivalence ratio for a constant inlet pressure. This shows that a fuel leaning by 0.1 lambda results in a reduction of approximately two octane numbers, which roughly compares to trends stated by Russ [22]. This is the trend with which lean operation is often associated; however, it is critical to note the NIMEP decreases along with the ONR. Figure 3-8 shows the decrease in NIMEP associated with these operating conditions. There is a decrease in ONR with increasing lambda, and as the intake manifold pressure is reduced.

3.2.3 Role of Inlet Pressure on ONR

Figure 3-9 presents data along contours of constant lambda. The lines of constant lambda are plotted against MAP and NIMEP. As the MAP rises the NIMEP increases as well. The ONR for each node or operating condition is noted in the symbol. Note that the ONR and NIMEP increase as the inlet pressure is raised. (4-5 increase in ONR per 0.1 bar MAP).

Figure 3-10 generalizes the data from Fig. 3-9 by showing lines of constant ONR and lambda. This illustration answers the question: "Does the knock-limited NIMEP change with lean operation?" From the contours of constant ONR, it is clear that the knock-limited NIMEP decreases slightly as a leaner mixture is burned.

Since the ONR appears to follow clear trends with MAP, lambda, and NIMEP, all the data were put into one graph to show the relationship between these four variables. Figures 3-11 and 3-12 show three-dimensional plots of ONR versus lambda and MAP. The plots resemble a plane with a few deviations. There are two prominent trends which can be visualized by referring to Fig. 3-11: – following a given value of MAP (following a line running left to right on the surface), one can see a side to side tilt

that shows the decrease in ONR with lean operation at constant inlet pressure. The front to back tilt is associated with the dependence of ONR on MAP, regardless of lambda. Figure 3-12 shows the individual data points as well as contours of constant ONR.

The top view (plan view) of this data is presented in Fig. 3-13. The top view maintains the axis of lambda and MAP. On this graph, the shading corresponds to the ONR in addition; contours of constant NIMEP have been added. The important characteristic to note is that the colors change approximately with the contours of NIMEP, which indicates that the ONR is strongly a function of NIMEP.

3.3 Knock Behavior with Hydrogen and Carbon Monoxide Addition

The next set of data investigates the knock trends when hydrogen and plasmatron reformate gas are added to the gasoline. Seven of the original data points, comprised of lambda sweeps at two different loads, were repeated with different fuel mixtures. Two types of fuel mixtures were tested: 1.) Gasoline with plasmatron reformate and 2.) Gasoline with H_2 addition, each with two mixture fractions. The hydrogen addition tests matched the H_2 energy fraction corresponding to the plasmatron cases. While completing these tests, the ONR of the engine is presumed to be unchanged at the same NIMEP and speed. Plasmatron reformate and H_2 improve the ON of the fuel mixture; hence, the ON of the primary reference fuel at audible knock can be reduced.

Figures 3-14 and 3-15 show the ON of the PRF at the onset of audible knock of the seven operating conditions with two plasmatron fractions, 15% and 30%. The gasoline-only case is shown for a baseline reference. This is taken to be the engine ONR at a given load, lambda, and speed, since it was measured with traditional primary reference fuels. In the case where H_2 + CO + N_2 are added to the mixture, the ON of the primary reference fuel, or base fuel, at the audible knock limit decreases. Over the range tested, the decrease in the ON of the PRF is nearly linearly for increasing plasmatron fractions. The equivalent graphs for hydrogen addition are shown in Figs. 3-16 and 3-17. This shows a similar trend – that a lower octane number of base fuel is required to reach the audible knock limit when part of the engine fuel energy is from H_2.

Since the base fuel ON reduction at audible knock is relatively consistent for all loads and air/fuel ratios, Figs. 3-18 - 3-20 were created to compare the effect of adding plasmatron gas and hydrogen for each operating condition. Each figure consists of a series of lines; there is one line for each operating condition. The lines represent the decrease in ON of PRF at audible knock for a fixed engine load (NIMEP), lambda, and speed as the plasmatron reformate fraction or H_2 fraction is increased.

For the plasmatron reformate addition, the ON of the PRF at knock decrease is defined as the difference in hydrocarbon ONR at the onset of knock when running primary reference fuels only versus the ON of PRF at audible knock when running with PRF and plasmatron reformate. A similar subtraction is done to find the decrease in ON of primary reference fuel at the knock limit for the H_2 addition cases.

Figures 3-18 and 3-19 illustrate that the decrease in the ON of PRF at knock goes up for higher plasmatron reformate fractions. The advantage with plasmatron gas seems to be independent of lambda and load since there is not any clear trend between the different engine operation lines. The data shows that when 15% and 30% of the fuel is converted to H_2 and CO, the octane number of fuel required to reach knock decreases by about 8 ONs and 20 ONs, respectively. A similar but less substantial trend is found with pure H_2 addition, shown in Fig. 3-20. Where the decrease in ON of PRF is plotted versus the fraction of the energy that was derived from hydrogen. For 5% energy from H_2, the ON of hydrocarbon fuel at the audible knock limit is 5 lower than without H_2. For 11% energy from hydrogen, there is a decrease of 10 octane numbers.

By comparing the decrease in ON of PRF at knock with the addition of plasmatron reformate (H_2+CO+N_2) versus the decrease with just H_2, the role of CO can be deduced. Figure 3-21 illustrates the inferred role of CO, based on the simple subtraction at each point. This figure shows that CO contributes about equally to H_2 to lowering the ON of PRF at audible knock.

This section has presented results for the ON of PRF required for audible knock for tests involving lean operation; with and without H_2 and plasmatron reformate addition. The results show that lean operation reduces the ONR when the inlet pressure is fixed and fuel decreased to increase the air/fuel ratio. If torque is maintained at lean operating conditions, the ONR is expected to increase slightly. The testing also illustrates that H_2 and CO have an octane number increasing effect, demonstrated by a decrease in ON of PRF at audible knock when operating with fuel mixtures containing H_2 and plasmatron reformate in addition to the PRFs. The fuel mixtures are described according to the fraction of energy derived from each fuel. In the "H_2-only" tests, 5.5% and 11%of the fuel mixture energy was derived from H_2. The H_2 contributed to the antiknock quality of the fuel; the ON of the PRF could be reduced by 5-10 octane numbers until the onset of knock was reach, compared to the ON of the PRF at knock when no H_2 was present. In the plasmatron reformate testing, 12% and 25% of the mixture energy was derived from the reformate (H_2 + CO). The contribution of both gaseous fuels increased the knock resistance of the mixture, and the octane number of the PRF at audible knock onset was 8-20 octane numbers lower than the octane number when no H_2 or CO was added.

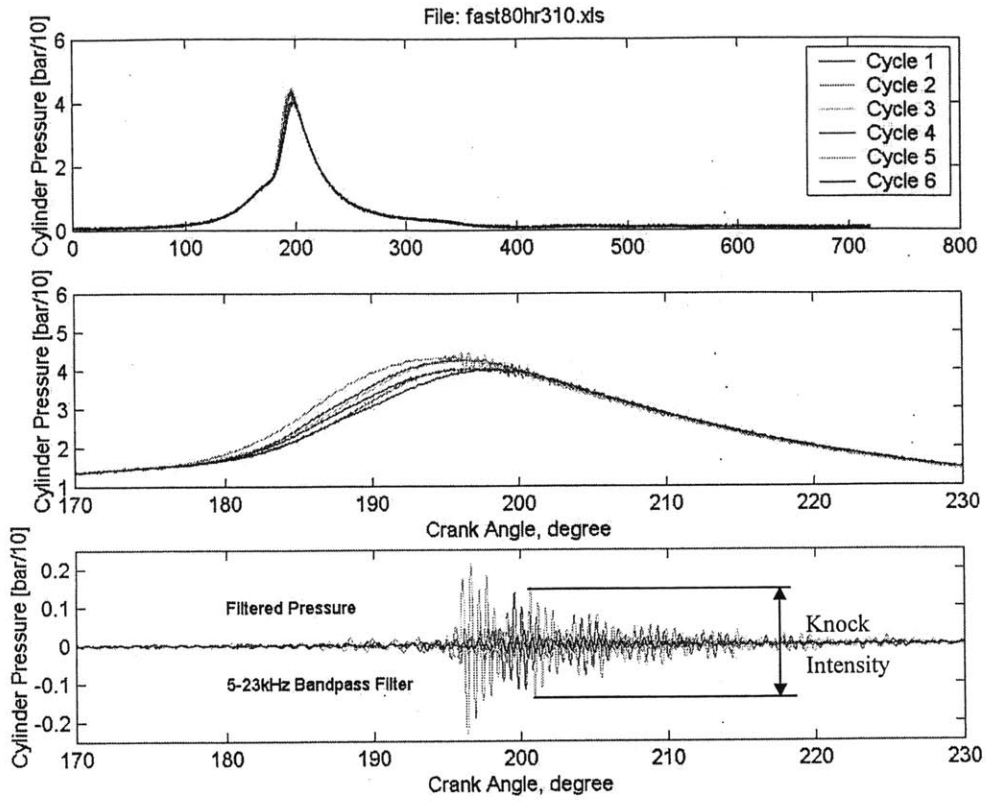

Fig. 3-1 **Typical in-cylinder pressure trace at onset of audible knock. Top graph shows six individual pressure traces (180 deg is TDC). Middle graph is enlarged portion around peak pressure. Bottom graph is the filtered pressure data illustrating the definition of KI.**

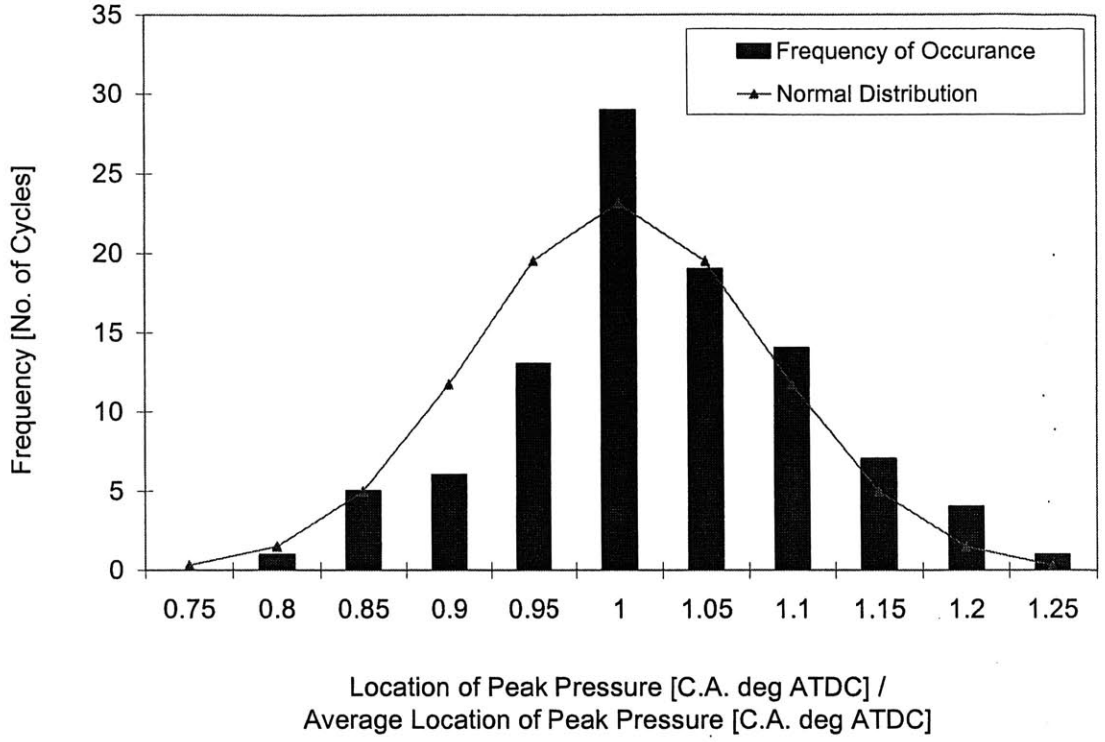

Fig. 3-2 **Distribution of location of peak pressure /average location peak pressure for 100 pressure cycles.**

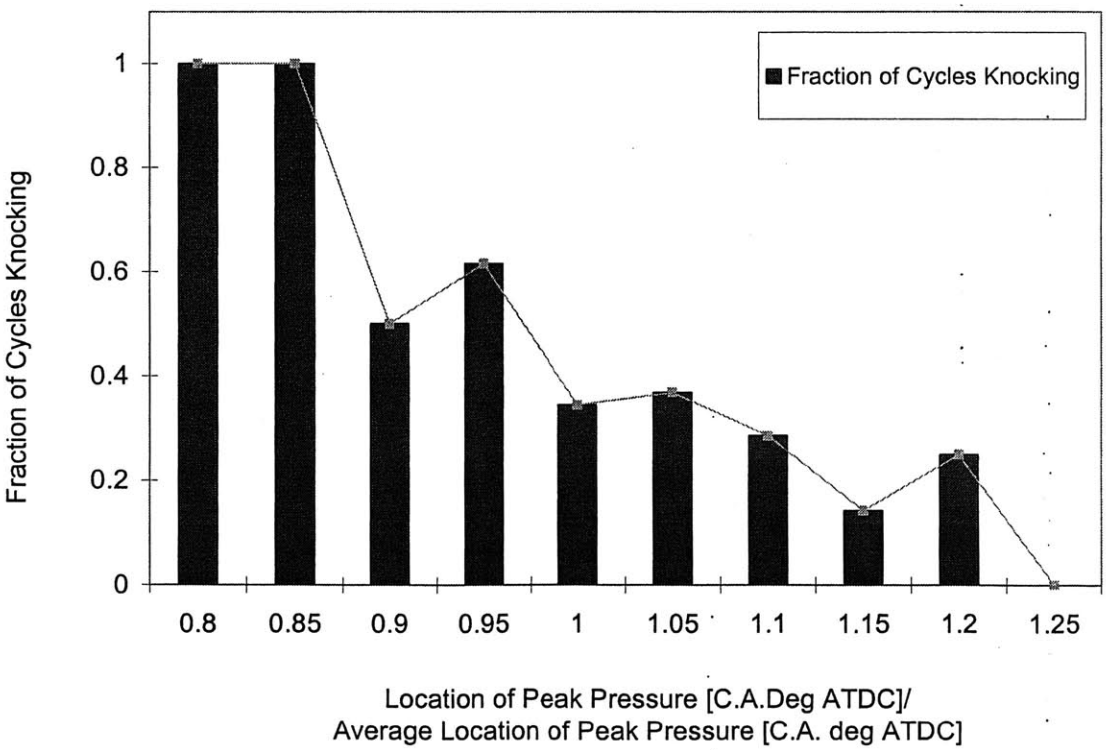

Fig. 3-3 **Frequency of knocking cycles (K.I. > 1 bar) as a function of location of peak pressure.**

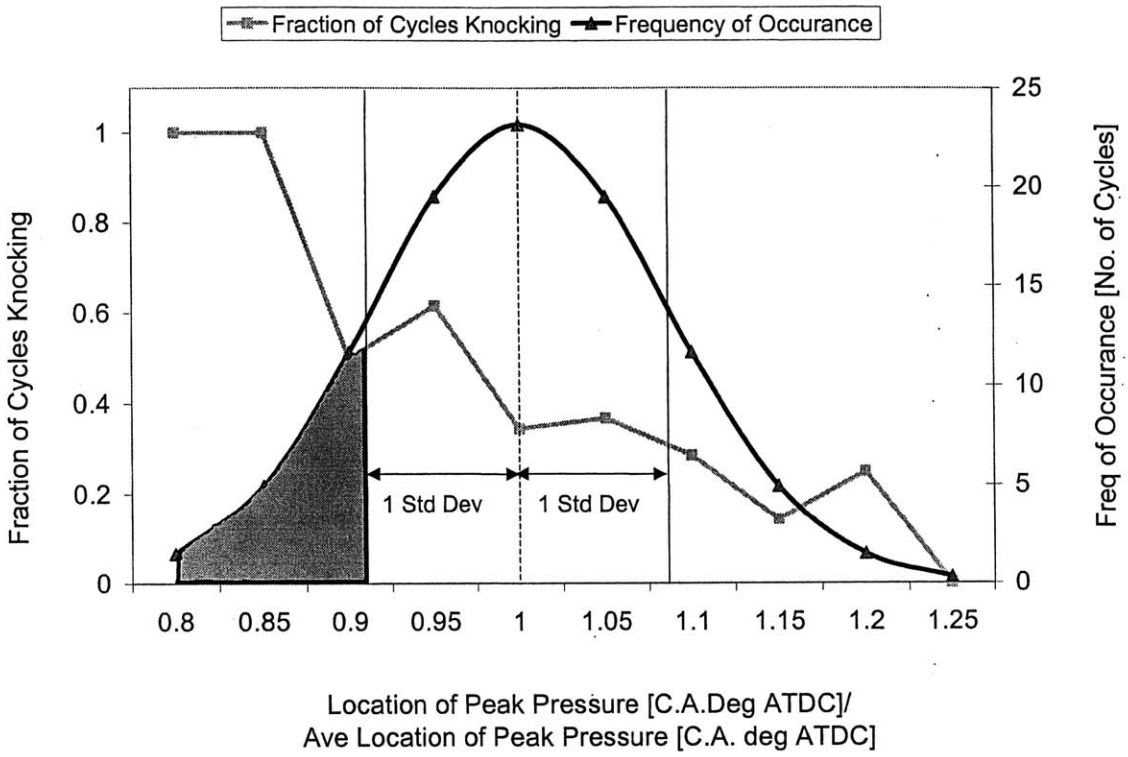

Fig. 3-4 **Pressure cycle selection criteria established by analyzing 100 pressure cycles at audible knock. Shaded area represents the pressure cycles that are most likely to show autoigntion at the onset of audible knock. This graph illustrates why cycles with an early location of peak pressure were chosen as inputs for the engine knock simulation.**

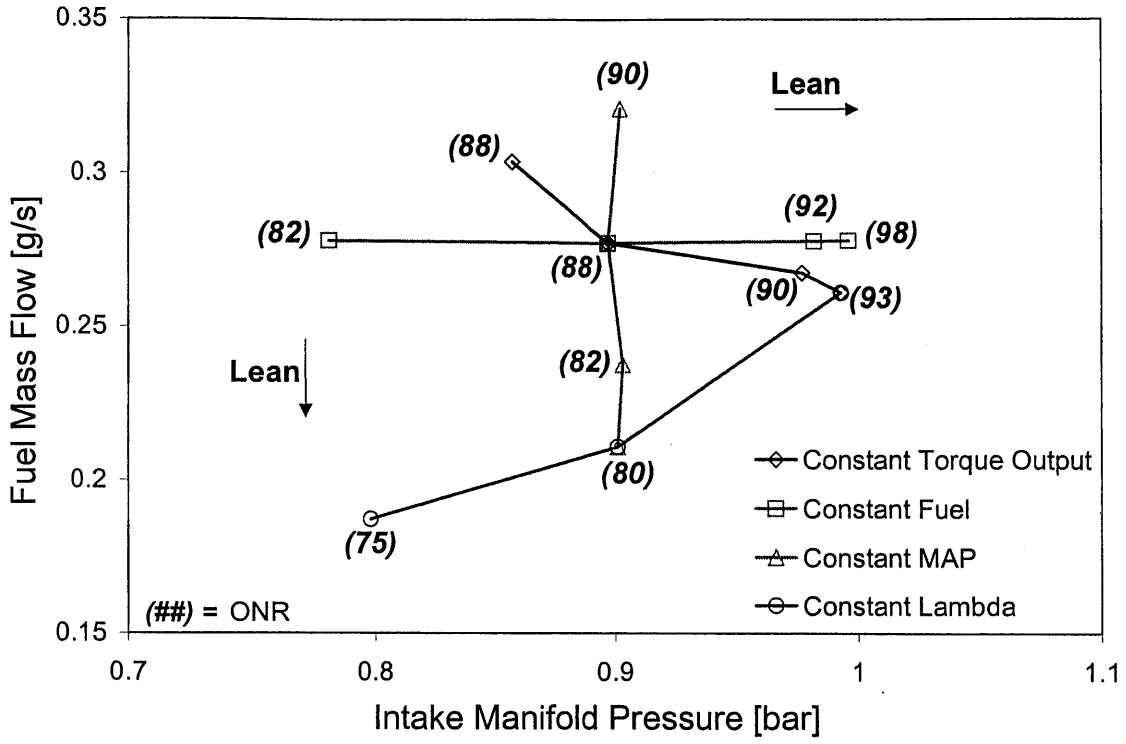

Fig. 3-5 **Octane number requirements determined with primary reference fuels. The constant torque series is 6.7 bar NIMEP.**

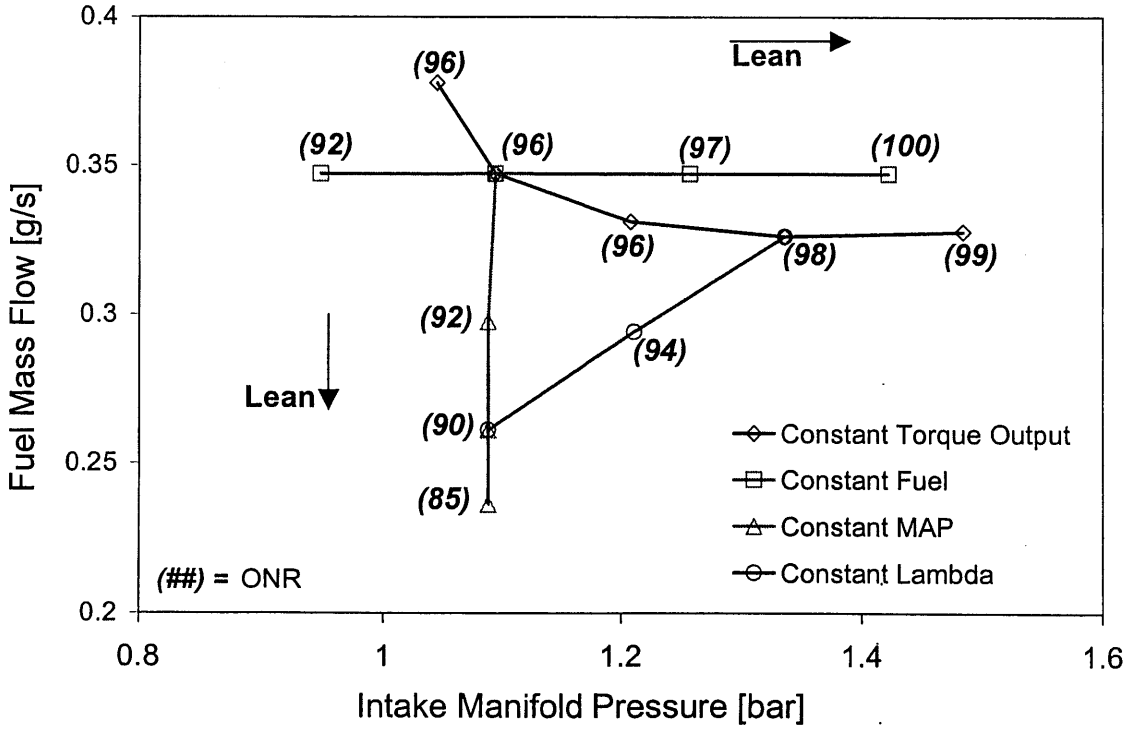

Fig. 3-6 **Octane number requirements determined with primary reference fuels. The constant torque series is 8.5 bar NIMEP.**

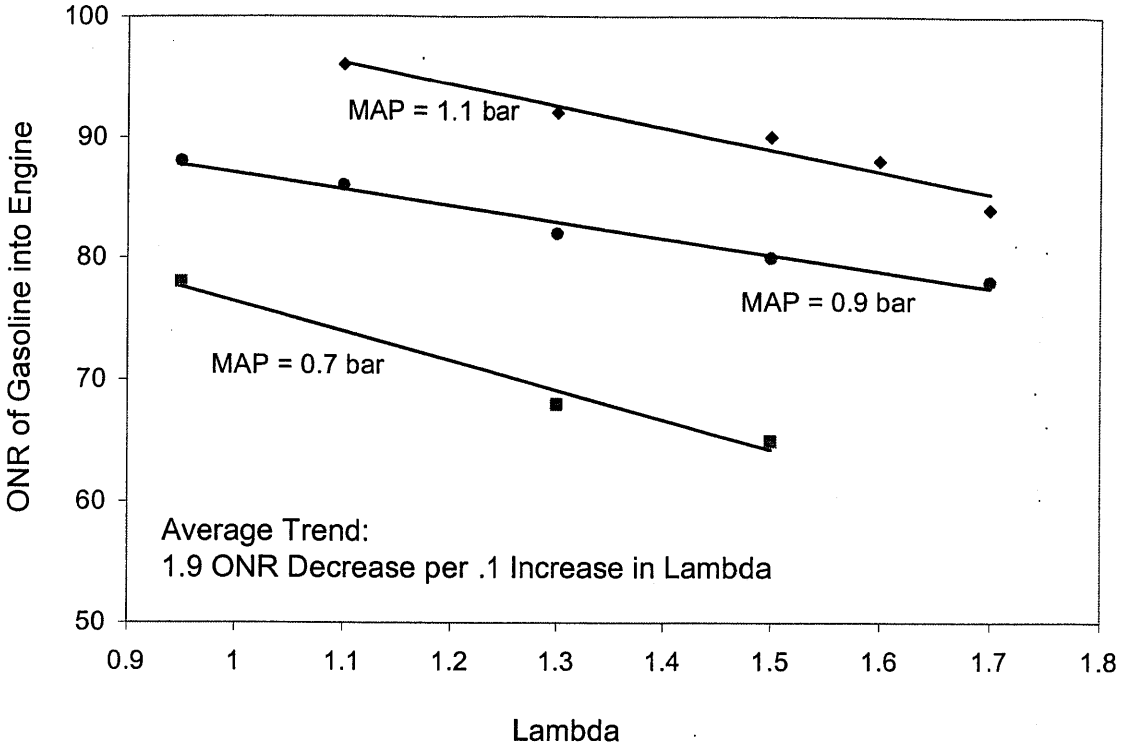

Fig. 3-7 **Experimental ONR trends for lean mixtures at constant intake pressures. This illustrates the dependence of ONR on lambda alone.**

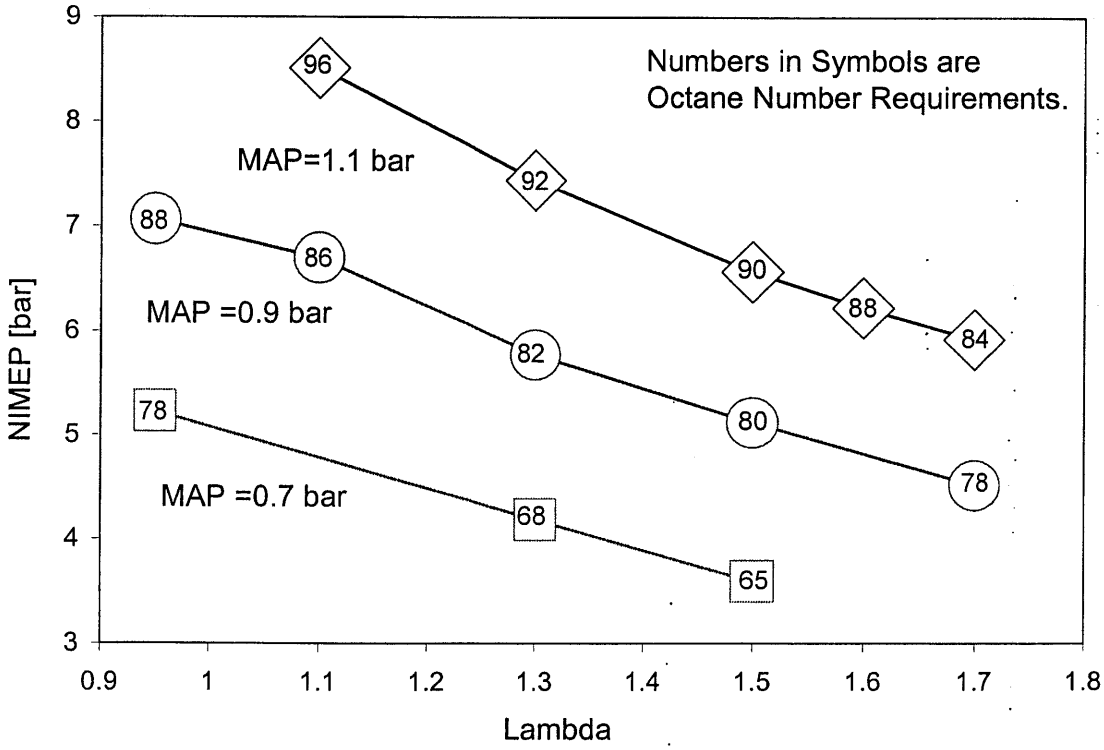

Fig. 3-8 **NIMEP decreases with ONR for a series of points at constant intake pressure and increasing lambda. This illustrates the coupling of NIMEP and ONR.**

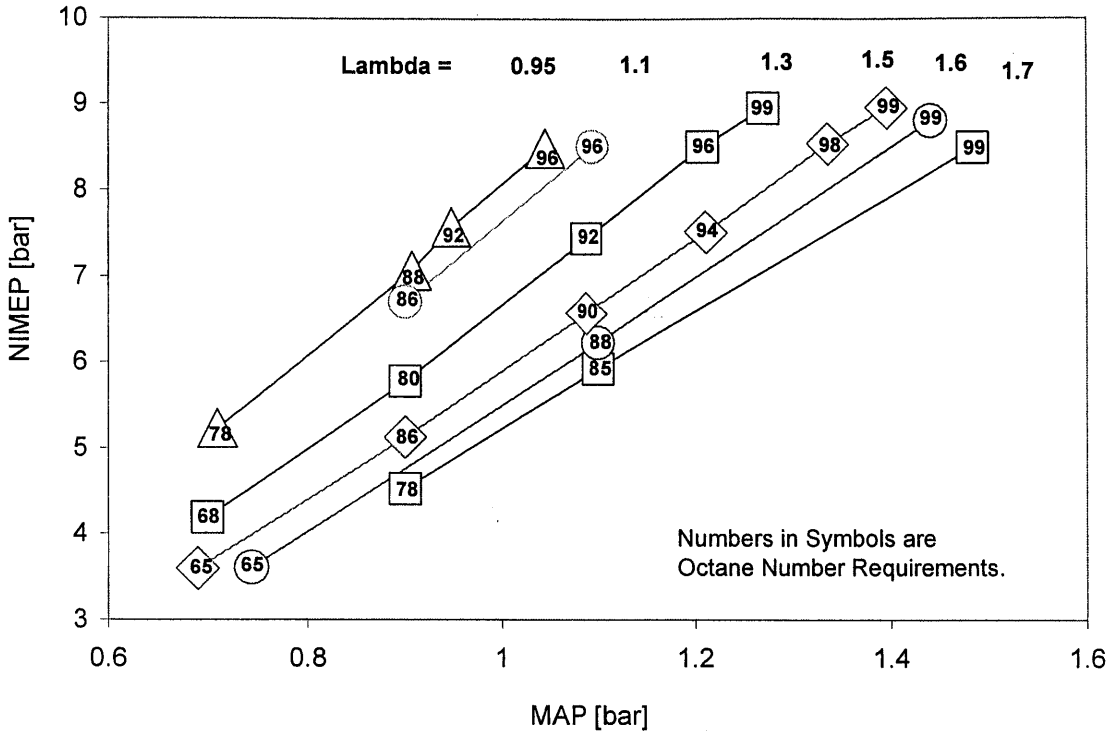

Fig. 3-9 **Experimental ONR trends for increasing manifold air pressure at constant lambda. This illustrates the dependence of ONR on MAP alone.**

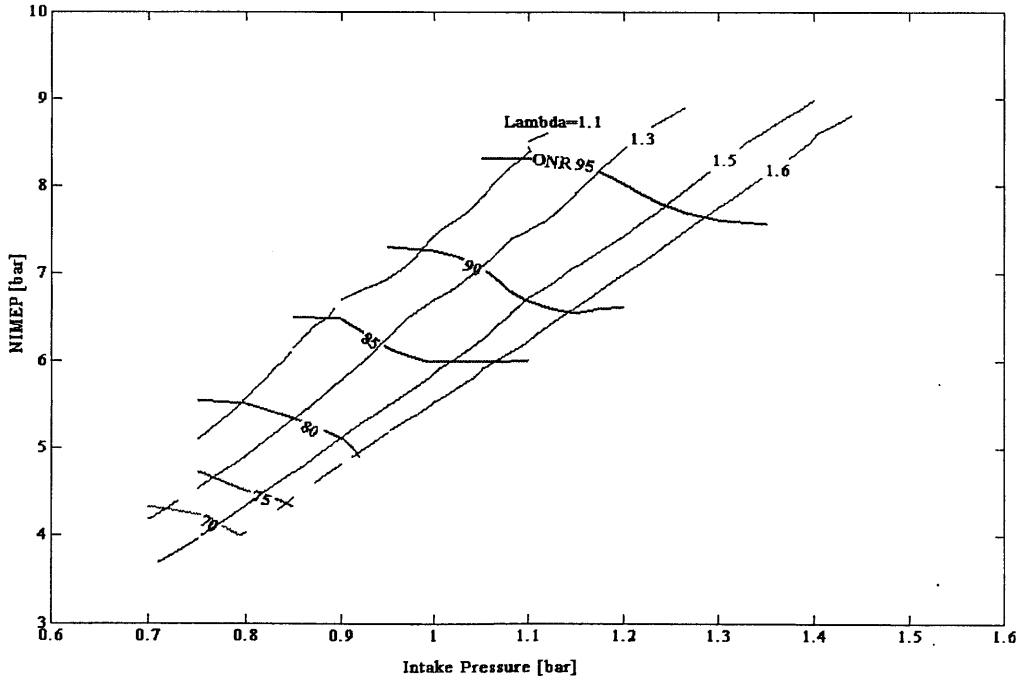

Fig. 3-10 **Contours of ONR and lambda show a slight decrease in knock-limited NIMEP for leaner operation.**

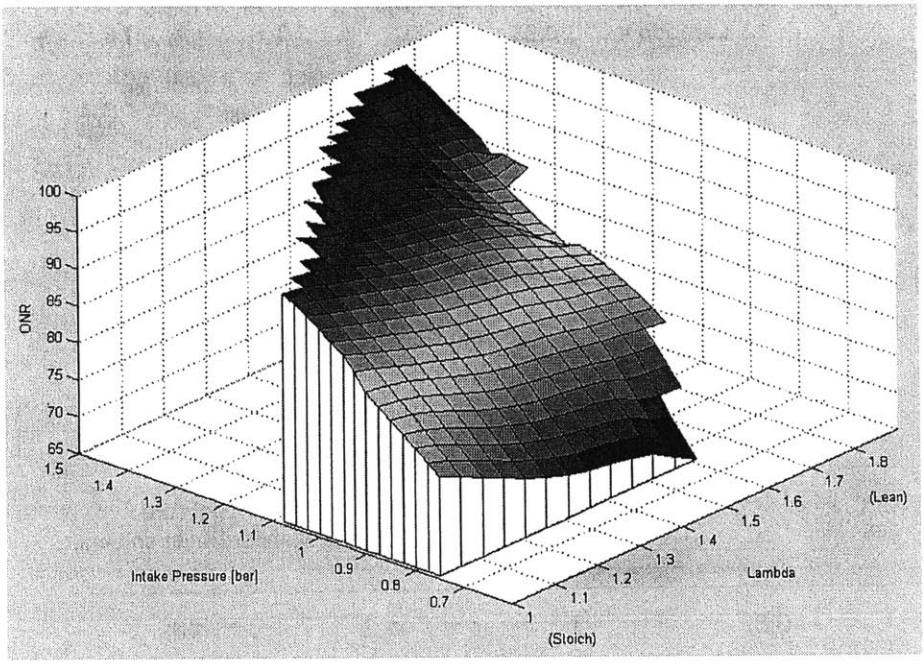

Fig. 3-11 **Three-dimensional surface showing relation between ONR, MAP, and lambda, for data collected with primary reference fuels. Knock resistance increases with lean operation and decreasing intake pressure.**

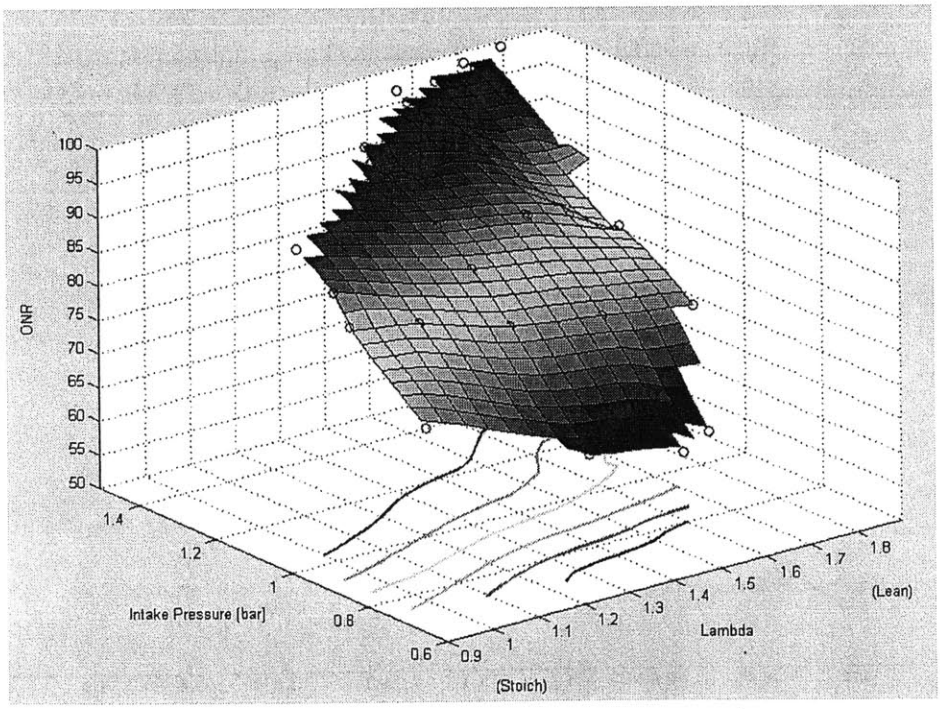

Fig. 3-12 **Three-dimensional surface showing relation between ONR, MAP, and lambda, for data collected with primary reference fuels. Lines of constant ONR are shown on the XY plane. Circles represent actual data points.**

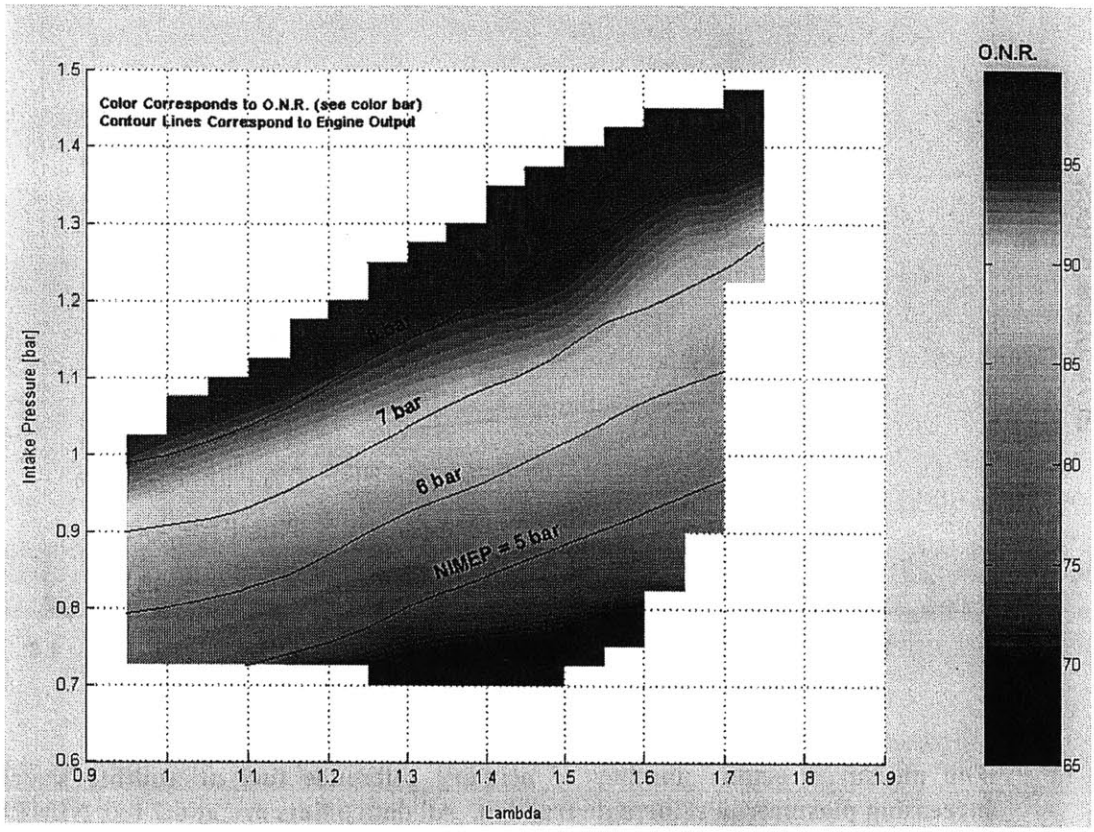

Fig. 3-13 **Top view of three-dimensional surface generated with leaning mixtures of primary reference fuel. Shade represents the ONR. Lines of constant NIMEP show ONR increases with load.**

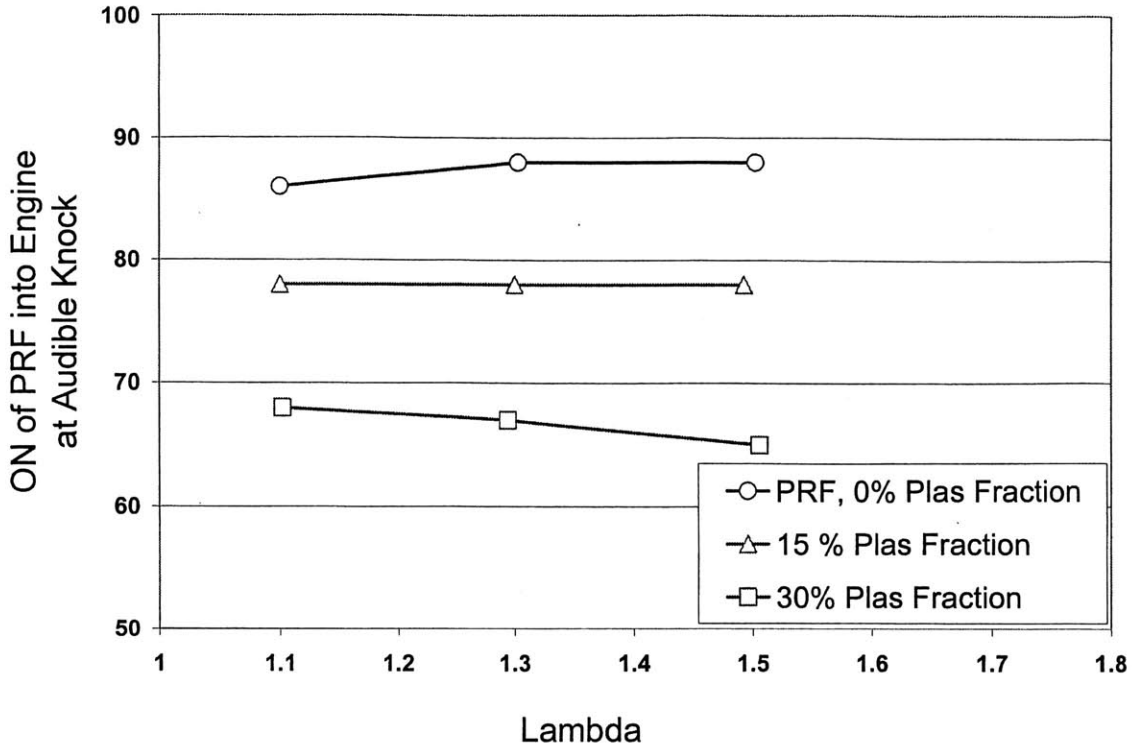

Fig. 3-14 **The measured octane number of primary reference fuel at audible knock with increasing plasmatron reformate fraction. All data points are at 6.7 bar NIMEP.**

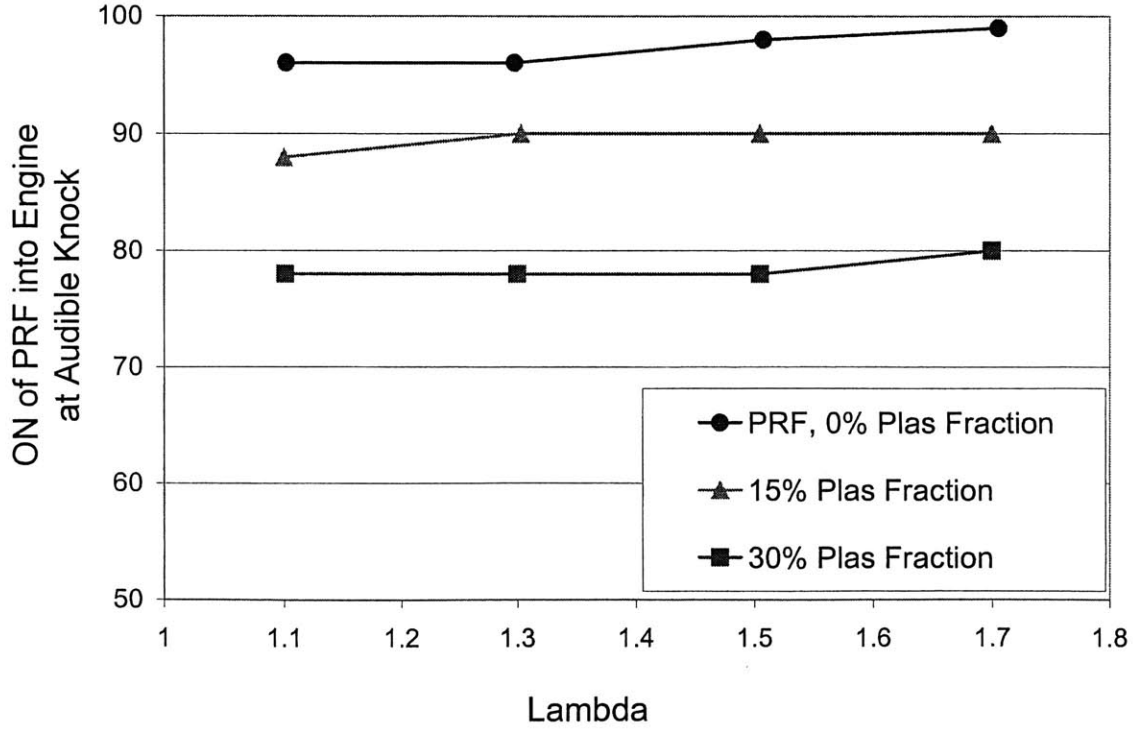

Fig. 3-15 **The measured octane number of primary reference fuel at audible knock with increasing plasmatron reformate addition. All data points are for 8.5 bar NIMEP.**

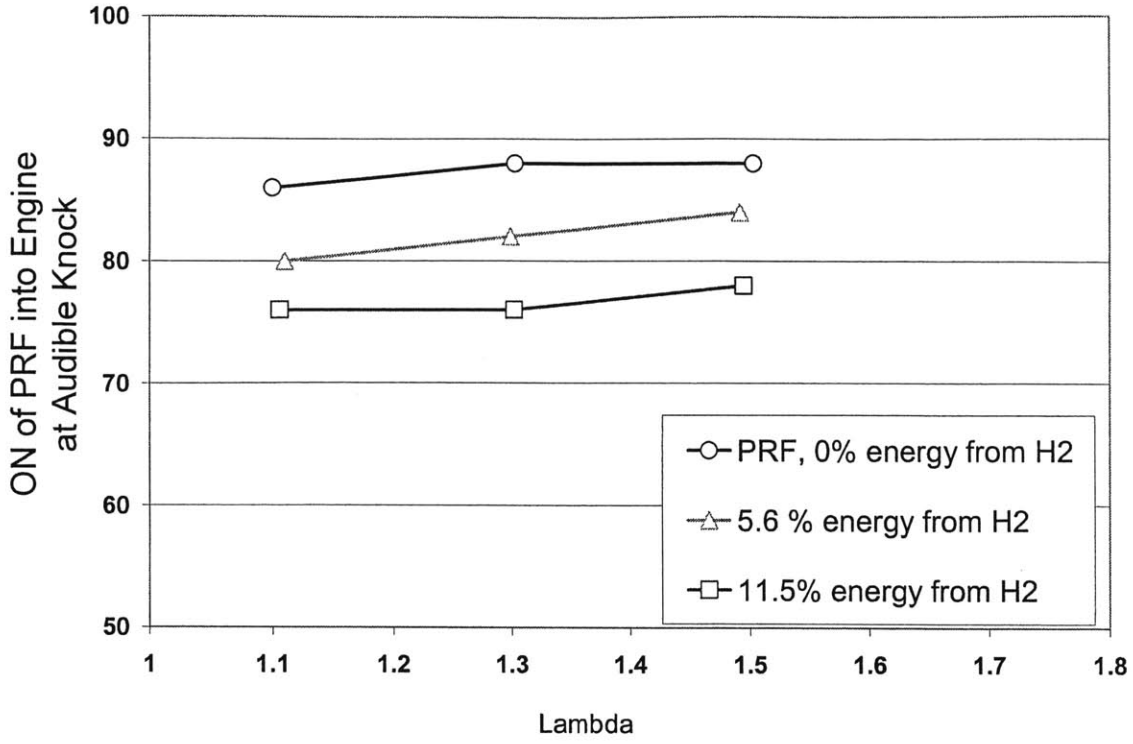

Fig. 3-16 **The measured octane number of primary reference fuel at audible knock with increasing H_2 addition. All data points are 6.7 bar NIMEP.**

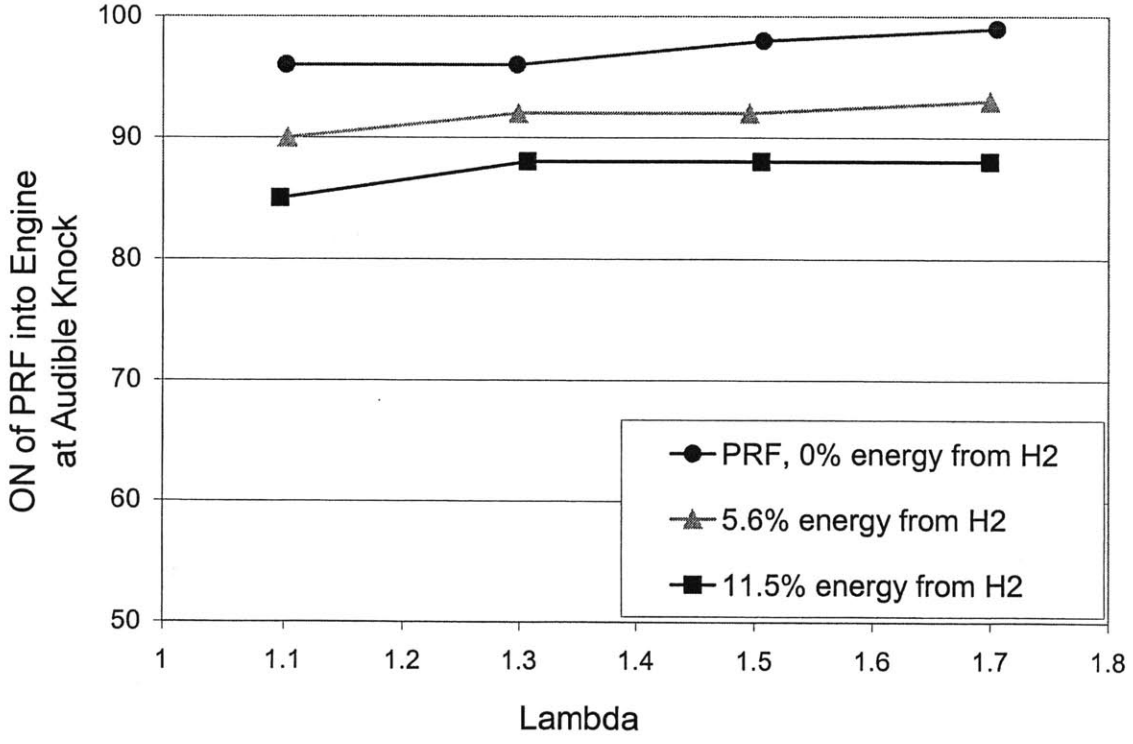

Fig. 3-17 **The measured octane number of primary reference fuel at audible knock with increasing H_2 addition. All data points are 8.5 bar NIMEP.**

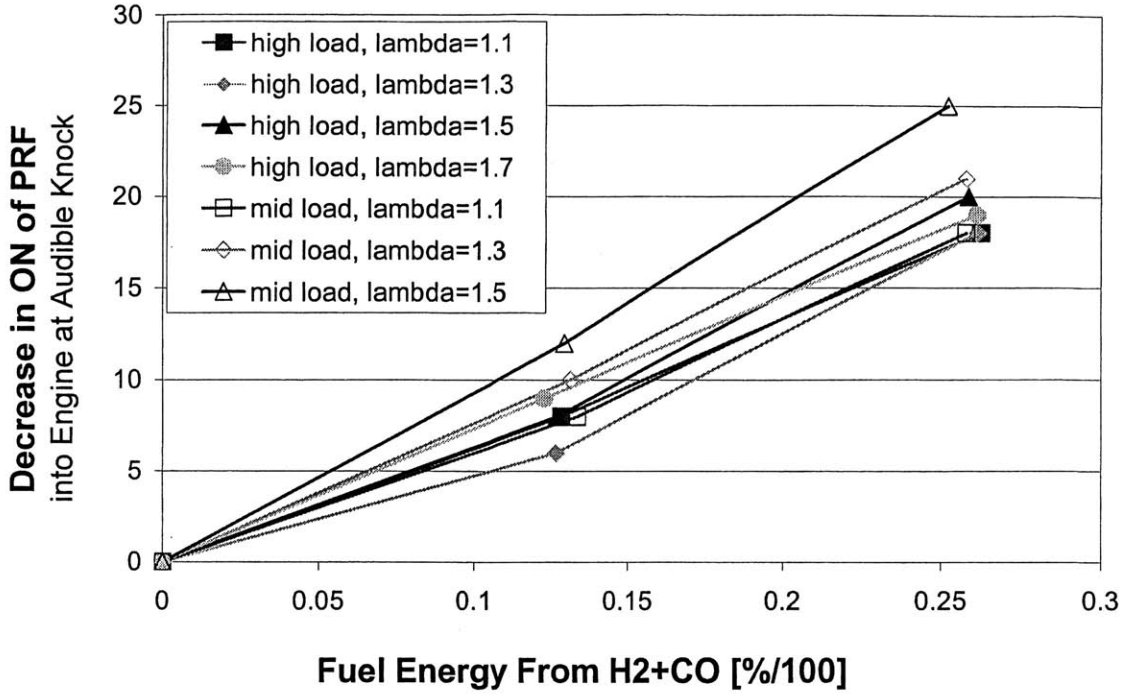

Fig. 3-18 **Decrease in octane number of the primary reference fuel at audible knock with plasmatron addition (0%, 15%, and 30%) for several operating conditions**

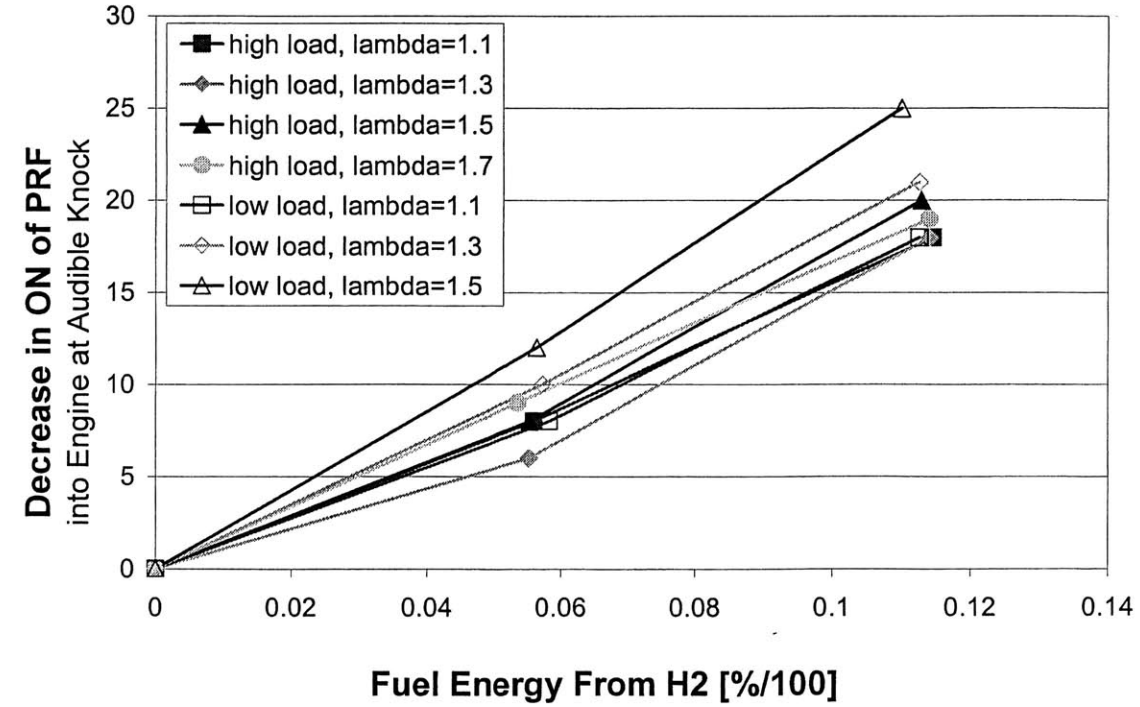

Fig. 3-19 **Decrease in octane number of the primary reference fuel at audible knock with plasmatron addition for several operating conditions. Horizontal axis is the energy fraction from H_2, which is found in 15% and 30% plasmatron reformate fraction.**

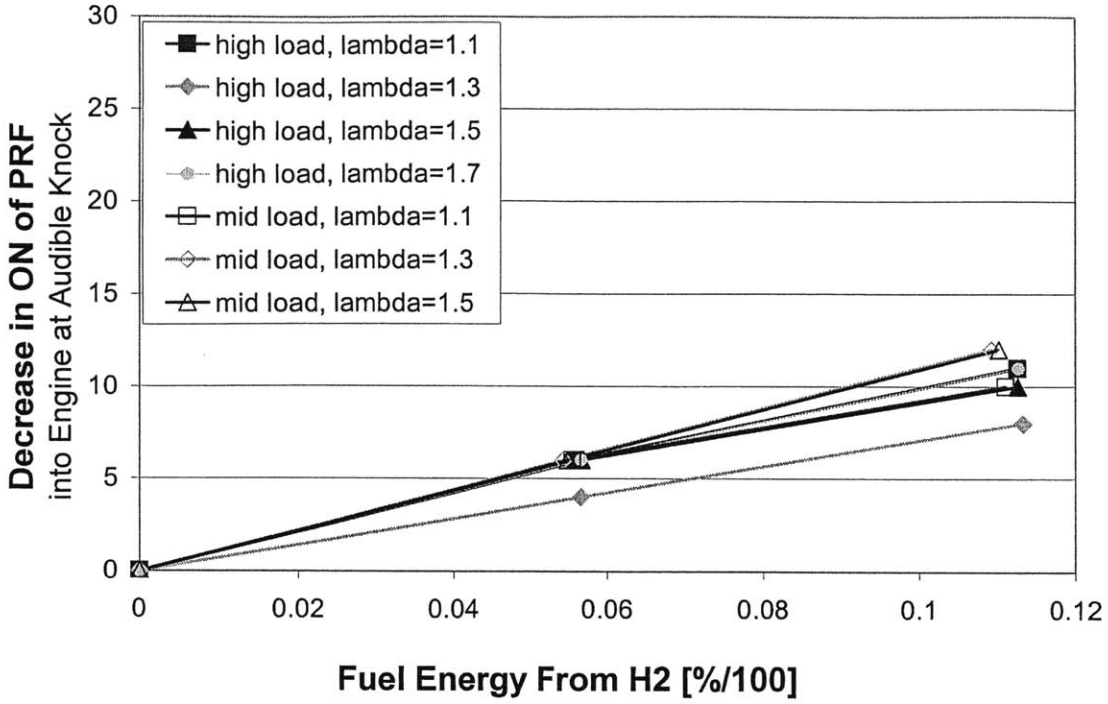

Fig. 3-20 **Decrease in octane number of primary reference fuel with increasing fuel energy from H_2 for several operating conditions. Data shown for the H_2 addition test cases.**

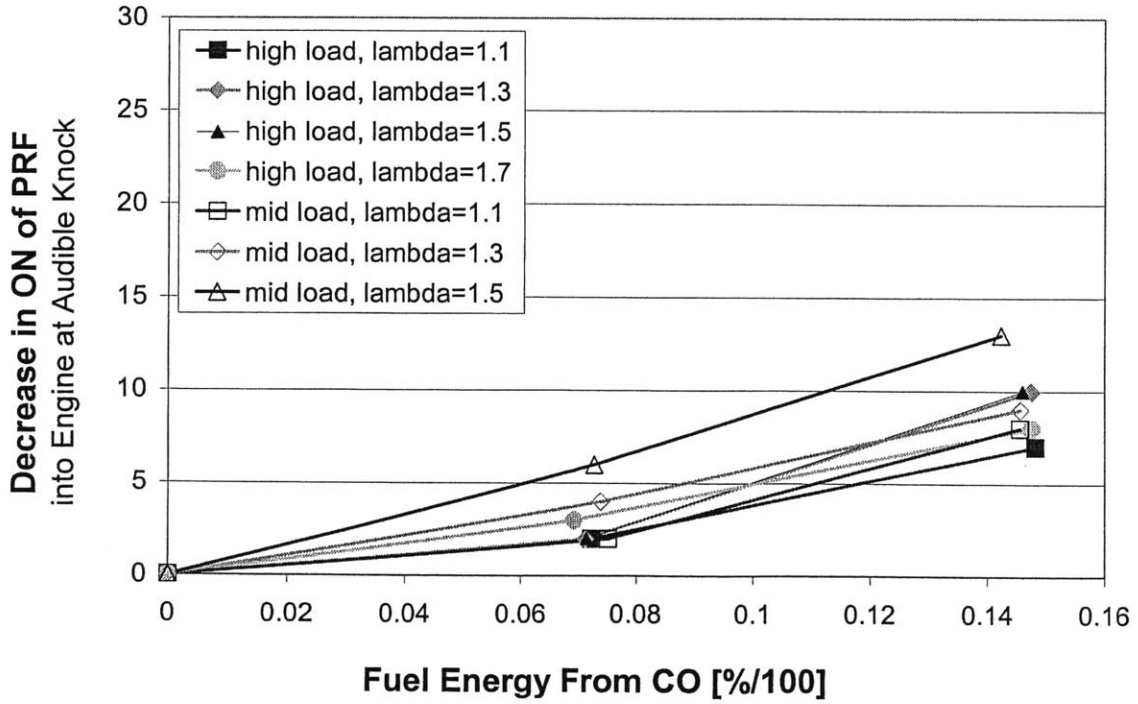

Fig. 3-21 **Inferred role of CO and additional N_2 dilution, estimated as the difference between the plasmatron addition and equivalent H_2 addition results.**

(This page was intentionally left blank.)

Chapter 4 Effective Octane Number Calculations

4.1 Overview

Fuel octane number is the traditional method to describe a fuel's resistance to knock in an SI engine. Octane number is an empirical measure established by comparing the knock tendency of a fuel to a mixture of two primary reference fuels as described in Sect. 2.6.1. Results of this study show that when H_2, or a combination of H_2 and CO, are added to a gasoline-air mixture, the octane number is increased above that of the gasoline alone. The effects of H_2 and CO are similar to octane-enhancing additives such as tetraethyl lead (TEL) or methyl tertiary butyl ether (MTBE). TEL and MTBE are known to increase the octane number of a mixture by a determined amount based on the mass or volume of additive mixed into a given amount of hydrocarbon fuel.

A new method for estimating the octane number was developed for blends of H_2, CO, and primary reference fuels. The method consists of calculating an average octane number based on a weighted average of the individual fuel components' octane numbers. The individual octane numbers were weighted based on various fundamental properties.

4.2 Background

Octane number is a comparative fuel measurement, which is particularly useful because it applies directly to spark-ignition engines. The effects of octane on feasible engine operating conditions and geometry are well explored and understood [22][23].

Although the octane number is the accepted knock index for SI engine fuel, current methods of estimating octane numbers do not account for H_2 or CO in the mixture. Nevertheless, this study shows that the addition of H_2 and CO serves to increase the octane number of the primary hydrocarbon fuel to which these gaseous fuels are added. A method to quantify the octane number increase as a function of the amount of H_2 and CO added would be useful for estimating possible impacts on engine operation. This method of accounting relies on knowing the relative knock behavior of H_2 and CO.

Blending octane numbers, or blending indexes, are typically established for fuels that are added in small quantities to a base fuel. The blending index describes the octane contribution of a fuel when it is added to a base fuel, in contrast to octane number, which describes the antiknock effect of a pure fuel. Blending octane numbers would be appropriate to use for this situation, but were not available for H_2 and

CO. Estimates for the research octane number were used instead, along with a weighting method, to establish octane numbers for fuel blends.

4.2.1 Octane Number of Hydrogen

Most literature estimates of the octane number of H_2 to be high, between 120 and 140 [12][13][14]. This value appears reasonable when inspecting the spontaneous ignition temperature of H_2, which is significantly higher than those of isooctane and n-heptane, as shown in Table 4-1. Fuels with high knock resistance will have a high spontaneous ignition temperature; thus, H_2 should have an octane number higher than 100.

Table 4-1 Selected properties of H_2, CO, isooctane, and n-heptane.

Fuel	Spontaneous Ignition Temp [2]	Research Octane Number
Isooctane	447 C	100
N-Heptane	247 C	0
Hydrogen	572 C	~140 [13]
Carbon Monoxide	609 C	~106 [13]

It is noted however, that a H_2 octane number is difficult to define. Octane number rating procedures were developed for liquid fuels. Another complication, which could arise in knock testing, is preigntion. Hydrogen is prone to preignition, defined as ignition of the charge by a hot surface before the spark is fired, which results from the low surface ignition energy of hydrogen. Knock tests on pure hydrogen engines must be carefully executed to ensure that the ignition phenomenon is indeed the autoignition of the end gas, and not preignition.

4.2.2 Octane Number of Carbon Monoxide

The octane number of CO has not been found in current literature. However, there are several reasons CO would have a high octane number. First, the spontaneous ignition temperature for CO is high. Secondly, this study found that CO has a similar effect to hydrogen on knock, when added to a fuel mixture. Discussions indicate that some recent tests, using the standard octane rating procedure, found the research octane number of CO to be 106 [14]. Therefore, the calculations in this study use the octane number of CO to be 106. The octane numbers for each pure fuel are summarized in Table 4-1.

4.3 Effective Octane Number Calculation

Following the determination of the octane numbers for H_2 and CO, a proper weighting attribute was sought. The current method to calculate average octane number for mixtures of hydrocarbon fuels uses volume or mass. These measures are not appropriate when dealing with a mixture of liquid fuels and H_2 and CO since these gaseous fuels take up a large volume fraction. Mass-weighting gives too little influence to H_2 since it is a very light molecule, while volume-weighting give too much influence to H_2 and CO since they constitute a significant volume fraction of the mixture. Since mass and volume do not represent the respective effects of the fuels, molecular attributes were considered. The fraction of critical chemical bonds and energy fraction provided weighting factors that worked with some success.

To test whether the methods are good, the calculated octane number at trace knock (using an estimation that accounts for C_8H_{18}, C_7H_{16}, H_2 and CO) is compared to the octane number at trace knock when using primary reference fuels only. These two octane numbers should match, under the assumption that the octane requirement at an operating condition is consistent. The critical bond-weighted and energy-weighted octane numbers are compared with the octane number that was determined while running primary reference fuels only for seven engine operating conditions. The comparisons show that the methods are generally good.

4.3.1 Bond-Weighted Octane Number

The ignition process initiates with the extraction of a hydrogen atom from a fuel molecule. This fundamental process led to a concept by which the effective octane number of a mixture of fuels could be estimated. The fuel proportions are quantified by the fraction of critical bonds they supply to the mixture. Critical bonds are those bonds that could take part in the spontaneous ignition process. For hydrocarbons, critical bonds are taken as the H-C bonds. For example, each molecule of isooctane (C_8H_{18}) contributes 18 H-C bonds; hence, the tendency of these H-C bonds to let loose determines if an isooctane-air mixture will spontaneously ignite. For molecules such as H_2 and CO, all of the bonds are critical. Thus, H_2 has one critical bond and CO has three. It is noted, however, that the effect of CO on the ignition process likely is different from that of H_2 and other hydrocarbons. Therefore, further investigation will re-evaluate the bond "weight" given to CO. Table 4-2 summarizes the critical bond assumptions and shows the structure of the fuel molecules.

Table 4-2 Number of critical bonds and molecular structure for fuels used in this study.

Fuel	Critical Bonds per Molecule of Fuel	Fuel Structure
Isooctane	18	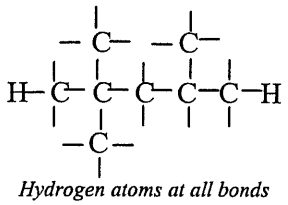 *Hydrogen atoms at all bonds*
Normal heptane	16	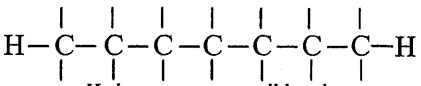 *Hydrogen atoms at all bonds*
Hydrogen	1	H–H
Carbon Monoxide	3	C≡O

The first step to calculate the bond-weighted octane number requires finding the number of CRitical Bonds (CRB) contributed by each pure fuel *i* as shown in Eq. (4-1).

$$CRB_i = X_i \times (\text{Critical Bonds/Molecule})_i \qquad \textbf{Eq. 4-1}$$

where X_i is the number of moles of fuel *i* in the mixture.

The number of critical bonds originating from each pure fuel component is then multiplied by the fuels' respective octane number. Summing this product over all fuel components, and dividing by the total number of critical bonds in the mixture, provides a bond-weighted octane number as shown in Eq. (4-2).

$$ON_{\text{bond-weighted}} = \frac{\sum (CRB_i \times ON_i)}{\sum CRB_i} \qquad \textbf{Eq. 4-2}$$

The results from this method of estimating an effective octane are shown in Fig. 4-1.

4.3.2 Energy-Weighted Octane Number

Another method of determining an effective octane number for a fuel mixture is to weight the octane number of each fuel component by the fraction of energy that it represents in the cylinder. The energy-weighted effective octane number is defined in Eq. (4-3).

$$ON_{\text{energy-weighted}} = \frac{\sum\left(LHV_i \times \dot{m}_i\right) \times ON_i}{\sum\left(LHV_i \times \dot{m}_i\right)} \qquad \textbf{Eq. 4-3}$$

where i is a pure fuel component, LHVi is the lower heating value, and $\dot{m}$ is the mass flow rate of fuel i. The results from this method of octane number calculation are shown in Fig. 4-1.

When fuel mixtures contain H_2 and CO in addition to gasoline, a method of estimating the octane number of the mixture is needed. In this section, two methods were presented to establish a way to calculate effective octane number for the fuel mixtures. The methods use information about the octane number of the pure fuels and find a weighted average. One approach looks at the number of critical bonds contributed by each fuel to find the influence of each fuel. The other approach uses energy of each fuel to predict the octane contribution of each fuel in the mixture. The bond-weighted octane number is accurate to ± 4 octane numbers, while the energy-weighted octane number is accurate to ± 8 octane numbers.

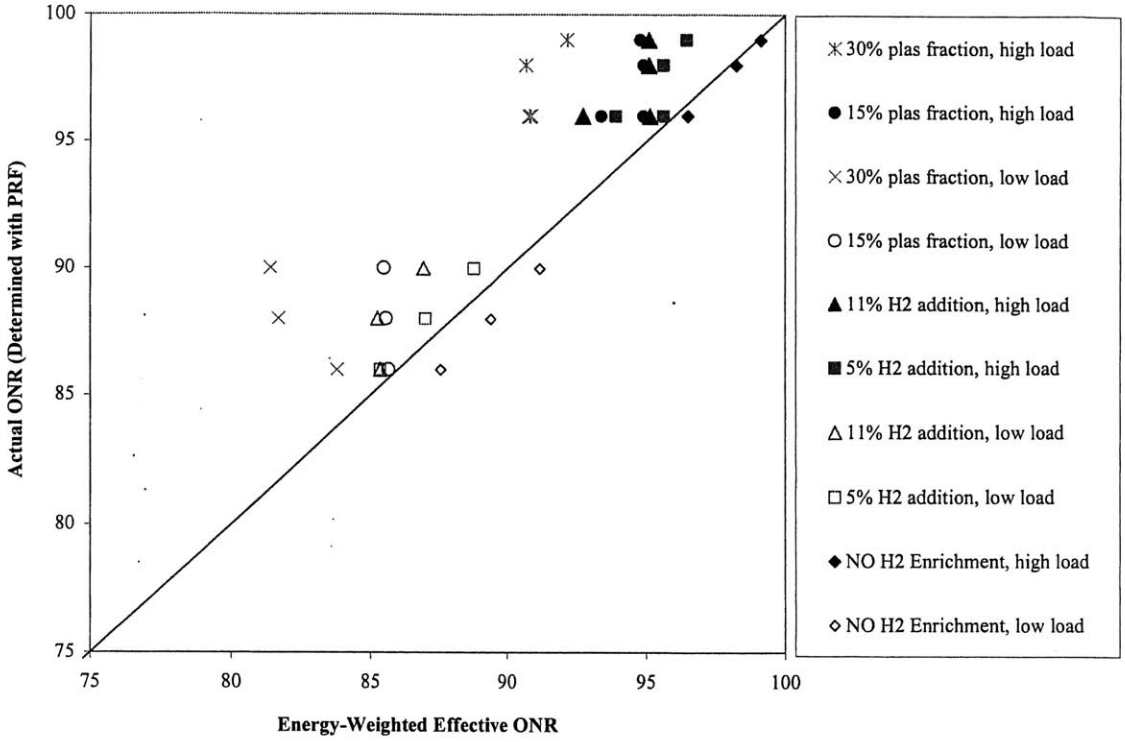

Fig. 4-1 **Agreement between the energy-weighted ON and the actual ON (as determined by a mixture of primary reference fuels) at audible knock.**

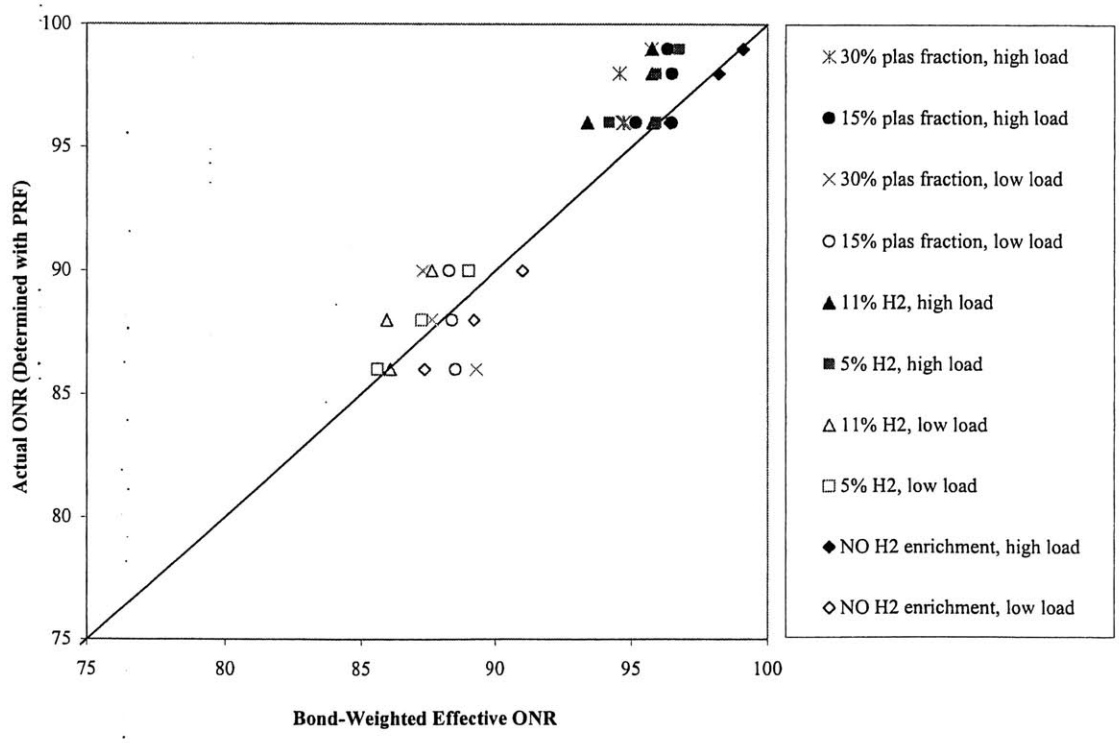

Fig. 4-2 **Agreement between the critical bond-weighted ON and the actual ON (as determined by a mixture of primary reference fuels) at audible knock.**

Chapter 5 Chemistry Modeling Study

5.1 Overview

A reduced chemistry model was used to predict the onset of autoignition in the homogeneous end-gas of a SI engine. The model was used in parallel with the experiments to help interpret the experimental data as well as to predict conditions that were not tested experimentally. The model has the ability to predict the octane number of hydrocarbon fuels (via a primary reference fuel model), which results in knock, given a characteristic pressure trace and the corresponding initial conditions.

5.2 Background

There are three types of chemical kinetic models used to predict autoignition: Empirical relations taking the form of overall Arrhenius equations, elementary reaction models, and models based on reduced chemistry reactions. Empirical models are simple and typically apply only to the specific situation for which they were calibrated. A comprehensive model based on elementary reactions offers the most complete approach; however, elementary reaction models require intensive computational time and detailed mechanisms are not available for all hydrocarbon fuels in engine-like conditions. A reduced chemistry model is a useful compromise between the previous types of models.

For this work, the reduced chemistry model uses the Hu-Keck ignition mechanisms for hydrocarbons. The ignition model was first calibrated with experiments, which measured the explosion limits in a constant combustion volume bomb [24][25]. Several MIT researchers have applied the chemistry model to SI knock prediction [21][26][27] with some success.

Recently, the reduced chemistry model has been extended and calibrated, making it useful for this research. Tanaka et al [28] added mechanisms for hydrocarbon breakdown and CO oxidation, as well improved the calibration for the entire model. The model currently contains 55 reactions and 32 species. After calibration, the model was shown to predict the ignition delay and oxidation of various primary reference fuel mixtures in a Rapid Compression Machine (RCM) extremely well.

Table 5-1 compares the calibration range of the reduced chemistry model [29] with the range of parameters used in this study. The comparison shows that the ignition model calibration regime is similar that of the end-gas in an SI engine.

Table 5-1 Regimes of chemistry model calibration and current research.

Parameter	Calibration [29]	Current Research
RON Range	0 – 120 PRF	65-100
Equivalence ratio (ϕ)	0.2-0.5	0.667-1.05
Initial pressure [MPa]	0.1	1.5-2
Initial temperature [K]	300-341	600-700
End of compression temp [K]	798-878	700-900
End of compression pressure [MPa]	4.04-4.19	3-5
Compression time [ms]	10-30	2-4

In summary, the mechanisms have been shown to be valid and the fuel hydrocarbon breakdown calibrated for appropriate conditions. However, because the mechanisms are global, they are not expected to directly transfer to different situations. T he reaction rates have n ot been calibrated f or our particular experimental situation; therefore, the model results are not expected to precisely match the quantitative experimental data. The model is being used to primarily investigate trends in ignition delay.

5.3 Ignition Chemistry

The reduced chemistry mechanism used in the engine knock model includes the Hu-Keck ignition model. The core ignition model is summarized below, and is illustrated in Fig. 5-1. There are four main steps of thermokinetic development [24]:

- Chain initiation: The first step in the process consists of the abstraction of a hydrogen atom from a saturated hydrocarbon. This yields an alkyl radical and a hydroperoxy radical (reaction 1[Ψ]).
- Chain Propagation: The alkylperoxy radical oxidizes a large alkane (four or more carbons) based on the isomerization theory (shown in reactions 2-6). The chain propagation is completed with the reaction of a hydroxyl (OH) radical with a fuel molecule.
- Chain Branching

  Low Temperature: Reaction 7 describes the chain branching reaction where hydroperoxide splits to become an OH and ORO.

[Ψ] Reaction numbers refer to Fig. 5-1.

These reactions (reactions 1-7) are considered the principle steps for oxidation of normal alkanes, with four or more carbons, at temperatures below 800° K in an oxygen-rich environment. This low temperature loop describes the first stage ignition delay.

High Temperature: In the high temperature and low oxygen concentration regime, hydrogen peroxide becomes the branching agent. The decomposition of hydrogen peroxide produces hydroxide radicals which accelerate the reaction process. Reactions 8-10 are the critical reactions in the high temperature loop.

- Chain Termination: Chain termination occurs when the radicals are consumed leading to the formation of water.

Reactions 1-10 are responsible for describing the complete two-stage ignition process. These reactions have high sensitivity to temperature and specie concentration. The rates of reaction also are dependent on the fuel type.

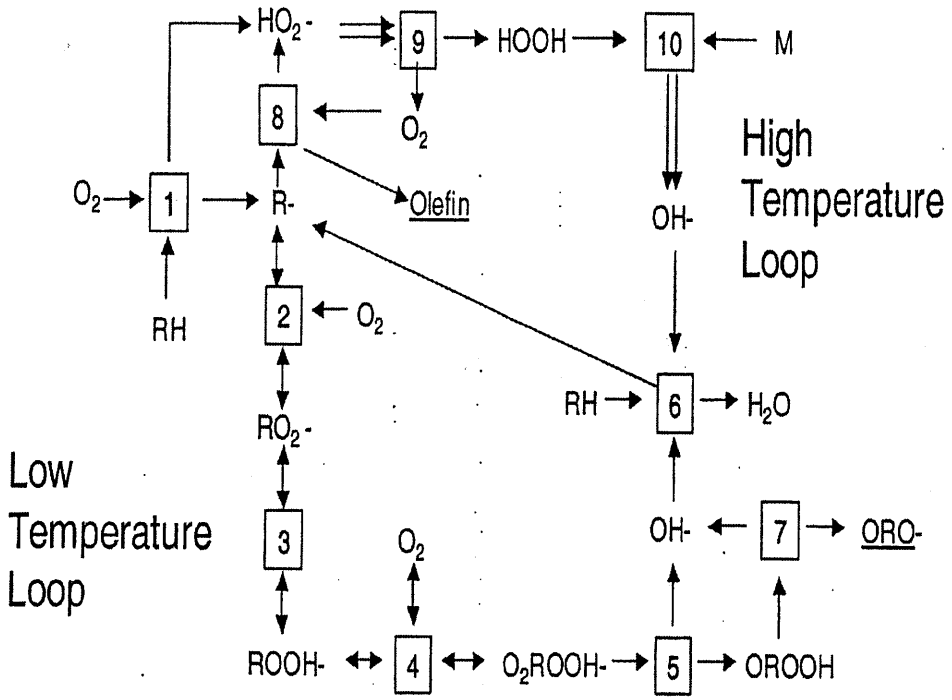

(Courtesy of D. Schmidt and F. Ayala [30])

Fig. 5-1 Schematic of the Hu-Keck ignition model. Reaction numbers are indicated in boxes.

5.4 Physical Situation and Assumptions

In our application, the model follows a small element of end-gas, subject to a known pressure constraint (pressure as a function of time.) The calculation begins at the time of spark, where the volume, composition, and pressure are known. After the spark, the end-gas is compressed adiabatically. Until autoigntion, the temperature of the end-gas increases mainly due to adiabatic compression and slow chemical energy release.

Other critical assumptions are:

1. The measured cylinder pressure is homogenous throughout the cylinder, and therefore representative of the end-gas pressure history.
2. The calculations assume that each cycle ingests the same amount of fuel and air, as measured by the steady state flow devices. The residual fraction in the end gas is estimated with the improved version of the Fox correlation described in Eqs. (5-11) and (5-12).

5.5 Governing Equations

To predict the autoignition delay, the state and composition of the end-gas are determined at each time step. The time step was taken to be 1×10^{-6} seconds.

The rate equation for each chemical specie was defined by reduced chemical equations where the change in specie concentration is a function of the rate constant defined in Eq. (5-1).

$$\frac{dn_{\text{specie}(i)}}{dt} = function(k)$$
$$k = A \cdot T^{n} \cdot \exp\left(-E/_{RT}\right) \qquad \textbf{Eq. 5-1}$$

where A, n and E are constants, which are listed in the Appendix C.

To calculate the state from one time step to the next, the change in pressure (dp), change in temperature (dT), the change in the volume (dV), and change in number of moles (dn) must be determined. Pressure as a function of time is a direct input; therefore, the change in pressure is known at each model time step. The change in number of moles in the element of end-gas due to the chemical reactions is calculated by the chemical kinetic equations. The remaining parameters, which are change in temperature and volume,

can be calculated by applying the energy equation and the ideal gas law. Eqs. (5-2)-(5-8) summarize the process to arrive at *dp*, *dT*, *dV*, and *dn*.

$$\frac{dp}{dt} = \text{known from experiment} = p(t) \qquad \textbf{Eq. 5-2}$$

$$\frac{dn}{dt} = \text{known from chem} = f(T, p) \qquad \textbf{Eq. 5-3}$$

This leaves two unknowns , $\mathrm{d}V/\mathrm{dt}$ and dT/dt , and two equations (5-5 and 5-8). The first equation involves the ideal gas law, Eq. (5-4).

$$p \cdot V = n \cdot R \cdot T \qquad \textbf{Eq. 5-4}$$

Where *p* is pressure in Pascals, *V* is volume in cubic meters, *n* is number is number of moles. *R* is the gas constant, $8.314\, J/(moles \cdot K)$, and *T* is temperature in degrees Kelvin. Differentiating Eq. (5-4) in terms of dt and solving for dV/dt gives Eq. (5-5).

$$\frac{dV}{dt} = \frac{n \cdot R}{p}\frac{dT}{dt} + \frac{R \cdot T}{p}\frac{dn}{dt} - \frac{V}{p}\frac{dp}{dt} \qquad \textbf{Eq. 5-5}$$

The second equation required is the first law of thermodynamics, or conservation of energy, Eq. (5-6).

$$dU = \left(\delta Q_{\text{energy released}} + \delta Q_{\text{heat loss}}\right) - \delta W \qquad \textbf{Eq. 5-6}$$

The isentropic assumption gives $\delta Q_{\text{heat loss}}$ to be zero and $\delta W = pdV$. Differentiating this equation with respect to dt leads to Eq. (5-7).

$$n[mol] \cdot c_v \left[\frac{J}{mol \cdot K}\right] \cdot \frac{dT}{dt}\left[\frac{K}{\text{sec}}\right] = \frac{\delta Q_{en\_rel}}{dt}\left[\frac{J}{\text{sec}}\right] - \frac{pdV}{dt}\left[\frac{J}{\text{sec}}\right] \qquad \textbf{Eq. 5-7}$$

Solving for dT/dt gives Eq. (5-8).

$$\frac{dT}{dt} = \frac{1}{n \cdot c_v} \frac{dQ_{en\_rel}}{dt} - \frac{p}{n \cdot c_v} \frac{dV}{dt} \qquad \textbf{Eq. 5-8}$$

Equations (5-1), (5-5) and (5-8) are solved simultaneously at each time step to determine the specie concentration and thermodynamic state of the end-gas. The structure and flow of the model is also illustrated in Fig. 5-10.

5.6 Inputs to the Model

The initial conditions include: specific volume, mixture composition expressed as mass fractions and the overall pressure as measured from an experimental data. This section describes the methods to find the inputs. The process to choose a representative pressure trace from experimental data is described, as well as the calculation of specific volume.

5.6.1 Pressure Trace Selection

Autoigntion does not occur in every cycle during audible knock operation. As described in Chapter 3, the fast-burning cycles are more likely to experience autoigntion. When approximately 40% of the cycles exhibit autoignition, near the time of peak pressure, the knock will most likely be audible. To accurately predict knock for a given operating condition, the model would be executed for a large sample of pressure traces, representing the distribution of possible end gas pressure histories. In this work, running the model for many pressure cycles was not convenient; therefore, a *"critical pressure trace"* was tested for knock in the model. The critical pressure trace represents a cylinder pressure cycle, which likely experiences substantial autoigntion at a given condition.

This is defined as a fast-burning cycle as described in Chapter 3. In this work, the measure of a particular cycle's burning speed was found by comparing the cycle's location of peak pressure to the average location of peak pressure. A cycle with a location of peak pressure occurring at least one standard deviation before the mean location of peak pressure was chosen. The cycle was extracted from the slow sampled data, collected when operating with a fuel giving trace knock.

5.6.2 Specific Volume Calculation

Specific volume is a value required by the program at the initial condition encountered at spark, it is defined as the volume divided by the mass, as shown in Eq.(5-9).

$$v_{spark} = \left(\frac{volume}{mass} \right)_{spark} \qquad \textbf{Eq. 5-9}$$

Both volume and mass at time of spark can be estimated. Volume in the cylinder at the time of spark can be found by relating the geometry to crank angle [1]. The mass in the cylinder can be estimated by the steady state flow rate of fuel and air, and residual gases as shown in Eq. (5-10).

$$mass\left[\frac{g}{cycle}\right] = \left(\dot{m}_{air} + \dot{m}_{fuel}\right)\left[\frac{g}{\sec}\right] * \frac{1}{25}\left[\frac{\sec}{rev}\right] * 2\left[\frac{rev}{cycle}\right] + residuals\left[\frac{g}{cycle}\right] \qquad \textbf{Eq. 5-10}$$

The Fox model was used to estimate residual fraction [31], and accounts for backflow of exhaust gas into the cylinder and the burned gas that is trapped in the cylinder before the valve overlap period. The residual mass fraction is related to six independent parameters: engine speed (N), inlet and exhaust pressures (p_i, p_e), a valve overlap factor (OF), compression ratio (r_c), and fuel/air equivalence ratio (ϕ).

$$\chi_{res} = \frac{\dot{m}_{residual}}{\dot{m}_{total}} = f(OF, N, p_i, p_e, \phi, r_c) \qquad \textbf{Eq. 5-11}$$

The overlap factor, Eq. (5-12), defines the characteristics of the flow passage during the valve overlap event; and is a function of valve characteristics and engine displacement. The Fox residual model is used with updated constants to reflect modern engine design.

$$OF = \frac{(D_i \cdot A_i + D_e \cdot A_e)}{V_d} \qquad \textbf{Eq. 5-12}$$

The calculation for specific volume is theoretically correct; however, slight errors in the mass trapped in the cylinder result in changes in temperature. A 5% change in mass can change temperature by 30 K. To obtain a better estimate of the conditions at spark the isentropic temperature history of the end-gas was considered. Equation (5-13) shows the appropriate form.

$$\left(\frac{P_2}{P_1}\right)^{\frac{\gamma-1}{\gamma}} = \frac{T_2}{T_1} \qquad \text{Eq. 5-13}$$

The initial temperature (state 1), at bottom dead center, was estimated as the mixing temperature of the fresh inlet charge and the residual gases. The ambient air temperature was 293 K ± 1. After passing though the air intake system, port, and valve area, the air temperature in the cylinder was estimated to be 340 K. The residual gas was assumed to have a temperature of 550° C (823 K), which is a typical exhaust gas temperature at high loads. The pressure at state 1 is clearly taken to as the intake manifold pressures. The ratio of specific heats (γ) was calculated using STRAP, the intake charge mixture was assumed to consist of only major species (fuel and air) at 500 K. Supplying these inputs and the pressure at spark (state 2), allows one to solve for the temperature at spark.

The temperature estimation at spark was first calculated with the ideal gas law, and then checked with isentropic compression temperature just described.

5.6.3 Mixture Composition

The end-gas mixture composition was entered into the model as mass fractions. The species that are available as inputs are: C_8H_{18}, O_2, N_2, CO_2, H_2O, C_7H_{16}, CO, OH, HO_2, H_2O_2, H, O, Ar and H_2. Although residuals were calculated for in the mass estimation, they were not reflected in the specie composition entered into the program. The mass composition input to the model is comprised of fuel and air only.

5.7 Model Methodology and Interpretation

The model predicted the octane number of hydrocarbon fuel giving audible knock. The model was executed with fuels corresponding to the experiments to see if the same trends in ONR were reached with the model. This section describes how the ONR was determined from the model. In order to compare all the cycles, a standardized methodology was used.

The model was run several times to find the ONR for one data point. For the runs, everything was held constant except the relative amount of C_8H_{18} and C_7H_{16}, to simulate operation with a range of octane numbers. By observing the calculated temperature of the mixture and applying the methodology described below, the octane number of fuel that results in autoignition occurred was predicted.

An example of the model results is shown in Fig. 5-2. The pressure trace is the input, starting at time of spark. The temperature at spark is calculated with pressure, specific volume, and the gas constant.

The temperature increases due to compression and chemical energy release. The temperature behaves differently for each fuel used. When the reactions in the end-gas become significant, the temperature rises quickly and autoignition is implied. The time when autoigntion occurs can be associated with the corresponding location in the pressure traced. Autoigntion at the cylinder peak pressure was interpreted as corresponding to audible knock, since experimental pressure traces show oscillations beginning around peak pressure. In addition, autoigntion should occur at peak cylinder pressure which corresponds to peak end-gas temperature.

The simulation is only valid until autoigntion and was used to obtain autoigntion times only. After autoigntion, the assumption of a homogeneous mixture is no longer valid and the input pressure trace does not apply to the element of end-gas that ignitied.

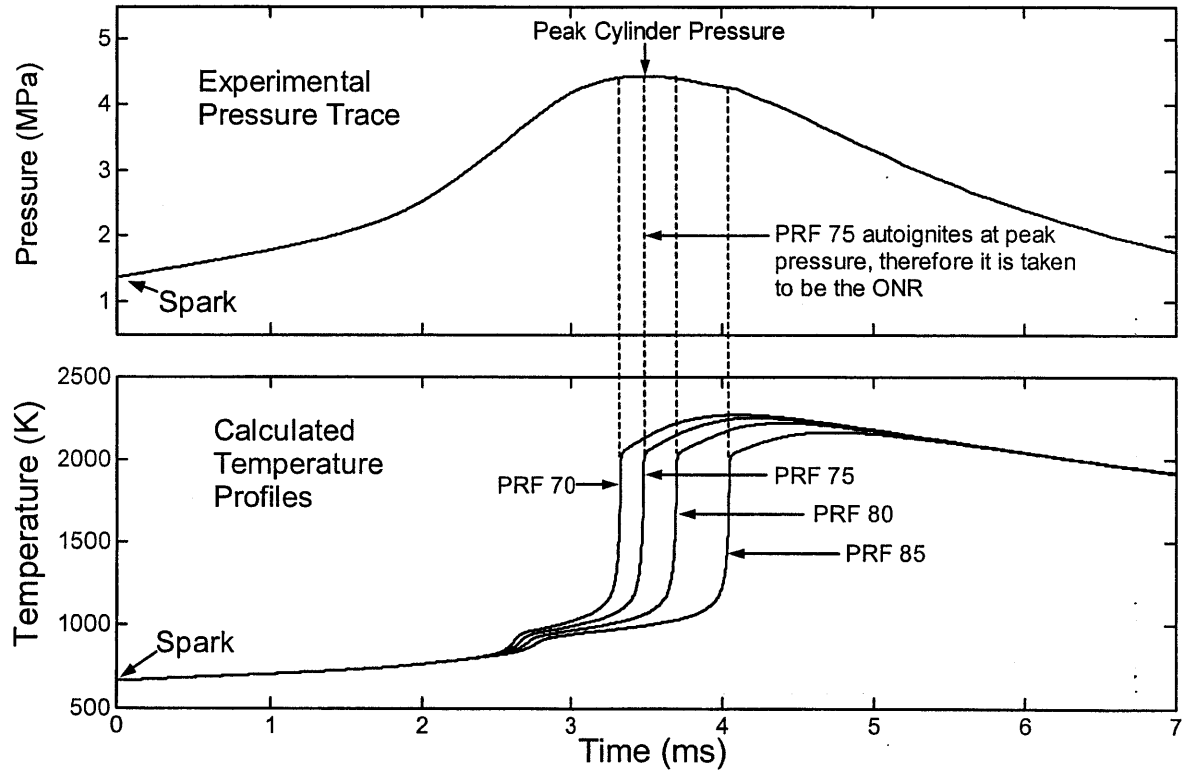

Fig. 5-2 **Sample of chemistry knock simulation results (illustrative case only.) Large energy release is interpreted as autoigntion.**

5.8 Results of the Engine Knock Simulation

Tables 5-2 and 5-3 show the experimental and the predicted octane number requirement (ONR) for two load cases where primary reference fuels were used. The simulation shows approximately correct results. The ONR predicted by the model are typically within 5 octane numbers of experimental results. Cases were tested for a range of operating conditions.

Figures 5-3 and 5-4 show a representative sample of results from the engine knock simulation. The pressure cycle chosen for the input is a moderately fast-burning cycle, which shows small amount of knock. The pressure oscillations typically associated with audible knock are not clearly visible in the pressure trace because the sampling rate was too slow (9kHz) to capture the pressure oscillations, which occur at primarily at 6-10 kHz. The goal of the engine knock simulation is to find the octane fuel, which shows autoigntion at peak pressure, just ahead of the visible irregularities in the pressure trace. Therefore, the pressure irregularities in the sampled pressure after the point of maximum pressure are thought to be insignificant for the knock simulation. In Fig. 5-3 the engine knock simulation predicts that the ONR is slightly over 90. The experimental ONR was found to be 96. In Fig. 5-4 the engine knock simulation predicts and ONR of 88, while the experimental result was 93.

Table 5-2 Model and experimental results at mid-load with primary reference fuel mixtures.

	NIMEP = 6.7 bar		
ONR	**λ=1.1**	**λ =1.3**	**λ =1.5**
Experimental	88	90	93
Predicted	86	85	88

Table 5-3 Model and experimental results at high-load with primary reference fuel mixtures.

	NIMEP = 8.5 bar		
ONR	**λ=1.1**	**λ =1.3**	**λ =1.5**
Experimental	96	96	98
Predicted	91	90	90

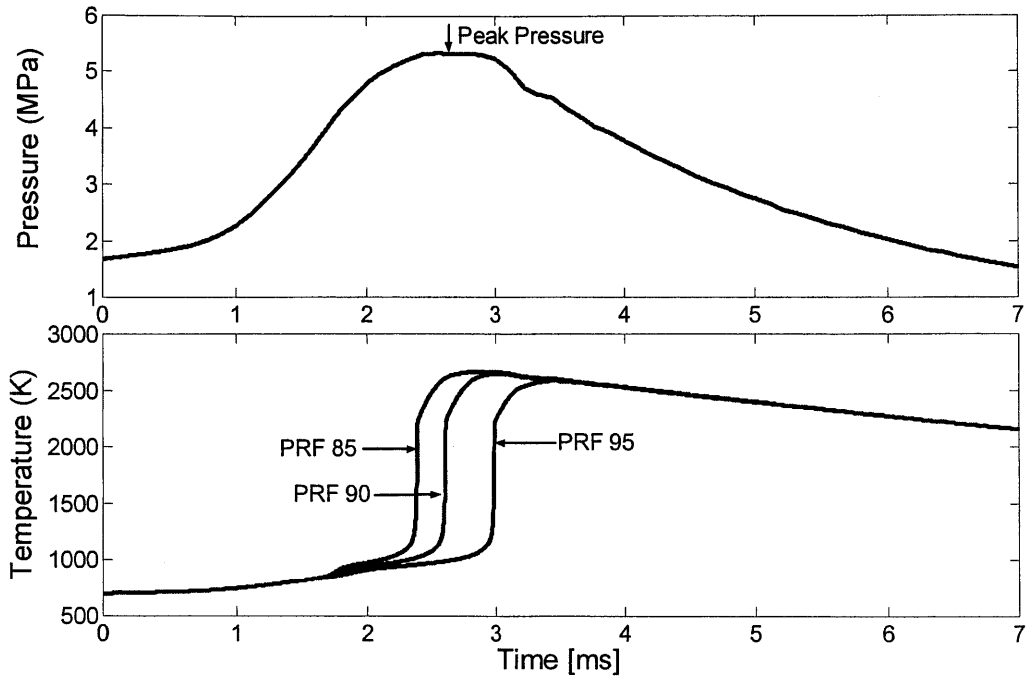

Fig. 5-3 **Engine knock simulation result for PRF case CC [lambda =1.1, NIMEP=8.5 bar, MAP = 1.1 bar, Spark Timing = 11 deg BTDC.] The experimental ONR for this case is PRF 96, the model predicts PRF 91.**

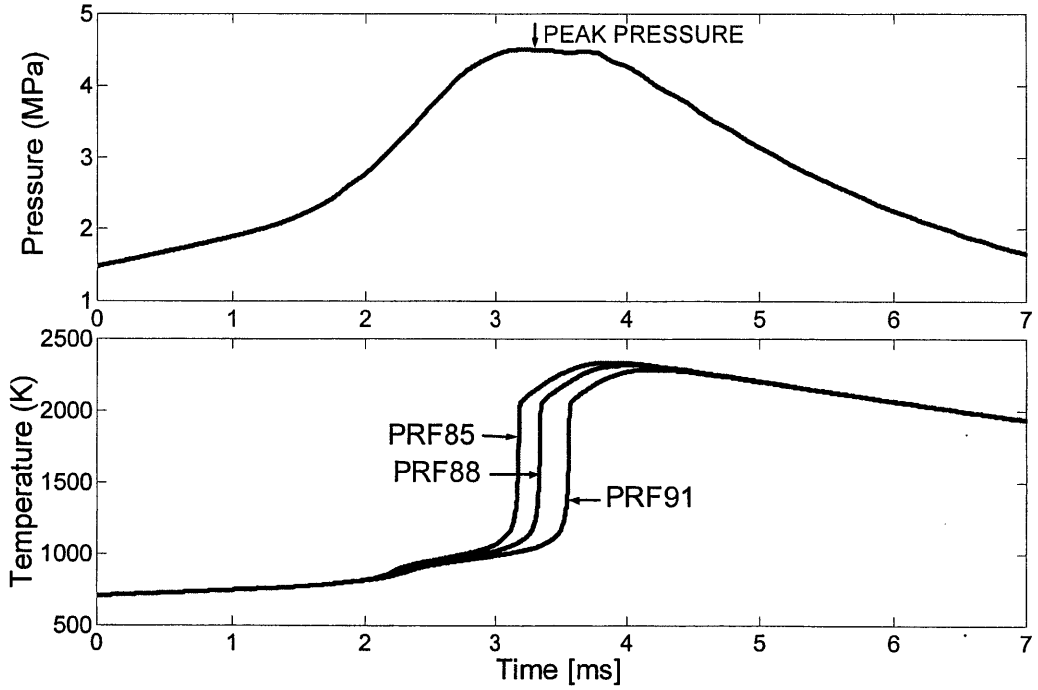

Fig. 5-4 **Engine knock simulation result for PRF case A [lambda =1.5, NIMEP=6.7 bar, MAP bar = 1.0, Spark Timing = 18 deg BTDC.] The experimental ONR for this case is PRF 93, the model predicts PRF 88.**

The result from the engine knock simulation is typically within five octane numbers to the experimental results, for the cases where traditional liquid hydrocarbons (primary reference fuels) are used. The simulation allows for input of H_2 and CO in addition to the primary reference fuel, so the plasmatron reformate and hydrogen addition tests can be modeled in the simulation. In the cases where plasmatron reformate and H_2 are added to the fuel mixture, the simulation suggests that an unreasonably low octane number of primary reference fuel is needed to achieve autoigntion near peak pressure. The experimental results show only a modest decrease in the octane number of the primary reference fuel to reach knock in these cases. Therefore, it is believed that the influence of hydrogen on autoignition appears to be overestimated in the model. Figure 5-5 shows the result from the engine knock simulation with 30% plasmatron reformate fraction. For this case, the experimental octane number of primary reference fuel giving audible knock was 65. However, the simulation predicts an octane number much lower than 50.

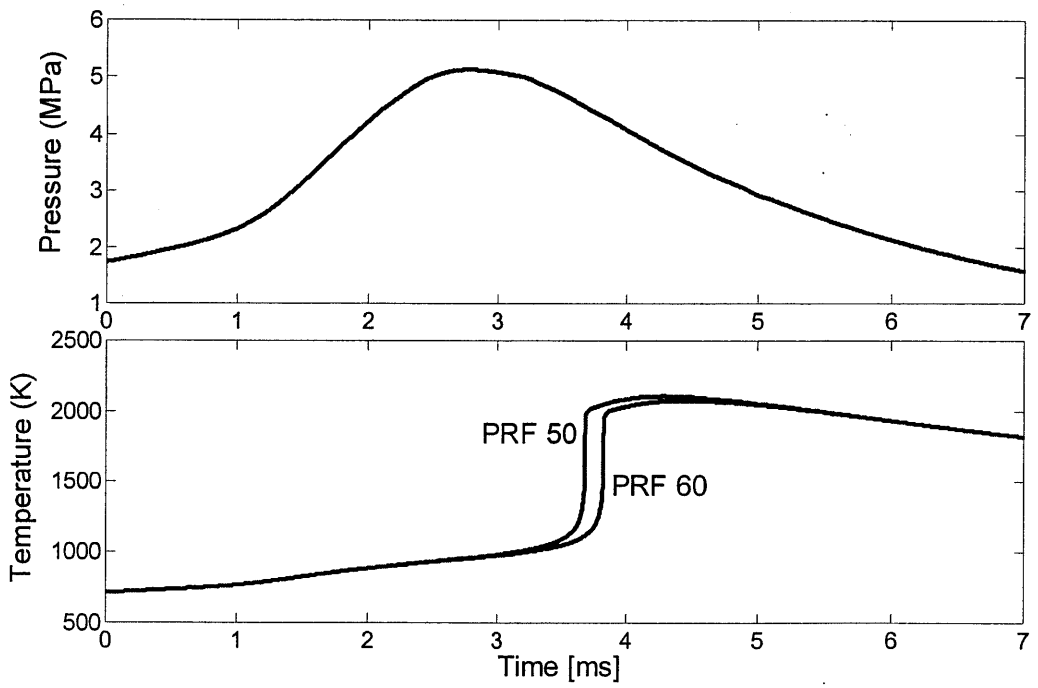

Fig. 5-5 **Engine knock simulation result for 30% plasmatron addition. [Case U, lambda=1.5, NIMEP=6.7 bar, MAP =1.2 bar, Spark Timing = 16 deg BTDC.] Experimental octane number of PRF supplied to the engine at audible knock was 65. The predicted octane number for audible knock extremely low.**

In the engine knock simulations, many end-gas parameters are accounted for, including density, composition, temperature and time. It is believed that the primary effect of CO and H_2 in extending the ignition delay is a chemical effect due to the mixture composition, with lesser dependencies on mixture pressure, temperature, and residence time in the cylinder. To give insight and explanation for the results

observed in experiments with H_2 and CO addition, work was done to understand the independent effect of mixture composition on ignition delay. This was achieved by completing ignition delay simulations in a constant volume situation.

5.9 Constant Volume Ignition Delay Predictions

Simple simulations were done to investigate the chemical effect of blending H_2, CO, and plasmatron reformate with isooctane on ignition delay time. One set of simulations was completed with the reduced chemistry mechanisms as described in Chap. 5. Another set of constant volume simulations was completed with a comprehensive chemistry mechanism for isooctane [32]. This chemistry mechanism is specifically for the break-up of isooctane. However, H_2 and CO are species formed and consumed in the break-up of isooctane; therefore, mechanisms should be included to account for their effect. The simulations shown in Fig. 5-6 – 5-9 are constant volume predictive runs, which begin at a given pressure and temperature. The initial temperature and pressure correspond to typical conditions at peak pressure in the cylinder, 875 K and 45 bar. Additional runs were completed at a lower temperature of 800 K to illustrate the temperature sensitivity of the reactions. The simulations were completed for four different mixtures; the energy fractions are shown in Table 5-4. All mixtures had a relative air/fuel ratio of 1.5. Table 5-5 gives the mole fractions used for these simulations. These mole fractions were used as the input to Senkin for the comprehensive model. The mole fractions were scaled and converted to masses, for input for the reduced chemistry model.

Figures 5-6 and 5-7 show the result of the comprehensive isooctane model. For both temperatures, the relative results of the autoigntion delay time agree with the experimental trends. The constant volume simulations show the ignition of isooctane and air to occur in the shortest time; the mixture of CO and isooctane has a slightly longer ignition delay period. The H_2 and isooctane mixture has a significantly longer ignition delay time, while the addition of H_2, CO and extra N_2 dilution (plasmatron reformate addition) results in the longest ignition delay. Experimental results show that mixtures of PRF (e.g. isooctane) and air are most susceptible to knock, suggesting these mixtures have shortest ignition delays. A mixture enhanced with plasmatron reformate is the most effective in resisting knock in the engine, which is consistent with the longest predicted ignition delay for this mixture.

Figures 5-8 and 5-9 show the constant volume ignition delay predictions given by the reduced mechanism. The absolute and relative differences between the two figures (875 K vs 800 K) suggest that the reduced chemistry is very temperature sensitive. The isooctane + CO mixture ignites before the isooctane mixture at high temperature, but not at the lower temperature. The addition of H_2 consistently lengthens the ignition delay.

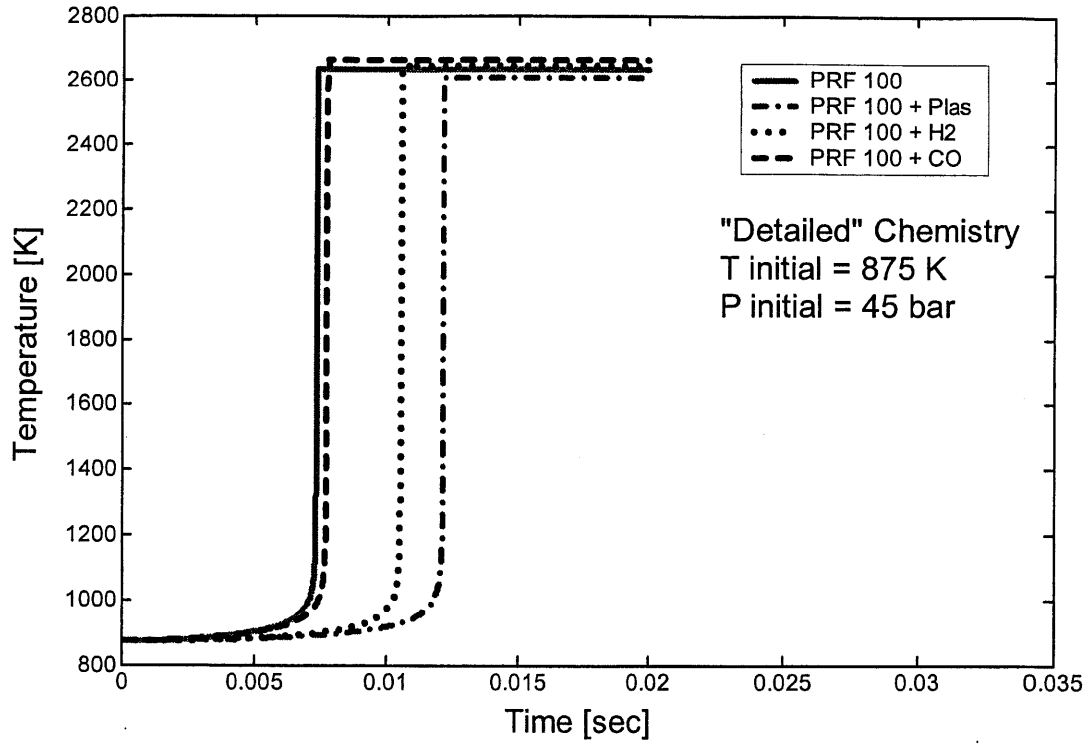

Fig. 5-6 **Constant volume calculation with the detailed chemistry model. (Initial Temp = 875K , initial pressure =45 bar.)**

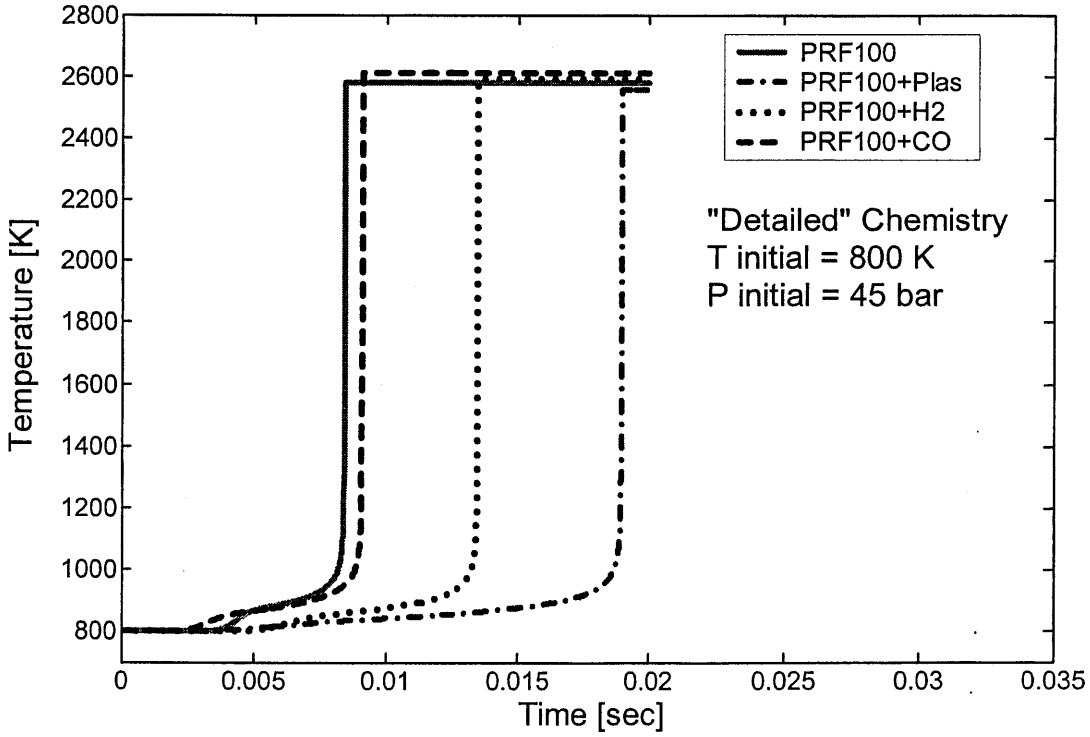

Fig. 5-7 **Constant volume calculation with the detailed chemistry model. (Initial Temp = 800K , initial pressure =45 bar.)**

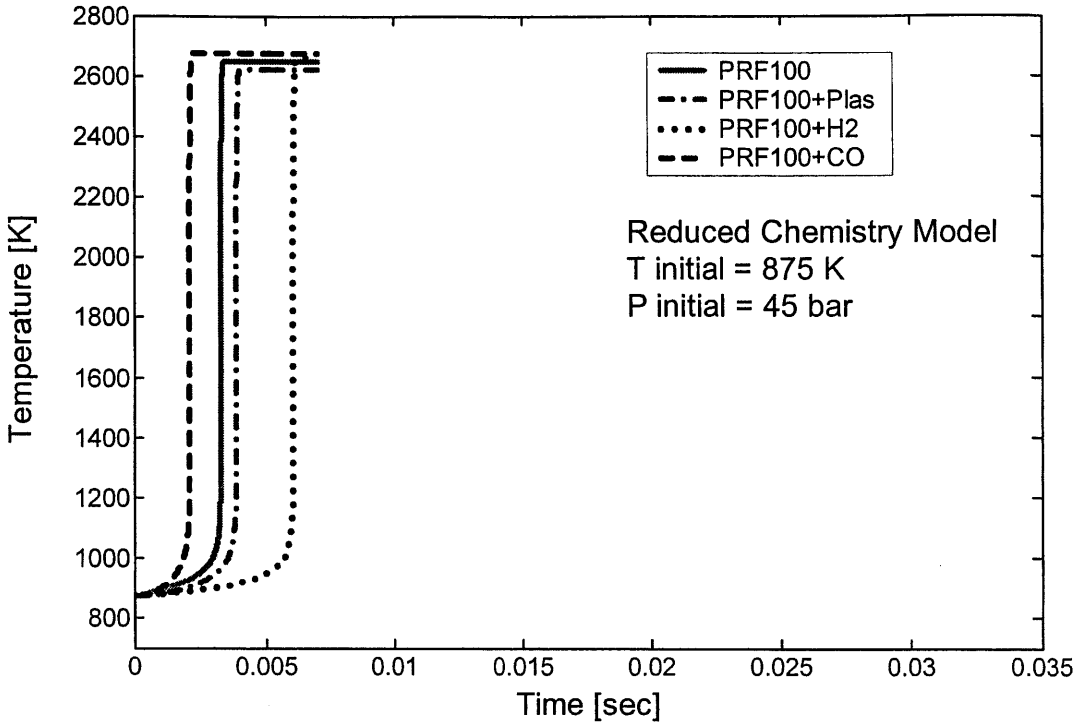

Fig. 5-8 **Constant volume calculation with the detailed chemistry model. (Initial Temp = 875K , initial pressure =45 bar.)**

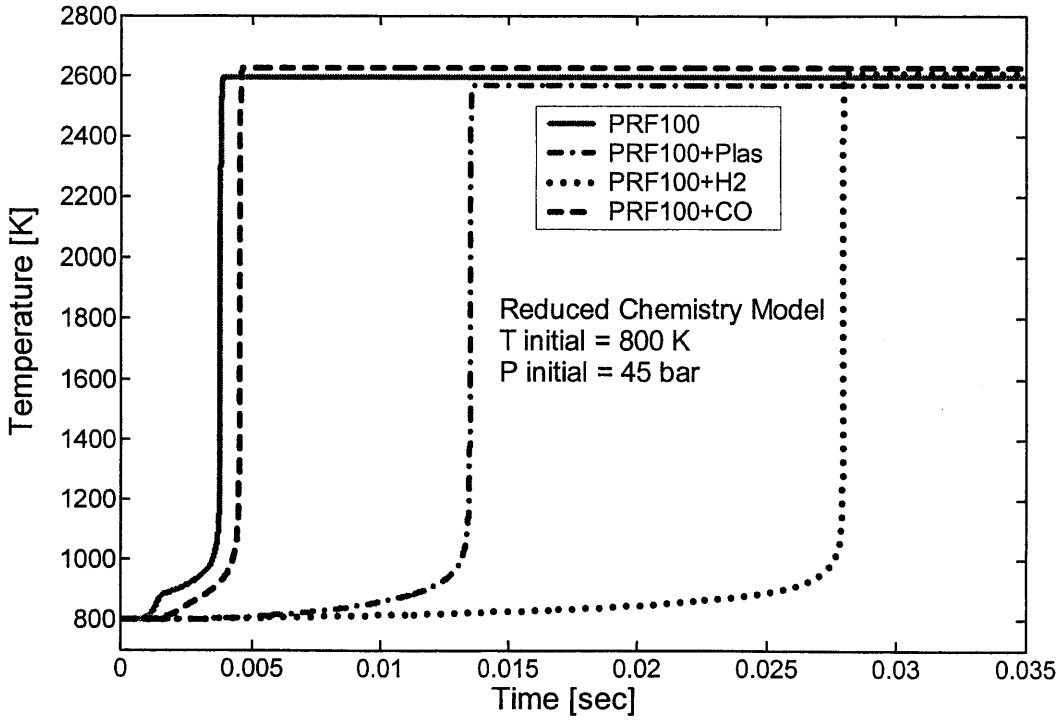

Fig. 5-9 **Constant volume calculation with the detailed chemistry model. (Initial Temp = 800K , initial pressure =45 bar.)**

Table 5-4 Fuel energy fractions for the four cases tested in the constant volume cases.

Energy Fraction	Isooctane only	Isooctane + CO	Isooctane + H_2	Isooctane + Plas
C_8H_{18}	1.0	0.85	0.9	0.75
H_2	0.0	0.0	0.1	0.1
CO	0.0	0.15	0.0	0.15

Table 5-5 Mixture composition used for the constant volume cases.

Mole Fraction	Isooctane only	Isooctane + CO	Isooctane + H_2	Isooctane + Plas
C_8H_{18}	0.011050	0.009528	0.009888	0.007936
H_2	0.0	0.0	0.022979	0.022131
CO	0.0	0.030076	0.0	0.028388
O_2	0.207197	0.201214	0.20262	0.186681
N_2	0.781753	0.759181	0.764507	0.754865

An engine knock simulation was used to predict the autoignition time of the end-gas. The model shows good autoigntion predictions for blends of primary reference fuels. This is likely due to the RCM calibration of the reduced mechanisms for these mixtures. The SI end-gas autoigntion agreement in the primary reference fuel cases help to validate the methodology used in the engine knock simulation. Uncertainties, which have been addressed briefly include: initial condition specification (i.e. temperature at spark), pressure trace selection, and identification autoigntion resulting in audible knock. Finally, the autoigntion predictions (using the reduced chemistry model) of mixtures that include small amounts of H_2 and CO are questionable. Constant volume calculations (using a comprehensive chemistry model) were used to show that H_2 and CO lengthen the ignition delay of fuel-air mixtures when added in small quantities. This agrees with experimental knock trends.

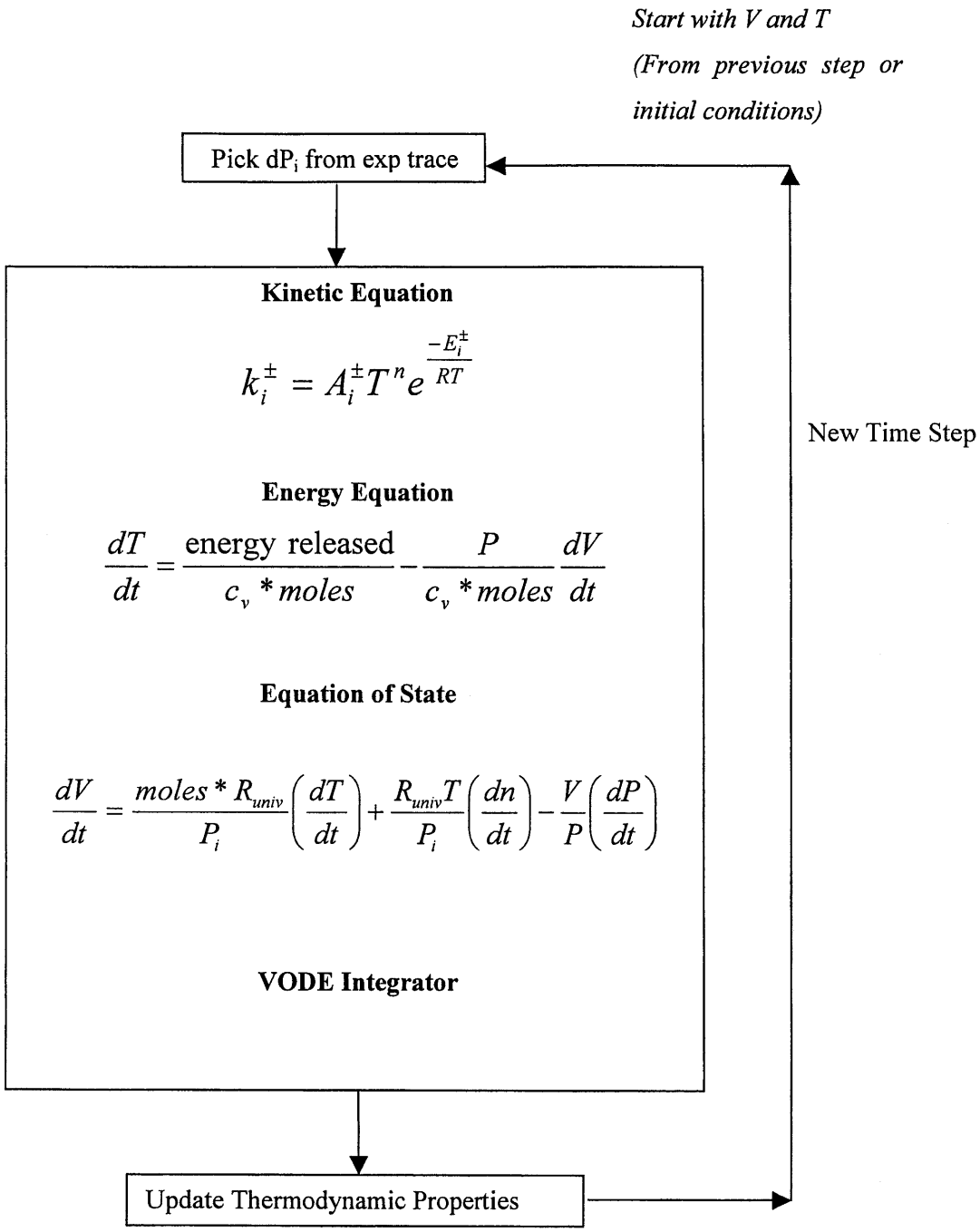

Fig. 5-10 Structure and governing equations in the engine knock simulation.

(This page was intentionally left blank.)

Chapter 6 Discussion

This research investigated knock trends in lean fuel/air mixtures and such mixtures enhanced with H_2 and CO. Experiments to identify the knock trends were performed on a single-cylinder Ricardo research engine with boosting capability. The experimental method used to investigate knock trends consisted of determining the octane number (ON) of primary reference fuel supplied to the engine that results in audible knock. All tests were completed at 1500 rpm, MBT spark timing, with coolant temperature at fully warmed-up conditions and intake air temperature at 293° K. Various relative air-fuel ratio (lambda) sweeps were performed, each while holding different parameters constant. First, lean operation knock limits were investigated with primary reference fuel. Selected tests were then repeated with H_2 and CO enhancement. The added mixture simulated 15% and 30% of the gasoline mass being reformed in the plasmatron fuel reformer.

Experimental knock trends associated with lean operation depend on what parameters are held constant, as the mixture is made leaner. If leaner operation is achieved by decreasing the fuel flow, while holding airflow constant, the knock tendency of the engine decreases, along with the torque output. This trend of decreasing knock with leaner mixtures is similar to what is displayed in Gruden and Hahn's work in Fig 1-6. Among other things, this is a result of lower fuel concentration in the end-gas and lower maximum end-gas temperatures. Holding the fuel flow constant and introducing more air to achieve a leaner mixture increases the knock tendency of the engine, as well as the engine output. To achieve constant torque with leaner operation, a combination substantially increased airflow and slightly decreased fuel flow is required. In this constant torque scenario, the knock tendency increases slightly. This information implies that a lean, boosted engine is less resistant to knock than a stoichiometric engine operating at the same torque output.

To understand this trend, the end-gas temperature - which is the dominant factor in determining knock - is estimated. The end-gas can be modeled as a homogeneous mixture, which experiences an isentropic compression (Eq. 1-3) from the start of compression until the peak pressure. Comparing an engine operating with stoichiometric and lean mixtures, while maintaining constant torque, shows that lean unburned mixtures have an equal or higher maximum temperature. (see Table 6-1)

Table 6-1 Isentropic compression calculation for constant output operation, with stoichiometric and lean mixtures.

Test Case	NIEMP [bar]	MAP [bar]	Initial T [K]	Peak Pressure [bar]	c_p/c_v at 500° K, 25 bar	Calculated peak end-gas T [K]
PRF only, Lambda=1.5	8.5	1.5	340	53	1.35	889
PRF only, Lambda=1.0	8.5	1.1	340	50	1.33	877

Lean mixtures have a higher γ due to reduced concentration of fuel molecules (which have lower γ than N_2 and O_2 due to their larger molecule size.) Higher unburned mixture γ results in a higher unburned mixture temperature at peak pressure, for the same pressure ratio, P_{max}/P_{intake}. This shows that the end-gas in a lean mixture reaches a higher maximum temperature due to compression than a stoichiometric mixture, promoting the end-gas reactions that ultimately lead to knock. These results are consistent with findings by research groups at Chalmers and Lund Universities [11]. The researchers found that leaner mixtures reach the critical temperature at a lower compression than richer mixtures. As a consequence the leaner mixtures will autoignite earlier, which results in a higher knock intensity.

Experiments show that H_2 and CO have an octane-enhancing effect when added to a hydrocarbon-air mixture. H_2 and CO-enhancement causes numerous changes that could affect the end-gas autoignition characteristics. One change is that the flame speed is increased, shortening the time that the end-gas is subject to at high temperatures and pressures. However, since MBT spark timing changes by only a few crank angles, this is not believed to be the primary factor responsible for the change in knock trends. The dominant factor is believed to involve the chemical reactions in the end-gas, which are slowed with the addition of H_2 and CO. These gaseous fuels contribute [high] octane to the gasoline. Experiments with H_2 addition show the same trends of increasing the knock resistance of the mixture. A method has been developed by which the octane number of fuel blends that include primary reference fuels, H_2 and CO can be estimated. The method involves calculating a average ON for the mixture, where the ON of each pure fuel is weighted by the fraction of bonds it supplies to the mixture.

A chemical kinetic ignition model was used to understand the reactions in the end-gas for various conditions and fuel-air mixtures. A reduced chemistry mechanism for mixtures of primary reference fuels - previously calibrated with rapid compression machine experiments - was used in the engine knock simulation. According to our methodology and definition of knock, the predicted ONR of the primary reference fuel at audible knock are close to the measured values. Since the reduced chemical model was

not calibrated for H_2 and CO addition, the engine knock simulation was not successful in predicting the onset of knock in mixtures containing plasmatron reformate and hydrogen.

To investigate the chemical ignition delay trends with CO and H_2 (individually and together) a constant volume ignition simulation was completed with a comprehensive chemistry mechanism for isooctane. The ignition delay times, which represent the fuels resistance to knock, agree with the experimental conclusion. The model shows that mixtures of isooctane and air have the shortest ignition delay time, followed by mixtures of isooctane + CO, and next by isooctane + H_2,. Addition of plasmatron reformate (H_2, CO, and N_2) results in the longest ignition delay. Experiments showed plasmatron reformate addition was the most effective way to delay the onset of knock, while hydrogen addition had less effect. Fuel mixtures without enhancement by plasmatron reformate or hydrogen showed the least knock resistance. Thus, the results from the comprehensive ignition model are consistent with the experimental trends.

(This page was intentionally left blank.)

Chapter 7 Conclusions

The main conclusions that can be drawn from this work are summarized below:

- Operating the engine with increasingly lean mixtures, while maintaining constant engine torque, slightly increases knock tendency. To maintain constant torque, the airflow is increased, and the fuel flow slightly decreased. A fuel lean mixture has a higher ratio of specific heats, compared with stoichiometric mixtures, and therefore experience higher temperatures rise during compression. Higher temperatures accelerate the end-gas chemical reactions, which ultimately lead to knock. The ONR was higher for lean mixtures compared with near-stoichiometric mixtures at the same engine output, implying that lean operation increases the knock tendency.

- The end-gas can be modeled as a mixture, which experiences an isentropic compression from the time of spark until the peak pressure. A reduced chemistry engine knock simulation was used to effectively model a small element of end-gas. The model calculated the thermodynamic state and composition of the end-gas at each time step, given the initials conditions and pressure profile as a function of time. Autoignition is assumed when the reactions become significant. Autoigntion of primary reference fuels agree well with the experimental data. Predicted autoigntion trends do not agree for mixtures that include H_2 and CO as fuel.

- A comprehensive chemistry model was used to investigate the autoigntion delay times for various fuel mixtures in a constant volume situation where initial conditions were similar to that of the end-gas at peak pressure. The fuel mixtures used in the simulation corresponding to primary reference fuels alone, and with the addition of plasmatron reformate, H_2, and CO. The comprehensive chemical mechanism predicts relative autoigntion delay times that agree with what are expected based on experimental results.

- H_2 and CO have high octane numbers and therefore increase the overall octane number of the fuel mixture when blended with hydrocarbons such as primary reference fuels. For example, when 11% of the fuel energy was from H_2, the ON of the mixture increased by 10. When 13% of the fuel energy was from CO and 11% from H_2, the ON was increased by 20. An effective octane number - for a mixture of H_2, CO and hydrocarbon - can be estimated with a bond-weighted average of the individual fuels' octane numbers. The octane benefits from H_2 and CO do not appear to vary with load or relative air/fuel ratio.

- H_2 and CO help to inhibit knock by slowing the autoigntion reaction and slightly speeding the flame travel. In vehicles with onboard reforming, the octane number of the fuel mixture that would reach the engine is higher. For example, if 15% of the fuel is reformed, the resulting fuel mixture will be approximately ten octane numbers higher than the original hydrocarbon fuel. Based on previous research relating a change in compression ratio to octane requirements (e.g. Russ and Chevron[22][23]), an increase in ten octane numbers would permit an increase of two compression ratios.

References

[1] Heywood, J.B., Internal Combustion Engine Fundamentals, McGraw-Hill, Inc., New York, 1988

[2] Glassman, I., Combustion, Academic Press, Inc., California, 1996.

[3] Tully, E., *Lean-Burn Characteristics of a Gasoline Engine Enriched with Hydrogen from a Plasmatron Fuel Reformer*, M.S. Thesis, MIT, May 2002.

[4] Franklin, M. and Murphy, T., "A Study of Knock and Power Loss in the Automotive Spark Ignition Engine," SAE 890161.

[5] Nakada T., Itoh T., and Takagi Y., "Application of CARS to Development of High Compression Ratio Spark Ignition Engine," SAE 932644.

[6] Taylor, C., The Internal Combustion Engine in Theory and Practice, M.I.T. Press, Cambridge, MA 1985.

[7] Chon, D. and Heywood, J., "Performance Scaling of Spark-Ignition Engines: Correlation and Historical Analysis of Production engine Data," SAE 2000-01-0565.

[8] Gruden, D. and Hahn., R., "Performance, Exhaust Emissions and Fuel Consumption of a IC Engine Operation with Lean Mixtures," I Mech E Publication (C111/79), 1979.

[9] Betts, W., Gozzelino, R., Poullot, B., and Williams, D., "Knock and Engine Trends," Coordinating European Council Second International Symposium, 1985.

[10] Stokes, J., Lake, T., Osborne, R., "A Gasoline Engine Concept for Improved Fuel Economy – The Lean Boost System," SAE 2000-01-2902.

[11] Grandin, B., et al., "Heat Release in the End-Gas Prior to Knock in Lean, Rich and Stoichiometric Mixtures With and Without EGR," SAE 2002-01-0239.

[12] Tang, X., Heffel, J., et al., "Ford P2000 Hydrogen Engine Dynamometer Development", 2002-01-0242.

[13] Green, R. and Pearce, S., "Alternative Transport Fuel," Energy World Journal, pp. 8-11, October 1994.

[14] Natkin, R., Ford Motor Company, Private Communication, June, 2003.

[15] Liu, Z. and Karim G., "Knock Characteristics of Dual-Fueled Engines Fuelled with Hydrogen Fuel," International Journal of Hydrogen, Volume 20, No. 11, 1995.

[16] Shudo, T, Ono, Y. and Takahashi, T., "Ignition Control by DME-Reformed Gas in HCCI Combustion of DME," SAE 2003-01-1824 / JSAE 20030167.

[17] Cheung, H. and Heywood, J., "Evaluation of a One-Zone Burn Rate Analysis Procedure Using Production SI Engine Pressure Data," SAE 932749, 1993.

[18] Chun, K. and Heywood, J., "Estimating Heat-Release and Mass-of-Mixture Burned from Spark-Ignition Engine Pressure Data," Combustion Science and Technology, Vol. 54, pp 133-143, 1987.

[19] Chun, K. and Heywood, J., "Characterization of Knock in a Spark-Ignition Engine," SAE 890159, 1989.

[20] Valtadoros, T., Wong, V., and Heywood, J., "Engine Knock Characteristics at the Audible Level," SAE 910567.

[21] Chun, K., Heywood, J., and Keck, J., "Prediction of Knock Occurrence in a Spark Ignition Engine," 22nd International Symposium on Combustion, The Combustion Institute, pp 455-463, 1988.

[22] Russ, S., "A Review of the Effect of Engine Operating Conditions on Borderline Knock," SAE 960497.

[23] Chevron Technical Review, "Motor Gasolines," 1996.

[24] Hu, H. and Keck, J., "Autoigntion of Adiabatically Compressed Combustible Gas Mixtures", SAE 872110.

[25] Keck, J. and Hu, H., "Explosions of Adiabatically Compressed Gases in a Constant Volume Bomb," 21st International Symposium on Combustion, The Combustion Institute, 1986, pp 521-529.

[26] Cowart, J., and Heywood, J., "The Intensity of Knock in an Internal Combustion Engine: An Experimental and Modeling Study," SAE 922327, 1993.

[27] Brussovansky, S., Heywood, J., Keck, J., "Predicting the Effects of Air and Coolant Temperature, Deposits, Spark Timing and Speed on Knock in Spark Ignition Engine," SAE 922324.

[28] Tanaka, S., Ayala, F., and Keck, J., "A Reduced Chemical Kinetic Model for HCCI Combustion of Primary Reference Fuels," Combustion and Flame, Volume 133, pp 467-481, 2003.

[29] Tanaka, Ayala, Keck, and Heywood, "Two-stage ignition in HCCI combustion and HCCI control by fuels and additives," Combustion and Flame, Volume 132,pp 219-239, 2003.

[30] Ayala, F., *Data Base Generation and Modeling of Homogeneous Charge Compression Ignition Using a Rapid Compression Machine*, M.S. Thesis, MIT, 2001.

[31] Fox, J., Cheng, W., and Heywood J., "A Model for Predicting Residual Gas Fraction in Spark-Ignition Engines," SAE 931025.

[32] Curran, H., Gaffuri, P., Pitz, W., and Westbrook, C., "A Comprehensive Modeling Study of Isooctane Oxidation," Combustion and Flame, 129:253-280 (2002).

Appendix A: Operating Condition Specifications

Mid-Load
Primary Reference Fuels, No Plasmatron Tests
1500 rpm

Run	Lambda [Rel AFR]	MAP [bar]	Fuel IPW [ms]	MBT Spark [deg BTDC]	NIMEP [bar]	O.N.R.
A	1.5	.995	8.3	18	6.7	93
B	1.3	.977	8.5	14	6.7	90
C	1.1	.90	8.8	12	6.7	88
D	.95	.86	9.59	10	6.7	88

Run	Lambda [Rel AFR]	MAP [bar]	Fuel IPW [ms]	Spark [deg BTDC]	NIMEP [bar]	O.N.R.
E (A)	1.5	1.0	8.3	18	6.7	93
F	1.5	.9	6.8	27	5.1	80
G	1.5	.8	6.1	29	4.4	75

Run	Lambda [Rel AFR]	MAP [bar]	Fuel IPW [ms]	Spark [deg BTDC]	NIMEP [bar]	O.N.R.
H (F)	1.5	.9	6.79	27	5.1	80
J	1.3	.9	7.73	17	5.9	82
K (C)	1.1	.9	8.8	12	6.7	88
L	.95	.9	10.1	10	7.14	90

Run	Lambda [Rel AFR]	MAP [bar]	Fuel IPW [ms]	Spark [deg BTDC]	NIMEP [bar]	O.N.R.
M	.95	.781	8.8	11	6.0	82
N (C)	1.1	.9	8.8	12	6.7	88
P	1.3	.981	8.8	14	6.9	92
Q	1.5	.996	8.8	18	7.2	98

High Load
Primary Reference Fuels, No Plasmatron Tests
1500 rpm

Run	Lambda [Rel AFR]	MAP [bar]	Fuel IPW [ms]	MBT Spark [deg BTDC]	NIMEP [bar]	O.N.R.
ZZ	1.7	1.48	10.3	27	8.5	99
AA	1.5	1.33	10.2	21	8.5	98
BB	1.3	1.208	10.4	15	8.5	96
CC	1.1	1.09	10.89	11	8.5	96
DD	.95	1.045	11.8	10	8.5	96

Run	Lambda [Rel AFR]	MAP [bar]	Fuel IPW [ms]	MBT Spark [deg BTDC]	NIMEP [bar]	O.N.R.
EE (AA)	1.5	1.33	10.2	21	8.5	98
FF	1.5	1.2	9.29	22	7.5	94
GG (KK)	1.5	1.1	8.3	23	6.57	90

Run	Lambda [Rel AFR]	MAP [bar]	Fuel IPW [ms]	MBT Spark [deg BTDC]	NIMEP [bar]	O.N.R.
HH (CC)	1.1	1.045	10.89	11	8.5	96
JJ	1.3	1.09	9.4	16	7.5	92
KK	1.5	1.09	8.3	23	6.6	90
LL	1.7	1.09	7.56	32	5.8	85

Run	Lambda [Rel AFR]	MAP [bar]	Fuel IPW [ms]	MBT Spark [deg BTDC]	NIMEP [bar]	O.N.R.
MM	.95	.941	10.89	10	7.57	92
NN (CC)	1.1	1.045	10.89	11	8.5	96
PP	1.3	1.26	10.89	15	8.85	97
QQ	1.5	1.422	10.89	15	9.13	100

Mid-Load Plasmatron Points

	0% plas *0% H_2 energy*	**15% plas** *~5.75% H_2 energy*	**30% plas** *~11.2% H_2 energy*
Lambda = 1.1	**Run: C*** **04_07_03**	**Run: R** **03_31_03**	**Run: S** **03_31_03**
	MAP = 0.9 bar	MAP = 0.948 bar	MAP = .997 bar
	FUEL = 8.99	FUEL =7.71 ms	FUEL =6.61 ms
	PLAS = 0	PLAS = 32 psi (orf 31)	PLAS = 75 psi (orf 31)
	SP = 12 deg BTDC	SP = 10 deg BTDC	SP = 9 deg BTDC
	NIMEP = 6.7 bar	NIMEP = 6.7 bar	NIMEP = 6.7 bar
	ONR = 86	ONR = 78	ONR = 68
Lambda = 1.3	**Run: B*** **04_07_03**	**Run: X** **03_31_03**	**Run: Y** **03_31_03**
	MAP = 1.0 bar	MAP = 1.05 bar	MAP = 1.1 bar
	FUEL = 8.66	FUEL = 7.53 ms	FUEL = 6.39 ms
	PLAS = 0	PLAS = 30 psi (orf 31)	PLAS = 72 psi (orf 31)
	SP = 15 deg BTDC	SP = 13 deg BTDC	SP = 12 deg BTDC
	NIMEP = 6.7 bar	NIMEP = 6.7 bar	NIMEP =6.7 bar
	ONR = 88	ONR = 78	ONR = 65
Lambda =1.5	**Run: A*** **04_07_03**	**Run: T** **03_31_03**	**Run: U** **03_31_03**
	MAP = 1.1 bar	MAP = 1.15 bar	MAP = 1.21 bar
	FUEL = 8.41	FUEL = 7.33	FUEL =6.29
	PLAS = 0	PLAS = 28 psi (orf 31)	PLAS = 68 psi (orf 31)
	SP = 20 deg BTDC	SP = 18 deg BTDC	SP = 16 deg BTDC
	NIMEP =6.7 bar	NIMEP =6.7 bar	NIMEP = 6.7 bar
	ONR = 90	ONR = 78	ONR = 65

Test Points A*, B*, and C* were run with compressed air on 04_07_03.

High Load Plasmatron Points

	0% plas *0% H_2 energy*	**15% plas** *~5.5% H_2 energy*	**30% plas** *~11.4% H_2 energy*
Lambda = 1.1	**Run: CC** **Data of Tests: 03_30_03**	**Run: RR** **Data of Tests: 04_05_03**	**Run: SS** **Data of Tests: 04_05_03**
	MAP = 1.09 bar	MAP = 1.15 bar	MAP = 1.22 bar
	FUEL =10.89 ms	FUEL =9.49 ms	FUEL =8.11 ms
	PLAS = 0 psi	PLAS = 40 psi (orf 31)	PLAS = 72 psi (orf 35)
	SP = 11 deg BTDC	SP = 10 deg BTDC	SP = 9 deg BTDC
	NIMEP = 8.5 bar	NIMEP =8.5 bar	NIMEP = 8.5 bar
	ONR = 96	ONR = 88	ONR = 78
Lambda = 1.3	**Run: BB** **Data of Tests: 03_30_03**	**Run: XX** **Data of Tests: 04_05_03**	**Run: YY** **Data of Tests: 04_05_03**
	MAP = 1.2 bar	MAP = 1.28 bar	MAP = 1.33 bar
	FUEL =10.4 ms	FUEL =9.21 ms	FUEL =7.79 ms
	PLAS = 0 psi	PLAS = 38 psi (orf 31)	PLAS = 68 psi (orf 35)
	SP = 15 deg BTDC	SP = 13 deg BTDC	SP = 11 deg BTDC
	NIMEP = 8.5 bar	NIMEP = 8.5 bar	NIMEP = 8.5 bar
	ONR = 96	ONR = 90	ONR = 78
Lambda =1.5	**Run: AA** **Data of Tests: 03_30_03**	**Run: TT** **Data of Tests: 04_05_03**	**Run: UU** **Data of Tests: 04_05_03**
	MAP = 1.33 bar	MAP = 1.4 bar	MAP = 1.475 bar
	FUEL =10.26 ms	FUEL =9.01 ms	FUEL =7.71 ms
	PLAS = 0 psi	PLAS = 37 psi (orf 31)	PLAS = 66 psi (orf 35)
	SP = 21 deg BTDC	SP = 19 deg BTDC	SP = 16 deg BTDC
	NIMEP = 8.5 bar	NIMEP = 8.5 bar	NIMEP = 8.5 bar
	ONR = 98	ONR = 90	ONR = 78

Continued on next page

	Run: ZZ Data of Tests: 03_30_03	Run: zed Data of Tests: 04_05_03	Run: ZZZ Data of Tests: 04_05_03
Lambda=1.7	MAP = 1.5 bar	MAP = 1.5 bar	MAP =1.6 bar
	FUEL =10.3 ms	FUEL =8.99 ms	FUEL =7.61 ms
	PLAS = 0 psi	PLAS = 35 psi (orf 31)	PLAS = 66 psi (orf 35)
	SP = 27 deg BTDC	SP = 25 deg BTDC	SP = 24 deg BTDC
	NIMEP = 8.5 bar	NIMEP = 8.5 bar	NIMEP = 8.5 bar
	ONR = 99	ONR = 90	ONR = 80

Mid-Load Hydrogen Points

	0% H_2 energy *Equivalent H_2 to 0% plas*	**5.75% H_2 energy** *Equivalent H_2 to 15% plas*	**11.3% H_2 energy** *Equivalent H_2 to 30% plas*
Lambda = 1.1	**Run: C*** **04_07_03**	**Run: HR**	**Run: HS** **04_16_03**
	MAP = 0.9 bar	MAP = 0.911 bar	MAP =0 .928 bar
	FUEL = 8.99 ms	FUEL =8.66 ms	FUEL = 8.1 ms
	H2 = 0	H2 = 60 (orf #6)	H2 =38 psi (orf #11)
	SP = 12 deg BTDC	SP = 10	SP = 9 deg BTDC
	NIMEP = 6.7 bar	NIMEP = 6.7 bar	NIMEP = 6.7
	ONR = 86	ONR = 80	ONR = 76
Lambda = 1.3	**Run: B*** **04_07_03**	**Run: HX**	**Run: HY** **04_16_03**
	MAP = 1.0 bar	MAP = 1.0 bar	MAP = 1.0 bar
	FUEL = 8.66 ms	FUEL = 8.36 ms	FUEL = 7.81 ms
	H2 = 0	H2 = 56 (orf #6)	H2 = 35 (orf #11)
	SP = 15 deg BTDC	SP = 13	SP = 11
	NIMEP = 6.7 bar	NIMEP =6.7 bar	NIMEP =6.7 bar
	ONR = 88	ONR = 82	ONR = 76
Lambda =1.5	**Run: A*** **04_07_03**	**Run: HT**	**Run: HU** **04_16_03**
	MAP = 1.1 bar	MAP = 1.11 bar	MAP = 1.11 bar
	FUEL = 8.41 ms	FUEL = 8.19 ms	FUEL = 7.61 ms
	H2 = 0	H2 = 55 (orf #6)	H2 =34 psi (orf #11)
	SP = 20 deg BTDC	SP = 18	SP= 15
	NIMEP =6.7 bar	NIMEP = 6.7 bar	NIMEP = 6.76
	ONR = 90	ONR = 84	ONR = 78

High Load Hydrogen Points

	0% H_2 energy *Equivalent H_2 to 0% plas*	**5.75% H_2 energy** *Equivalent H_2 to 15% plas*	**11.3% H_2 energy** *Equivalent H_2 to 30% plas*
Lambda = 1.1	**Run: CC** **Data of Tests: 03_30_03**	**Run: HRR** **Data of Tests:**	**Run: HSS** **Data of Tests: 04_16_03**
	MAP = 1.09 bar	MAP = 1.11 bar	MAP = 1.12 bar
	FUEL =10.89 ms	FUEL =10.5 ms	FUEL = 9.9 ms
	H2 = 0 psi	H2 = 75 (orf # 6)	H2 = 50 (orf #11)
	SP = 11 deg BTDC	SP = 10	SP = 8
	NIMEP = 8.5 bar	NIMEP = 8.5 bar	NIMEP = 8.5 bar
	ONR = 96	ONR = 90	ONR = 85
Lambda = 1.3	**Run: BB** **Data of Tests: 03_30_03**	**Run: HXX** **Data of Tests:**	**Run: HYY** **Data of Tests: 04_16_03**
	MAP = 1.2 bar	MAP = 1.26 bar	MAP = 1.246 bar
	FUEL =10.4 ms	FUEL =10.16 ms	FUEL = 9.49 ms
	H2= 0 psi	H2 = 73 (orf #6)	H2 = 48 (orf #11)
	SP = 15 deg BTDC	SP = 13	SP = 10
	NIMEP = 8.5 bar	NIMEP = 8.5 bar	NIMEP = 8.5 bar
	ONR = 96	ONR = 92	ONR = 88
Lambda =1.5	**Run: AA** **Data of Tests: 03_30_03**	**Run: HTT** **Data of Tests:**	**Run: HUU** **Data of Tests: 04_16_03**
	MAP = 1.33 bar	MAP = 1.35 bar	MAP = 1.36 bar
	FUEL =10.26 ms	FUEL =9.91 ms	FUEL =9.26 ms
	H2= 0 psi	H2 = 71 (orf #6)	H2 = 46 (orf #11)
	SP = 21 deg BTDC	SP = 15	SP = 13
	NIMEP = 8.5 bar	NIMEP = 8.5 bar	NIMEP = 8.5 bar
	ONR = 98	ONR = 92	ONR = 88

Continued on next page

	Run: ZZ Data of Tests: 03_30_03	Run: Hzed Data of Tests:	Run: HZZZ Data of Tests: 04_16_03
Lambda=1.7	MAP = 1.5 bar	MAP = 1.47 bar	MAP = 1.5 bar
	FUEL =10.3 ms	FUEL = 9.81 ms	FUEL = 9.11ms
	H2= 0 psi	H2 = 70 (orf #6)	H2 = 45 (orf #11)
	SP = 27 deg BTDC	SP = 22	SP = 19
	NIMEP = 8.5 bar	NIMEP = 8.5 bar	NIMEP = 8.5
	ONR = 99	ONR = 93	ONR = 88

Additional Points

Primary Reference Fuels, No Plasmatron Tests, 1500rpm

Run	Lambda [Rel AFR]	MAP [bar]	Fuel IPW [ms]	MBT Spark [deg BTDC]	NIMEP [bar]	O.N.R.
Knock Limit & Lean limit	1.8	1.51	10.2	31	8.41	99+

Run	Lambda [Rel AFR]	MAP [bar]	Fuel IPW [ms]	MBT Spark [deg BTDC]	NIMEP [bar]	O.N.R.
Knock Limit	1.7	1.46	10.3	27	8.54	99+
ZA	1.7	1.1	7.79	33	5.92	84
Lean Lt (ZB)	1.7	0.9	6.3	38	4.52	78

Run	Lambda [Rel AFR]	MAP [bar]	Fuel IPW [ms]	MBT Spark [deg BTDC]	NIMEP [bar]	O.N.R.
Knock Limit	1.6	1.44	10.6	24	8.81	99+
ZE	1.6	1.10	8.09	29	6.22	88
Lean Lt (ZF)	1.6	.744	5.51	32	3.61	65

Run	Lambda [Rel AFR]	MAP [bar]	Fuel IPW [ms]	MBT Spark [deg BTDC]	NIMEP [bar]	O.N.R.
Knock Limit	1.5	1.40	10.89	20	8.96	99+
F*	1.5	.9	6.99	26	5.12	80
Lean Lt (ZD)	1.5	.693	5.4	29	3.40	65

Run	Lambda [Rel AFR]	MAP [bar]	Fuel IPW [ms]	MBT Spark [deg BTDC]	NIMEP [bar]	O.N.R.
Knock Limit	1.3	1.3	11.3	15	9.15	99+
J*	1.3	.89	7.81	17	5.77	80
Lean Lt. (ZJ)	1.3	.7	6.13	19	4.19	68

Run	Lambda [Rel AFR]	MAP [bar]	Fuel IPW [ms]	MBT Spark [deg BTDC]	NIMEP [bar]	O.N.R.
L*	0.95	.9	10.29	10	7.07	88
ZL	0.95	.71	8.1	11	5.23	78

Appendix B: Modified Fortran Codes

The FORTRAN programs for the engine knock simulation are presented in this appendix. The subroutines that were modified for this application are:

1. driver.f
2. realkin.f
3. reaction.f

```
      program driver
ccccccccccccccccccccccccccccccccccccccccccccccccccccccccccccccccccccccc
c a program for driving the HCCI combustion model
c written by David Schmidt, MIT Sloan Automotive Laboratory
c 2000
c modified by Shigeyuki Tanaka, MIT Sloan Automotive Lab.
c 2001
c remodified by Shigeyuki Tanaka, MIT Sloan Automotive Lab.
c for engine cycle simulation of HCCI combustion
c 2002
c remodified by Jennifer Topinka, MIT Sloan Automotive Lab.
c for spark-ignition engine end-gas autoignition prediction.
c 2003
c
c all units in meters, kilograms, kelvin, kmoles unless specified
c otherwise
c
c this is going to be "eine Katzenjammer" since ChemKin works in
c CGS units
ccccccccccccccccccccccccccccccccccccccccccccccccccccccccccccccccccccccc

      implicit none


c************ run parameters ***********

c time at which the simulation ends and time step size
      real*8 t_end, deltat, dPdt

c number of time steps and pressure data points
      integer nsteps, psteps

c number of data points in pressure file, change this as needed
       parameter (psteps = 12200)

c storage for pressure data
       real*8 presshistory(psteps)

c volume, temperature, pressure of the chamber
      real*8 volume , temp,  press

c specific volume at start of calculation
      real*8 vol0

c differential change in volume [cu. meters]
      real*8 dv


c************ species vectors ***********

c storage--intended only for use in kinetic calcultions
c numbers of moles of up to fourty real species in moles
      real*8 species(40)

c species initial masses--the first twenty species
c are storage for "real" species and the second twenty are for
c pseudo-species from the ignition chemistry.  This vector
c is used ONLY for initializing the moles.
      real*8 m_spec(40)


c************ chemistry variables ***********
```

```
c  energy of heat release[J] for this time step
      real*8 enrel

c internal energy [J]
      real*8 energy

c work out of the cylinder (p*dv) in [J]
      real*8 work

c universal gas constant in J/kmol-K
      real*8 R_gas
      parameter (R_gas = 8.314E3)

c ratio of specific heats
      real*8 gamma

c the total mass
      real*8 totmass


c************ variables for ChemKin ***********

c lengths of integer, real, and character work arrays
      integer leniwk,lenrwk,lencwk
      parameter (leniwk=4000,lenrwk=4000,lencwk=4000)

c delcare integer, real, and character work arrays
      integer   ickwrk(leniwk)
      real*8      rckwrk(lenrwk)
      character*16 cckwrk(lencwk)

c logical unit numbers for input and output
c linc is for the Chemkin binary file
c lout if for the real species output
      integer linc,lout
      parameter (linc=55,lout=66)

c numbers of elements, species, and reactions
      integer mm,kk,ii

c number of coefficents in fits to thermodynamic data
      integer nfit


c************ local work variables ***********

c which step number we are on
      integer istep

c the current time
      real*8 tim

c the state of the stiff ODE integrator
      integer istate

c the pressure at the last time step
      real*8 oldpress

c the volume before updating
      real*8 oldvol
```

```
c************ initialization  ***********

c order of initial species mass fractions.
c data is able to calculated by excel file.
c
c     species       C8H18,     O2,        N2,        CO2,        H2O,
      data m_spec / 0.039602979, 0.22149213, 0.722758004, 4.336e-4, 0.0,

c                   C7H16,     CO,        OH,        HO2,        H2O2,
     &              0.003435821, 0.00000,  0.0e-15,   0.0e-15, 0.0,
c
c                   H2,         O,         AR,        H,
     &             0.00000000,   0.000000,  0.01227484, 0.0000,
     & 26*0.0 /

      data species /40*0.0E-9/


c time stepping information
      tim   = 0.0
      t_end =.010
      deltat=1.00e-6
      nsteps = nint(t_end/deltat)

c initial conditions: vol0 is the specific volume [m3/kg],
c                                 press is the initial pressure [Pa].

       vol0 = 0.1327
      volume = vol0
       press = 1481500


c initial condition will be the energy datum
      energy = 0.0

c intialize state variable for stiff ODE solver
      istate = 1

c open ChemKin binary data file
      open(linc, file ='chem.bin',form='UNFORMATTED',status='old')

c open output file, overwriting previous contents
      open(lout, file='driver.txt', status ='unknown')

c initializes ChemKin arrays and reads data files
      call CKINIT(LENIWK, LENRWK, LENCWK, LINC, 6, ICKWRK,
     &                   RCKWRK, CCKWRK)

c initialize other arrays
      call CKINDX(ICKWRK, RCKWRK, MM, KK, II, NFIT)

c initializes species vectors
      call spec_init(cckwrk,kk,m_spec, species)

c calculate initial pressure in the chamber
      call intherm(temp,volume,species,kk,ickwrk,rckwrk,
     &             press,gamma)

      tim=0

c do initial output
```

```
c calculate mass
      call calcmass(CCKWRK,kk, species, totmass)

      call putout(gamma,lout,tim,kk, species,
     &     temp, press, cckwrk, totmass,volume)


      write(6,*)
      write(6,'(a,i6,a)')'Calculating ',nsteps,' time steps'
      write(6,*)

c read pressure file in, store in presshistory.
c Note:  The data points must occur once every timestep.
c Interprelate data before reading in.

       open (13, File='pressure_032504_54.txt', status='old')
       read (13, *) presshistory



c************ main time stepping loop *************
      do istep = 1, nsteps


         write(6,'(3a,f8.3,a,f8.3)')char(27),char(77),
     & 'Time [ms] : ',tim*1000.0,'   Temperature* : ', temp

c save pressure, calculate dPdt
         oldpress =press

          press = presshistory(istep)

       dPdt=(press-oldpress)/deltat


c step reactions forward one time step.
c updates the following variables:  time, preign, ignit, species,
c                                   temp, pressure, enrel, istate
c note:  Temperature is updated by conservation of energy.


         call reaction(dPdt,tim,deltat, species,
     &                 temp, press, volume,kk,ickwrk,rckwrk,
     &                 enrel,istate)



c update thermodynamic state, updates energy,
c and returns gamma
         call uptherm( kk,ICKWRK, RCKWRK, work,
     &   energy,enrel,species, volume, temp, press,gamma)

calculate mass
         call calcmass(CCKWRK,kk, species, totmass)

c write output to driver.txt
         call putout(gamma,lout,tim,kk, species,
     &               temp, press,cckwrk, totmass,volume)

      enddo
c************ end of main time stepping loop *************
```

```
close output file
      close(lout)

      write(6,*)
      write(6,*)'Work Completed.'

      stop
      end

c end of main program
```

```
c step reactions forward one time step
      subroutine reaction(dPdt, tim,deltat, species,
     &     temp, press, volume,kk,ickwrk,rckwrk,
     &     enrel,istate)

ccccccccccccccccccccccccccccccccccccccccccccccccccccccccccccccccccc
c a subroutine for driving the HCCI combustion model
c written by David Schmidt, MIT Sloan Automotive Laboratory
c 2000
c modified by Shigeyuki Tanaka, MIT Sloan Automotive Lab.
c 2001
c modified by Jennifer Topinka, MIT Sloan Automotive Lab.
c Call to VODE changed to include dPdt, 2003.

c this subroutine calculates the change in species concentrations and
c heat release for one time step.
c
ccccccccccccccccccccccccccccccccccccccccccccccccccccccccccccccccccc


      implicit none


c************subroutine parameters ***********

c time [s]
      real*8 tim

c time interval
      real*8 deltat

c storage--intended only for use in kinetic calcultions
c numbers of moles of up to fourty chemkin species in moles
      real*8 species(40)

c volume, temperature, pressure of the chamber
      real*8 volume , temp,  press, dPdt

c number of species
      integer kk

c energy released by combustion [J]
      real*8 enrel


c************variables for ChemKin ***********

c lengths of integer, real, and character work arrays
      integer lenick,lenrck,lencck
      parameter (lenick=4000,lenrck=4000,lencck=4000)

c delcare integer, real, and character work arrays
      integer   ickwrk(lenick)
      real*8      rckwrk(lenrck)


c***********External functions for Stiff ODE's
      external realkin, jac


c************local variables ***********
      integer i
```

```
c tells the state of the stiff ODE solver
      integer istate

c mole fraction of each real species
      real*8 molefrac(40)

c cv (converted from CGS to MKS units)
      real*8 cv

c total moles
      real*8 totmole

c end time of integration
      real*8 tout

c new and old sensible enthalpy [J]
      real*8 newenth, oldenth

c*******Local Variables--work and parameter arrays

c real and integer work space
      real*8 rpar(lenrck+2)
      integer ipar(lenick+1)
      real*8 yvec(42),ydot(42)

c work arrays for the stiff ODE solver
      real*8 RWORK(lenrck)
      integer IWORK(lenick)

c these variables should be saved between calls to VODE
      save RWORK,IWORK
      data rwork/lenrck*0.0/
      data iwork/lenick*0.0/


c************begin  ***********

c the stiff solver will need to re-initialize every time step
c because other routines may have changed temp & press
      istate=1

      tout = tim+deltat

c calculate total moles of all of the species (pseudo-species don't count)
      totmole = 0.0
      do i=1,kk
         totmole = totmole + species(i)
      enddo

c mole fractions
      do i=1,kk
         molefrac(i)= species(i)/(totmole)
      enddo

c calculate Cv--[ergs/mol]
      call ckcvbl(temp,molefrac,ickwrk,rckwrk,cv)

c convert cv to J/mol-K units
      cv = cv * 1.0D-7

c store sensible enthalpy
      oldenth = cv*temp*totmole
```

```
c------------- chemkin chemistry

c initialize parameter storage from variables
         yvec(1) = temp
         yvec(2) = volume
         do i=1,40
            yvec(i+2)=species(i)
         enddo

         rpar(1) = press
         rpar(2) = cv
         do i=1,lenrck
            rpar(i+2)=rckwrk(i)
         enddo

         ipar(1) = kk
         do i=1,lenick
            ipar(i+1)=ickwrk(i)
         enddo



c call the stiff ODE integrator
         iwork(6)=100000
         call dvode(realkin,kk+2,yvec,tim,tout,1,1.0d-6 ,1.0d-12,
     &         1,istate,1, RWORK,lenrck,IWORK,lenick,jac,
     &         22,rpar,ipar, dPdt)

c check for successful completion
         if (istate.lt.0) then
            write(6,*)'Failure in Stiff ODE solver.'
            write(6,*)'Stopping.'
            stop
         endif

c copy variables from parameter storage
         temp    = yvec(1)
         volume  = yvec(2)
         do i=1,40
            species(i)=yvec(i+2)
         enddo


         cv      = rpar(2)


c calc new sensible enthalpy--note that the number of moles may have changed
      totmole = 0.0
      do i=1,kk
         totmole = totmole + species(i)
      enddo
      newenth = cv*temp*totmole

c energy release is the change in sensible enthalpy
      enrel = newenth - oldenth

      do i=1,40
c check for negative moles
         if (species(i).lt.0.0) then
            write(6,*)
            write(6,*)"Warning:  ",
```

```
     &           "negative species concentration for species ",i
            write(6,*)"Mass is not conserved.  Reduce timestep.
     &           "

c zero out species
            species(i)=0.0
          endif
        enddo


        return
        end
```

```
      subroutine realkin(dPdt,neq,tim,yvec,ydot,rpar,ipar)

c Elementary Kinetics:

ccccccccccccccccccccccccccccccccccccccccccccccccccccccccccccccccc
c a subroutine for driving the HCCI combustion model
c written by David Schmidt, MIT Sloan Automotive Laboratory
c 2000
c modified by Shigeyuki Tanaka, MIT Sloan Automotive Lab.
c 2001
c remodified by Jennifer Topinka, MIT Sloan Automotive Lab.
c Changed governing equations, 2003.
c
c
c This subroutine is called by the stiff equation solver. It takes
c data stored in Rpar and Ipar and uses it to operate on a vector, yvec.
c Yvec contains all the highly transient variables. The subroutine
c returns their time derivatives in ydot.
c
ccccccccccccccccccccccccccccccccccccccccccccccccccccccccccccccccc


      implicit none

c**************Parameters***********************************

c the number of equations
      integer neq

c the time
      real*8 tim, oldpress

c the yvector and its derivative
      real*8 yvec(42),ydot(42)

c lengths of integer, real, and character work arrays
      integer lenick,lenrck,lencck
      parameter (lenick=4000,lenrck=4000,lencck=4000)

c real and integer work space
      real*8 rpar(lenrck+2)
      integer ipar(lenick+1)

c the Universal Gas Constant in J/mol-K
      real*8 Ru
      parameter (Ru=8.314)


c*************Local Variables--from Parameter storage*********

c the temperature is the first entry in yvec
      real*8 temp

c the pressure is the second entry in yvec
      real*8 press

c the species vector is stored in the yvec
      real*8 species(40)

c the volume is the first entry in rpar
      real*8 volume
```

```
c cv [J/kg-K] is the second entry in rpar
      real*8 cv

c the array rckwrk(lenrck) starts with the third entry in rpar
c don't need to declare, since we are just passing this

c the number of species, kk, is stored as the first entry in ipar
      integer kk

c the array ickwrk(lenick) starts with the second entry in ipar
c don't need to declare this, since we are just passing it


c**************Local Variables**************************

c molar enthalpies in CGS units
      real*8 uml(40)

c molar species production rates
      real*8 wdot(40)

c energy released [J]
      real*8 enrel

c mole fraction of each real species
      real*8 molefrac(40)

c total mass
      real*8 totmole

c pressure and volume in cgs units
      real*8 cgspress,cgsvol

c dTdt is the time derivative of temperature [K/s]
      real*8 dTdt

c dPdt is the time derivative of pressure [Pa/s]
      real*8 dVdt, dPdt

c dndt is the time derivative of the total number of moles [mol/s]
      real*8 dndt

c loop index
      integer i

c***************Executable Statments**************************

cinitialize energy release
      enrel = 0.0

c initialize variables from parameter storage
      temp   = yvec(1)
      volume  = yvec(2)
      do i=1,40
         species(i)=yvec(i+2)
      enddo

      press = rpar(1)
      cv     = rpar(2)
      kk     = ipar(1)

c convert pressure and volume to cgs units
```

```
      cgspress = press * 10.0
      cgsvol   = volume * 100**3

c calculate total moles of all of the species (pseudo-species don't count)
      totmole = 0.0
      do i=1,kk
         totmole = totmole + species(i)
      enddo

c mole fractions
      do i=1,kk
         molefrac(i)= species(i)/(totmole)
      enddo

c get species enthalpies
      call ckuml(temp,ipar(2),rpar(3),uml)

c get production rates ( wdot is in mol/cc/sec)
      call ckwxp(cgspress,temp,molefrac,ipar(2),rpar(3),wdot)

      dndt = 0


convert wdot to mol/s
      do i=1,kk
         wdot(i)=wdot(i)*cgsvol
         dndt=dndt + wdot(i)
      enddo

calculate energy release in ergs/sec:
c use the energy of the species * their change over the time sub-step
      do i=1,kk
         enrel=enrel-uml(i)*wdot(i)
      enddo

convert energy release from ergs/s to J/s units
      enrel = enrel * 1.0E-7

c use the ideal gas law and first law of thermodynamics

       dVdt=(-(volume/press*dPdt)+(Ru*temp/press*dndt)+
     & (Ru/(press*cv)*enrel))/(1+(Ru/cv))


      dTdt = (enrel/( cv * totmole))-(press/totmole/cv*dVdt)


c store the derivatives of y in ydot
      ydot(1) = dTdt
      ydot(2) = dVdt
      do i=1,40
         ydot(i+2)=wdot(i)
      enddo

      return
      end
ccccccccccccccccccccccccccccccccccccccccccccccccccccccccccccccccccccccccccccccc

c dummy jacobian routine
      subroutine jac
      end
```

Appendix C: Reduced Chemistry Mechanism

```
CHEMKIN INTERPRETER OUTPUT: CHEMKIN-II Version 3.6 Apr. 1994
                            DOUBLE PRECISION

                          --------------------
                          ELEMENTS     ATOMIC
                          CONSIDERED   WEIGHT
                          --------------------
                           1. H       1.00797
                           2. O       15.9994
                           3. N       14.0067
                           4. AR      39.9480
                           5. C       12.0112
                          --------------------
------------------------------------------------------------------------------
                        C
                      P H
                      H A
                      A R
SPECIES               S G MOLECULAR TEMPERATURE   ELEMENT COUNT
CONSIDERED            E E WEIGHT    LOW    HIGH   H  O  N  AR C
------------------------------------------------------------------------------
  1. H2               G 0   2.01594  300.0 5000.0  2  0  0  0  0
  2. H                G 0   1.00797  300.0 5000.0  1  0  0  0  0
  3. O2               G 0  31.99880  300.0 5000.0  0  2  0  0  0
  4. O                G 0  15.99940  300.0 5000.0  0  1  0  0  0
  5. OH               G 0  17.00737  300.0 5000.0  1  1  0  0  0
  6. HO2              G 0  33.00677  300.0 5000.0  1  2  0  0  0
  7. H2O2             G 0  34.01474  300.0 5000.0  2  2  0  0  0
  8. H2O              G 0  18.01534  300.0 5000.0  2  1  0  0  0
  9. N2               G 0  28.01340  300.0 5000.0  0  0  2  0  0
 10. N                G 0  14.00670  300.0 5000.0  0  0  1  0  0
 11. NO               G 0  30.00610  300.0 5000.0  0  1  1  0  0
 12. CO               G 0  28.01055  300.0 5000.0  0  1  0  0  1
 13. CO2              G 0  44.00995  300.0 5000.0  0  2  0  0  1
 14. AR               G 0  39.94800  300.0 5000.0  0  0  0  1  0
 15. C8H18            G 0 114.23266  300.0 5000.0 18  0  0  0  8
 16. OC2              G 0 113.22469  300.0 5000.0 17  0  0  0  8
 17. OC3              G 0 112.21672  300.0 5000.0 16  0  0  0  8
 18. OC4              G 0 128.21612  300.0 5000.0 16  1  0  0  8
 19. OC5              G 0 145.22349  300.0 5000.0 17  2  0  0  8
 20. OC6              G 0 145.22349  300.0 5000.0 17  2  0  0  8
 21. OC7              G 0 177.22229  300.0 5000.0 17  4  0  0  8
 22. OC8              G 0 160.21492  300.0 5000.0 16  3  0  0  8
 23. OC9              G 0 143.20755  300.0 5000.0 15  2  0  0  8
 24. OC10             G 0 113.18106  300.0 5000.0 13  1  0  0  7
 25. OC11             G 0  30.02649  300.0 5000.0  2  1  0  0  1
 26. OC12             G 0 142.19958  300.0 5000.0 14  2  0  0  8
 27. OC13             G 0 140.18364  300.0 5000.0 12  2  0  0  8
 28. C7H16            G 0 100.20557  300.0 5000.0 16  0  0  0  7
 29. HE2              G 0  99.19760  300.0 5000.0 15  0  0  0  7
 30. HE3              G 0  98.18963  300.0 5000.0 14  0  0  0  7
 31. HE4              G 0 114.18903  300.0 5000.0 14  1  0  0  7
```

32. HE5	G	0	131.19640	300.0	5000.0	15	2	0	0	7
33. HE6	G	0	131.19640	300.0	5000.0	15	2	0	0	7
34. HE7	G	0	163.19520	300.0	5000.0	15	4	0	0	7
35. HE8	G	0	146.18783	300.0	5000.0	14	3	0	0	7
36. HE9	G	0	129.18046	300.0	5000.0	13	2	0	0	7
37. HE10	G	0	57.07270	300.0	5000.0	5	1	0	0	3
38. HE11	G	0	72.10776	300.0	5000.0	8	1	0	0	4
39. HE12	G	0	128.17249	300.0	5000.0	12	2	0	0	7
40. HE13	G	0	126.15655	300.0	5000.0	10	2	0	0	7

REACTIONS CONSIDERED	(k = A T**b exp(-E/RT)) A	b	E
1. C7H16+O2<=>HE2+HO2	1.00E+16	0.0	46000.0
Reverse Arrhenius coefficients:	1.00E+12	0.0	0.0
2. HE2+O2<=>HE5	1.00E+12	0.0	0.0
Reverse Arrhenius coefficients:	2.51E+13	0.0	27400.0
3. HE5<=>HE6	1.51E+11	0.0	19000.0
Reverse Arrhenius coefficients:	1.00E+11	0.0	11000.0
4. HE6+O2<=>HE7	3.16E+11	0.0	0.0
Reverse Arrhenius coefficients:	2.51E+13	0.0	27400.0
5. HE7=>HE8+OH	8.91E+10	0.0	17000.0
6. C7H16+OH=>HE2+H2O	1.00E+13	0.0	3000.0
7. HE2+O2<=>HE3+HO2	3.16E+11	0.0	6000.0
Reverse Arrhenius coefficients:	3.16E+11	0.0	19500.0
8. HE3+HO2+7O2=>7CO+7H2O+HO2	3.16E+13	0.0	10000.0
9. HE8=>HE9+OH	3.98E+15	0.0	43000.0
10. HE9+O2<=>HE12+HO2	3.16E+11	0.0	6000.0
Reverse Arrhenius coefficients:	3.16E+11	0.0	19500.0
11. HO2+HE12+O2=>H2O2+HE13+HO2	3.16E+13	0.0	10000.0
12. HO2+HE13+5O2=>7CO+5H2O+HO2	3.16E+13	0.0	10000.0
13. C8H18+O2<=>OC2+HO2	1.00E+16	0.0	46000.0
Reverse Arrhenius coefficients:	1.00E+12	0.0	0.0
14. OC2+O2<=>OC5	1.00E+12	0.0	0.0
Reverse Arrhenius coefficients:	2.51E+13	0.0	27400.0
15. OC5<=>OC6	1.14E+11	0.0	22400.0
Reverse Arrhenius coefficients:	1.00E+11	0.0	11000.0
16. OC6+O2<=>OC7	3.16E+11	0.0	0.0
Reverse Arrhenius coefficients:	2.51E+13	0.0	27400.0
17. OC7=>OC8+OH	8.91E+10	0.0	17000.0
18. C8H18+OH=>OC2+H2O	1.00E+13	0.0	3000.0
19. OC2+O2<=>OC3+HO2	3.16E+11	0.0	6000.0
Reverse Arrhenius coefficients:	3.16E+11	0.0	19500.0
20. OC3+HO2+8O2=>8CO+8H2O+HO2	2.00E+13	0.0	10000.0
21. OC8=>OC9+OH	3.98E+15	0.0	43000.0
22. OC9+O2<=>OC12+HO2	3.16E+11	0.0	6000.0
Reverse Arrhenius coefficients:	3.16E+11	0.0	19500.0
23. HO2+OC12+O2=>H2O2+OC13+HO2	1.58E+13	0.0	10000.0
24. HO2+OC13+6O2=>8CO+6H2O+HO2	1.58E+13	0.0	10000.0
25. C8H18+HE2<=>C7H16+OC2	5.01E+12	0.0	0.0
26. OH+H2=H+H2O	2.14E+08	1.5	3449.0
27. O+OH=O2+H	2.02E+14	-0.4	0.0
28. O+H2=OH+H	5.06E+04	2.7	6290.0
29. H+O2(+M)=HO2(+M)	4.52E+13	0.0	0.0

```
     Low pressure limit:  0.10500E+20 -0.12570E+01  0.00000E+00
        H2O               Enhanced by    0.000E+00
        H2                Enhanced by    0.000E+00
        H2O               Enhanced by    0.000E+00
        H2                Enhanced by    0.000E+00
        N2                Enhanced by    0.000E+00
 30. H+O2(+N2)=HO2(+N2)                             4.52E+13    0.0        0.0
     Low pressure limit:  0.20300E+21 -0.15900E+01  0.00000E+00
 31. H+O2(+H2)=HO2(+H2)                             4.52E+13    0.0        0.0
     Low pressure limit:  0.15200E+20 -0.11330E+01  0.00000E+00
 32. H+O2(+H2O)=HO2(+H2O)                           4.52E+13    0.0        0.0
     Low pressure limit:  0.21000E+24 -0.24370E+01  0.00000E+00
 33. OH+HO2=H2O+O2                                  2.13E+28   -4.8     3500.0
     Declared duplicate reaction...
 34. OH+HO2=H2O+O2                                  9.10E+14    0.0    10964.0
     Declared duplicate reaction...
 35. H+HO2=OH+OH                                    1.50E+14    0.0     1000.0
 36. H+HO2=H2+O2                                    8.45E+11    0.7     1241.0
 37. H+HO2=O+H2O                                    3.01E+13    0.0     1721.0
 38. O+HO2=O2+OH                                    3.25E+13    0.0        0.0
 39. OH+OH=O+H2O                                    3.57E+04    2.4    -2112.0
 40. H+H+M=H2+M                                     1.00E+18   -1.0        0.0
        H2O               Enhanced by    0.000E+00
        H2                Enhanced by    0.000E+00
 41. H+H+H2=H2+H2                                   9.20E+16   -0.6        0.0
 42. H+H+H2O=H2+H2O                                 6.00E+19   -1.2        0.0
 43. H+OH+M=H2O+M                                   2.21E+22   -2.0        0.0
        H2O               Enhanced by    6.400E+00
 44. H+O+M=OH+M                                     4.71E+18   -1.0        0.0
        H2O               Enhanced by    6.400E+00
 45. O+O+M=O2+M                                     1.89E+13    0.0    -1788.0
 46. H2O2+H=HO2+H2                                  1.98E+06    2.0     2435.0
 47. H2O2+H=OH+H2O                                  3.07E+13    0.0     4217.0
 48. H2O2+O=OH+HO2                                  9.55E+06    2.0     3970.0
 49. H2O2+OH=H2O+HO2                                2.40E+00    4.0    -2162.0
 50. HO2+HO2=>H2O2+O2                               2.00E+10    0.0     5000.0
 51. H2O2+M=>OH+OH+M                                1.00E+16    0.0    48000.0
 52. O+CO(+M)<=>CO2(+M)                             1.80E+10    0.0     2385.0
     Low pressure limit:  0.60200E+15  0.00000E+00  0.30000E+04
        H2                Enhanced by    2.000E+00
        O2                Enhanced by    6.000E+00
        H2O               Enhanced by    6.000E+00
        CO                Enhanced by    1.500E+00
        CO2               Enhanced by    3.500E+00
        AR                Enhanced by    5.000E-01
 53. O2+CO<=>O+CO2                                  2.50E+12    0.0    47800.0
 54. CO+OH<=>CO2+H                                  4.76E+07    1.2       70.0
 55. HO2+CO<=>OH+CO2                                4.76E+13    0.0    23600.0

 NOTE:  A units mole-cm-sec-K, E units cal/mole


NO ERRORS FOUND ON INPUT...CHEMKIN LINKING FILE WRITTEN.

WORKING SPACE REQUIREMENTS ARE
   INTEGER:     1202
```